

Three-Dimensional Fire Weather Forecast

HRRR Cross-Section Analysis

SPC Day 1 Critical Fire Weather Areas

Valid: **10 February 2026** (06z Feb 10 – 06z Feb 11)

HRRR Cycle: **20260209 06z** | Forecast Hours: 24–48

*Autonomous Fire Weather Research Agent
wxsection.com Atmospheric Cross-Section Platform*

Generated: 9 February 2026

SPC CRITICAL FIRE WEATHER — Two Areas

Northern Rockies: Central Montana / Northern Wyoming

Four Corners: Arizona / New Mexico / Southern Colorado

This forecast supplements standard NWS/SPC guidance with three-dimensional atmospheric cross-section analysis not available in operational products.

Abstract

The Storm Prediction Center has issued a Day 1 Critical Fire Weather Outlook valid February 10, 2026, highlighting two regions of critical fire weather potential: the Northern Rockies corridor spanning central Montana and northern Wyoming, and the Four Corners region across Arizona, New Mexico, and southern Colorado. This report provides three-dimensional atmospheric analysis using vertical cross-sections extracted from the HRRR (High-Resolution Rapid Refresh) 3-km model via the wxsection.com cross-section data platform. Analysis encompasses 19 atmospheric products across multiple transects and forecast hours, revealing the vertical structure of wind fields, humidity distributions, temperature profiles, subsidence patterns, and composite fire weather conditions that standard two-dimensional forecast products cannot capture. Cross-section analysis reveals the altitude, depth, and intensity of critical fire weather parameters through the atmospheric column, enabling identification of mixing potential, terrain-channeled wind acceleration, subsidence-driven drying, and the vertical extent of extreme fire danger conditions.

Contents

1 Situational Overview and Current Guidance	2
1.1 SPC Outlook Analysis	2
1.1.1 Central High Plains Critical Area	2
1.1.2 Southern High Plains Critical Area	2
1.1.3 Elevated Risk Envelope	3
1.2 NWS Warnings and Watches	3
1.3 Current Fire Activity	4
1.4 Antecedent Conditions: Drought, Snowpack, and Fuels	4

1.4.1	U.S. Drought Monitor (as of 3 February 2026)	4
1.4.2	Snow Drought and Snowpack	5
1.4.3	Fuel Conditions and Fire Season Outlook	5
1.4.4	Synthesis	6
2	Northern Rockies Critical Area Analysis (Montana–Wyoming)	6
2.1	Wind Field Analysis	6
2.1.1	Surface and Low-Level Winds	6
2.1.2	Mid- and Upper-Level Flow	9
2.1.3	Temporal Evolution of Wind	9
2.1.4	Terrain Interactions	9
2.2	Humidity and Moisture Analysis	12
2.2.1	Surface Relative Humidity	12
2.2.2	Elevated Dry Layer and Entrainment Potential	12
2.2.3	Spatial Variability of Moisture	13
2.2.4	Diurnal RH Evolution	13
2.3	Temperature Structure and Stability	13
2.3.1	Surface Temperature Distribution	13
2.3.2	Vertical Temperature Profile	16
2.3.3	Lapse Rate and Atmospheric Stability	18
2.4	Vertical Motion and Subsidence	18
2.4.1	Large-Scale Vertical Motion Pattern	18
2.4.2	North–South Subsidence Variability	20
2.5	Vapor Pressure Deficit and Fire Weather Composite	23
2.5.1	VPD Analysis	23
2.5.2	Fire Weather Composite	24
2.5.3	Multi-Transect Fire Weather Assessment	24
2.6	Summary and Fire Weather Assessment	25
3	Four Corners Critical Area Analysis (Arizona–New Mexico–Colorado)	26
3.1	Wind Field and Terrain Channeling	27
3.2	Humidity Analysis	32
3.3	Temperature Structure and Mixing Height	38
3.4	Vertical Motion and Subsidence	42
3.5	Vapor Pressure Deficit	43
3.6	Fire Weather Composite	48
3.7	Summary and Risk Assessment	52
4	Synoptic-Scale Atmospheric Pattern	53
4.1	Upper-Level Flow and Jet Stream Configuration	54
4.2	Large-Scale Subsidence and the Western Ridge	59
4.3	Moisture Distribution and Dry Air Intrusion	60
4.4	Temporal Evolution Through February 10	66
4.5	Synoptic Mechanisms Driving Critical Fire Weather	71
4.6	Pattern Comparison to Historical Fire Weather Events	73

5 Quantitative Fire Weather Analysis	73
5.1 Diurnal Evolution of Fire Weather Parameters	74
5.2 Red Flag Threshold Exceedance Analysis	74
5.3 Regional Comparison: Northern Rockies vs. Four Corners	76
5.4 Peak Fire Danger Window Identification	76
5.5 Vertical Extent of Critical Conditions	77
6 Forecast Discussion and Operational Implications	81
6.1 Synthesis of Cross-Section Analysis	81
6.2 Peak Fire Danger Windows	81
6.3 What Cross-Sections Reveal That Surface Maps Cannot	81
6.4 Operational Recommendations	82
6.5 Confidence and Uncertainty	83

1. Situational Overview and Current Guidance

The Storm Prediction Center (SPC) Day 1 Fire Weather Outlook issued at **0715 UTC on 9 February 2026** (valid 09/1200Z–10/1200Z) delineates two **Critical** fire weather areas across the central High Plains, with broad **Elevated** risk surrounding both corridors. This section synthesizes the SPC technical discussion, active National Weather Service (NWS) warnings, current fire activity, and antecedent drought and fuel conditions that frame the threat for 10 February 2026.

1.1. SPC Outlook Analysis

Forecaster **Squitieri** identifies a synoptic pattern dominated by broad upper ridging overspreading the central and eastern CONUS, with a pronounced mid-level impulse poised to crest the ridge over the central Plains. An elongated surface low developing across the central Plains drives two distinct mechanisms that produce the twin Critical areas.

Central High Plains Critical Area

The northern Critical area covers **far southeastern Wyoming into far western Nebraska**, centered along the Interstate 80 corridor east of the Laramie Range. Behind a cold-frontal passage, dry northwesterly flow is forecast to produce **sustained surface winds of 20–25 mph** with relative humidity potentially falling to **15–20%**. The SPC discussion notes model uncertainty regarding the degree of post-frontal airmass dryness but concludes that “stronger post-cold frontal winds atop drying fuels should compensate to support wildfire spread” even if humidity does not reach the lowest projections.

The NWS Cheyenne office provides higher-resolution detail, forecasting a **65–70 kt mid-level jet** developing across the Laramie Range, with **700 mb winds of 50–55 kt** near the I-80 Summit area driving strong surface momentum transfer. Afternoon gusts of **58+ mph** are expected to become “more frequent and expand to more locations” across the southeast Wyoming plains. Minimum relative humidity is forecast in the **14–20% range** east of the Laramie Range, with overnight recovery limited to only **35–40%**—described as “very poor” by the Cheyenne forecast office, indicating that fire weather conditions may persist well beyond the peak afternoon heating window.

Southern High Plains Critical Area

The southern Critical area extends from **far northeastern New Mexico through the Oklahoma and Texas Panhandles, extreme northwestern Oklahoma, and far southwestern Kansas**. The SPC identifies “dry downslope flow, in combination with a very deep and dry boundary layer” as the primary driver, supporting relative humidity values **as low as 10–15%** with sustained west-southwesterly surface winds exceeding **20 mph for several hours**.

The NWS Amarillo discussion underscores the severity of conditions across the Panhandle corridor: afternoon temperatures are expected in the **mid-to-upper 70s °F** (with some locations approaching **80 °F**), while RH values are forecast to **bottom out below 10%**. Portions of the Canadian River Valley face RH values potentially dropping to an extreme **5%**. Southwesterly winds of **20–25 mph sustained with gusts to 35–45 mph** are forecast.

The NWS Albuquerque office reports that **25–35 kt winds at 700 mb** will align with the eastern Interstate 40 corridor, producing surface winds of **25–30 kt** along the I-40 corridor and near the Texas/New Mexico border. Temperatures will surge **15–22 °F above climatology** in the eastern zones, causing RH values to “plummet further.” The Albuquerque discussion specifically notes that “the recent fire activity over the past few days suggests fuels are combustible,” supporting the upgrade from a Fire Weather Watch to a Red Flag Warning.

Elevated Risk Envelope

Surrounding both Critical areas, broad Elevated risk extends across the central and southern High Plains, reflecting the regional-scale pattern of anomalous warmth, low humidity, and gusty winds. NWS Riverton reports that **elevated fire weather conditions are expected across much of central and southern Wyoming** on Monday, with temperatures running **20–30 °F above normal** and widespread gusty winds of **20–40 mph**. South Pass faces a **70% probability of gusts exceeding 60 mph**, while southern Casper has an **80% probability of gusts over 50 mph**.

The SPC Day 2 Outlook (also issued by Squitieri at 0748 UTC) indicates **no Critical areas** for 10–11 February, suggesting the threat window is concentrated in the Monday afternoon–evening period before the upper impulse translates east and the pattern relaxes.

1.2. NWS Warnings and Watches

As of 09 February 2026, **thirteen Red Flag Warnings** are active across seven NWS forecast offices spanning six states. The warnings collectively affect a corridor from southeastern Wyoming through the Nebraska Panhandle, across eastern Colorado, the Texas and Oklahoma Panhandles, southwestern Kansas, and east-central New Mexico. Key warnings are summarized below.

- **NWS Cheyenne (CYS):** Red Flag Warning for zones 430–437 (southeast Wyoming and the western Nebraska Panhandle) through **5 PM MST Monday**. Westerly turning northwest winds **20–30 mph sustained with gusts to 45 mph; RH 13–20%**.
- **NWS Albuquerque (ABQ):** Red Flag Warning for zones NMZ104, 123, 125, 126 (San Miguel, Guadalupe, Quay, and Curry counties in east-central New Mexico) from **11 AM to 6 PM MST Monday**. Southwest winds **20–25 mph sustained with gusts to 35 mph; RH as low as 7%**.
- **NWS Amarillo (AMA):** Red Flag Warning for Texas and Oklahoma Panhandle counties (TXZ001–013, 016–017, 317; OKZ001–003) from **noon to 6 PM CST Monday**. Southwest winds **20–25 mph with gusts to 40 mph; RH as low as 7%, with temperatures in the 70s °F**.
- **NWS Pueblo (PUB):** Red Flag Warning for zones COZ221–222, 225, 228–230, 233, 237 (the greater I-25 corridor from Pueblo south to the New Mexico border, including Teller, Fremont, Pueblo, Huerfano, Las Animas, and Baca counties) from **10 AM to 6 PM MST Monday**. West winds **10–20 mph with gusts to 40 mph; RH as low as 7–9%**.
- **NWS Denver/Boulder (BOU):** Red Flag Warning for zones 238, 242 (northeast Larimer and north Weld counties) from **11 AM to 5 PM MST Monday**. West winds **10–20 mph with gusts to 35 mph; RH as low as 13%**.
- **NWS North Platte (LBF):** Red Flag Warning for zones 204, 206, 209 (Nebraska Panhandle and Sandhills) from **9 AM CST to 6 PM CST Monday**. West winds **20–30 mph with gusts to 40 mph; RH as low as 14%; temperatures up to 75–76 °F**.
- **NWS Dodge City (DDC):** Red Flag Warning for southwestern Kansas counties (Stanton, Grant, Haskell, Morton, Stevens, Seward, Meade, Hamilton, Kearny, Finney, Gray, Ford, Clark) from **noon to 7 PM CST Monday**. Southwest winds **20–30 mph with gusts to 40 mph; RH as low as 9–12%**.
- **NWS Norman (OUN):** Red Flag Warning for northwestern Oklahoma (Harper, Ellis, Woodward counties) from **noon to 7 PM CST Monday**. South winds **15–25 mph with gusts to 35 mph; RH as low as 14%; temperatures up to 82 °F**.

The geographic breadth of these warnings—spanning from **41°N** in Nebraska to **34°N** in east-central New Mexico and from **106°W** to **100°W**—underscores the regional scale of this fire weather event. The most extreme conditions ($\text{RH} \leq 7\%$, gusts $\geq 40 \text{ mph}$) are concentrated in the two SPC Critical areas: the I-80 corridor of southeast Wyoming/western Nebraska and the Panhandle corridor from northeast New Mexico through the Texas/Oklahoma Panhandles into southwest Kansas.

1.3. Current Fire Activity

As of the most recent NIFC Incident Management Situation Report (6 February 2026), the **National Preparedness Level stands at 1** (the lowest on the 1–5 scale), and fire activity nationwide remains light. Year-to-date statistics through 6 February show **3,797 fires for 61,122 acres**, with only **three active large fires**—all in Florida—totaling **1,138 acres** and all at 70–80% containment. No large fires are being managed under a strategy other than full suppression.

Within the regions of concern for this outlook:

- **Rocky Mountain Area (RMA):** The RMA has experienced minimal fire activity in January 2026, with **30 fires totaling approximately 1,400 acres**, all contained by local initial-attack resources. Wildfire activity has been concentrated in **southwestern South Dakota and along the Colorado Front Range**, consistent with the exposed fine-fuel areas most susceptible to wind-driven fire spread.
- **Southwest Area:** A **25-acre fire** was reported on 1 February 2026 in the Magdalena Mountains on the Magdalena Ranger District of the Cibola National Forest & National Grasslands, cause unknown. The NWS Albuquerque forecast discussion notes that “recent fire activity over the past few days suggests fuels are combustible,” indicating additional small fires have occurred in eastern New Mexico leading into this event.
- **Front Range Corridor:** The NIFC monthly outlook identifies the Colorado Front Range as an area of **above-normal significant fire potential** in February, expected to manifest in “brief two- or three-day windows” coinciding with wind events—precisely the pattern materializing on 9–10 February.

While the current national fire situation is quiet, the low preparedness level should not obscure the potential for rapid escalation. The February 2024 precedent of a **60+ mph wind-driven grass fire near Cheyenne that closed both I-25 and I-80** demonstrates how quickly conditions in this corridor can produce significant incidents with major transportation and community impacts.

1.4. Antecedent Conditions: Drought, Snowpack, and Fuels

The fire weather threat on 10 February 2026 is underpinned by an exceptional antecedent drought and snowpack deficit across the western United States that has been building since late 2025.

U.S. Drought Monitor (as of 3 February 2026)

As of the most recent USDM release, **37.41% of the United States** (44.53% of the Lower 48) is classified in drought. A mostly dry January led to large drought degradations across the West, with specific conditions in the affected fire weather areas as follows:

- **Southeast Wyoming:** Severe Drought (D2) expanded from southeastern Wyoming into northeastern Colorado and the Nebraska Panhandle. Moderate Drought (D1) expanded across much of eastern Wyoming. Lowland snow cover is at its **lowest area extent and depth in at least 20 years**. Five SNOTEL stations report **record-low snow water equivalent (SWE)**.

- **Colorado:** Extreme Drought (**D3**) increased across central Colorado. The state reports **record-low statewide average SWE**, with most basins at **less than 60% of median**. **95% of Colorado SNOTEL stations** are classified as being in snow drought.
- **New Mexico:** **72% of the state** is under drought conditions with an additional 27% abnormally dry (as of late January). All basins report **less than 50% of median SWE**: the Upper Rio Grande at 48%, Rio Grande–Elephant Butte at 40%, and the Upper Canadian at just **28% of median**. **81% of New Mexico SNOTEL stations** are in snow drought.
- **Montana:** Limited recent precipitation, declining soil moisture, and below-normal streamflows. **46% of SNOTEL stations** report snow drought conditions. Most basins at **75–85% of median SWE**, with several locations approaching record lows. The state is experiencing a **top-five warmest winter on record**.
- **Southern/Central Plains:** Abnormal dryness (D0) and Moderate Drought (D1–D2) expanded across portions of Kansas, with the broader High Plains corridor experiencing continued deterioration.

Snow Drought and Snowpack

The drought conditions are compounded by a historic snow drought. Snow cover across the western United States on 1 February 2026 was **139,322 square miles**—the **lowest February 1 snow cover in the MODIS satellite record** (since 2001). January 2026 was exceptionally dry across central and eastern Montana and northwest North Dakota, with little to no precipitation reported since 8 January. Most western states received **50% or less of normal January precipitation**, and above-normal temperatures caused what precipitation did fall at higher elevations to arrive as rain rather than snow.

For the specific fire weather areas, this snowpack deficit translates directly to fire-receptive landscapes: the eastern Wyoming and Colorado plains and foothills are essentially **snow-free at low to mid elevations**, leaving dormant fine fuels (primarily cured grasslands) fully exposed. The NIFC monthly outlook notes that “exposed and dry fine fuels on the eastern plains and foothills continue to be the main concern” and that “infrequent snowfalls followed by warm dry periods have provided little relief for fine fuel moisture.”

Fuel Conditions and Fire Season Outlook

The NIFC National Significant Wildland Fire Potential Outlook issued 2 February 2026 identifies several critical fuel characteristics:

- **Eastern New Mexico:** “Well above normal fine fuel loading,” particularly across the northeastern plains, as the wind season begins. Above-normal significant fire potential is expected through March and potentially into April.
- **Colorado Front Range:** Above-normal significant fire potential forecast for February, occurring during transient wind events. From February into March, southeastern Colorado and western Kansas are “likely to experience elevated fire chances like the past two years.”
- **Wyoming–Montana:** Larger fuels are drier than average but “not nearing critical levels”; however, the fine-fuel (grass) component in eastern Wyoming is the dominant concern. The alignment of dry fine fuels and gusty winds “has been responsible for the fire growth observed so far this year.”
- **Fuel Moisture Classification:** The SWCC tracks dead fuel moisture in categories from Wet ($\geq 15\%$) through Extremely Dry ($\leq 3\%$). Current conditions across eastern New Mexico and the southern High Plains place fine fuels in the **Dry to Very Dry** categories, consistent with the SPC’s characterization of “continued drying fuels” and “fuel desiccation.”

NWS Senior Service Hydrologist Andrew Mangham summarized the seasonal outlook: “Given the fact that the Climate Prediction Center is calling for an overall warm, dry winter the whole way through, we are really getting set up for a particularly dangerous fire season.”

Synthesis

The 10 February fire weather event occurs against a backdrop of historically low snowpack, expanding multi-category drought, and dormant fine fuels that have received minimal precipitation relief since early January. While the national fire posture remains at Preparedness Level 1, the ingredients for rapid fire growth and spread—critically low RH (7–15%), strong sustained winds (20–30 mph with gusts to 45–60 mph), anomalous warmth (15–30 °F above normal), and receptive fuels—are converging across a broad swath of the central and southern High Plains. The SPC Critical risk area encompasses approximately **55,520 square miles** with a population of **553,237**, underscoring the potential societal impact of fire ignitions during this event window.

The cross-section analyses that follow will examine the vertical atmospheric structure driving these surface conditions, focusing on boundary-layer depth, momentum transfer mechanisms, and the interaction between terrain-channelled flow and the synoptic-scale pattern.

2. Northern Rockies Critical Area Analysis (Montana–Wyoming)

This section presents a detailed mesoscale analysis of the Northern Rockies fire weather environment for February 10, 2026, using HRRR cross-section diagnostics initialized at 06z February 9, 2026. Four transects are examined across the critical area of central Montana and northern Wyoming: an east–west main transect at 47°N spanning the Continental Divide to the western Dakotas (113°W to 103°W), a southern east–west transect at 45°N crossing southern Montana and northern Wyoming (112°W to 104°W), a north–south transect along 108°W from the Canadian border to central Wyoming (49°N to 43°N), and a terrain-following transect from the Bitterroot Range southeast to the Powder River Basin (47.5°N, 114°W to 46°N, 104.5°W). Focus is placed on forecast hours 36 (18z, 11 AM MST) and 39 (21z, 2 PM MST), corresponding to the period of maximum surface heating and peak fire danger. Temporal evolution sequences from overnight (06z) through late afternoon (00z February 11) provide context for the diurnal fire weather cycle.

2.1. Wind Field Analysis

Surface and Low-Level Winds

The HRRR wind speed cross-sections reveal a relatively benign surface wind environment across central Montana at peak heating on February 10. Along the E–W Main transect at 47°N (Figure 1), surface winds range from 1.3 to 8.8 kt with a mean of 5.7 kt—well below the critical 25 kt fire weather threshold. The predominant surface wind direction is from the west-southwest (mean 238°), reflecting the prevailing synoptic-scale westerly flow pattern. The strongest surface winds are concentrated along the eastern portion of the transect near 103.7°W, where terrain transitions from the Montana plains to the more rolling topography near the North Dakota border.

The low-level wind profile shows a gradual increase with altitude. At 850 hPa, maximum winds reach 10.9 kt, strengthening to 17.0 kt at 800 hPa near the eastern end of the transect (104.4°W). The 700 hPa level exhibits a more pronounced wind maximum of 20.4 kt centered near 108.3°W, reflecting the developing mid-level flow. This 700 hPa wind maximum is significant because it represents the upper boundary of the afternoon mixed layer and could be entrained to the surface through turbulent mixing during peak heating hours.

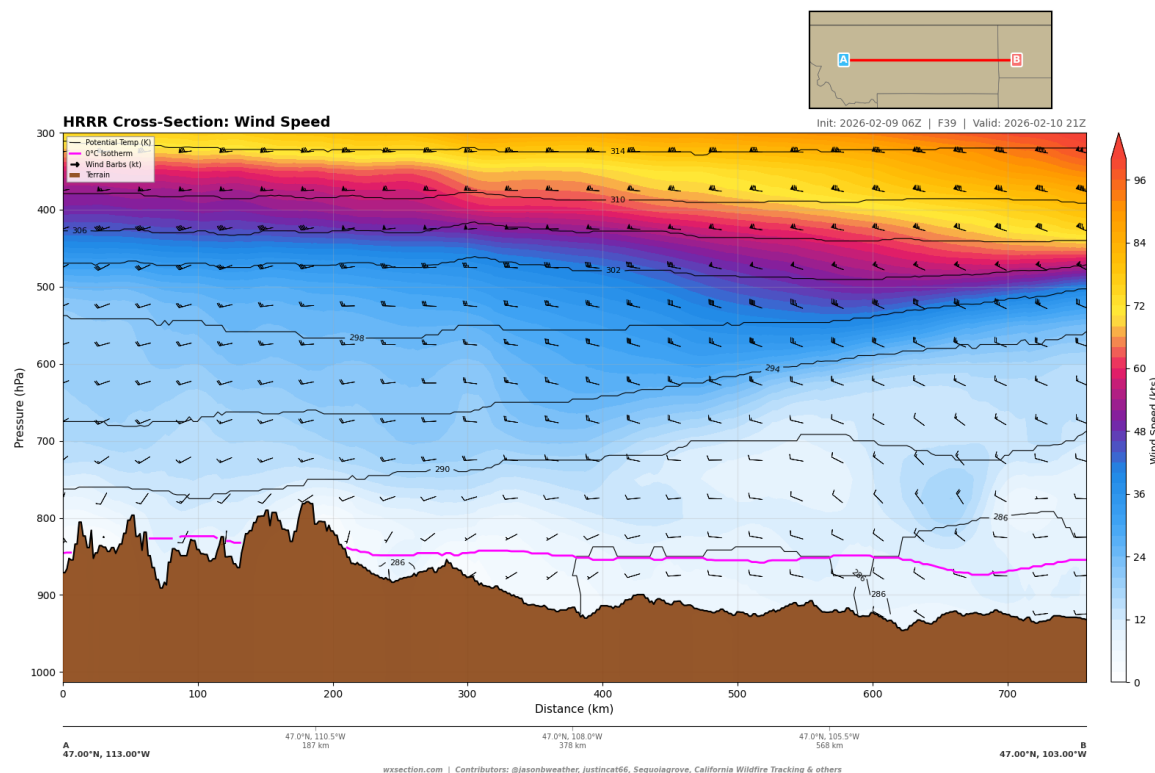


Figure 1: HRRR wind speed cross-section along the E–W Main transect (47°N , 113°W to 103°W) valid 21z February 10, 2026 (FHR 39). Wind barbs show flow direction and speed. Pink contour marks the freezing level. The jet stream core exceeds 100 kt above 300 hPa.

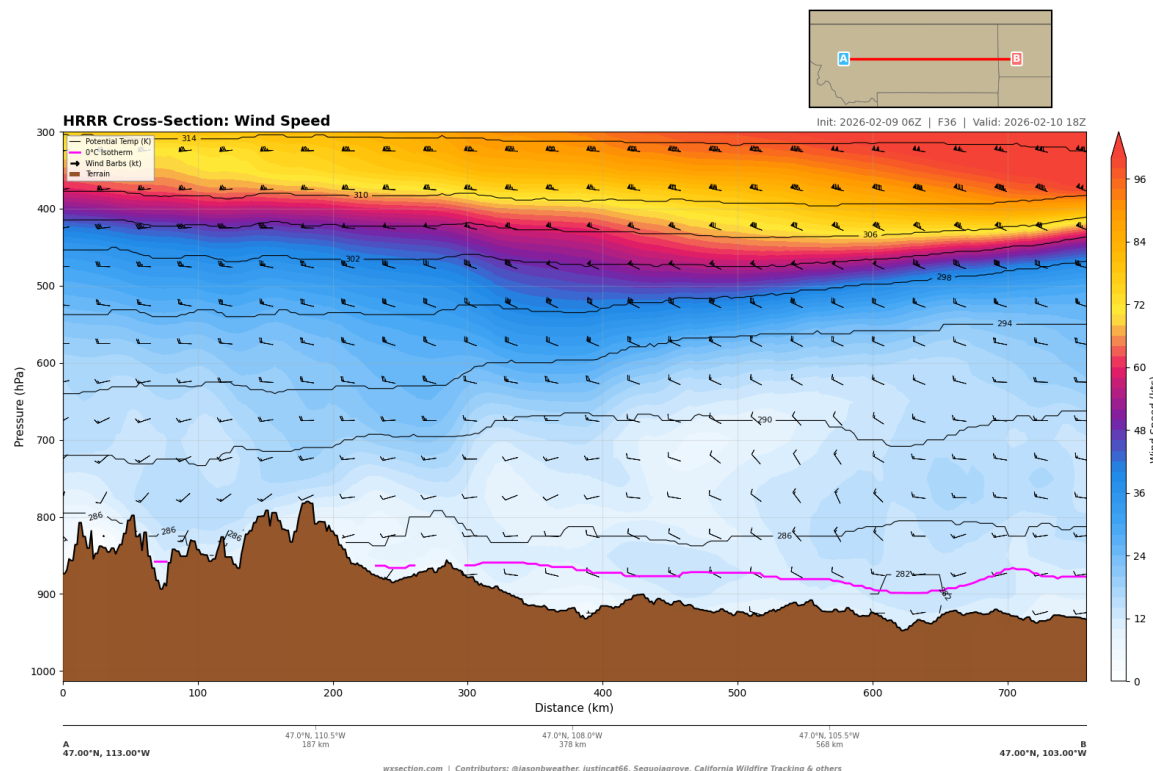


Figure 2: HRSS wind speed cross-section along the E-W Main transect valid 18z February 10, 2026 (FHR 36, 11 AM MST). Early heating phase shows the beginning of boundary layer development and wind acceleration.

Mid- and Upper-Level Flow

Above 700 hPa, winds increase substantially. The 650 hPa level reaches 25.2 kt near 108°W, while 600 hPa winds reach 30.6 kt centered at 106.8°W. At 500 hPa, the flow strengthens to 50.0 kt over the eastern Montana plains (105°W), accelerating rapidly to 80.5 kt at 400 hPa and 101.9 kt at 300 hPa near 103°W (Table 1). This strong upper-level jet streak positioned over eastern Montana has implications for the fire weather environment: the associated subsidence on the anticyclonic side of the jet entrance region can enhance drying aloft and promote deep mixing of low-humidity air toward the surface.

Table 1: Wind speed profile along the E–W Main transect at 21z February 10, 2026 (FHR 39). Values in knots.

Level (hPa)	Min (kt)	Mean (kt)	Max (kt)	Max Location
Surface (1013)	1.3	5.7	8.8	103.7°W
925	1.3	5.8	9.6	103.5°W
850	1.8	7.4	10.9	104.3°W
800	3.0	9.7	17.0	104.4°W
700	9.8	15.6	20.4	108.3°W
650	12.3	18.4	25.2	108.0°W
600	16.0	22.7	30.6	106.8°W
500	24.1	37.2	50.0	105.0°W
400	48.9	61.0	80.5	103.0°W
300	74.5	86.3	101.9	103.0°W

Temporal Evolution of Wind

The diurnal wind evolution (Figure 3) shows a marked progression from overnight quiescence to daytime acceleration. At 06z (FHR 24, overnight), winds are strongest aloft with a well-defined upper-level jet but minimal surface flow, consistent with a stable nocturnal boundary layer. By 15z (FHR 33, 8 AM MST), boundary layer mixing begins to erode the nocturnal inversion, and the mid-level flow starts to strengthen as the upstream trough amplifies. The wind speed maximum at the jet level shifts progressively eastward through the day, reflecting the eastward propagation of the upper-level wave. By 00z February 11 (FHR 42, 5 PM MST), the jet core has moved east of the transect, and surface winds remain light as the boundary layer begins to restabilize.

Terrain Interactions

The terrain-following transect from the Bitterroot Range (114°W) to the Powder River Basin (104.5°W) reveals important orographic wind interactions (Figure 4). Lee-side acceleration is evident downstream of the Rocky Mountain front, with enhanced wind speeds in the 800–700 hPa layer east of the Continental Divide. The complex terrain of western Montana forces channeling of the westerly flow through valleys, creating localized areas of enhanced surface wind where canyon exits open onto the Montana plains. These terrain-channeled winds, while not reaching critical thresholds in this forecast, represent areas where fire spread could be locally enhanced.

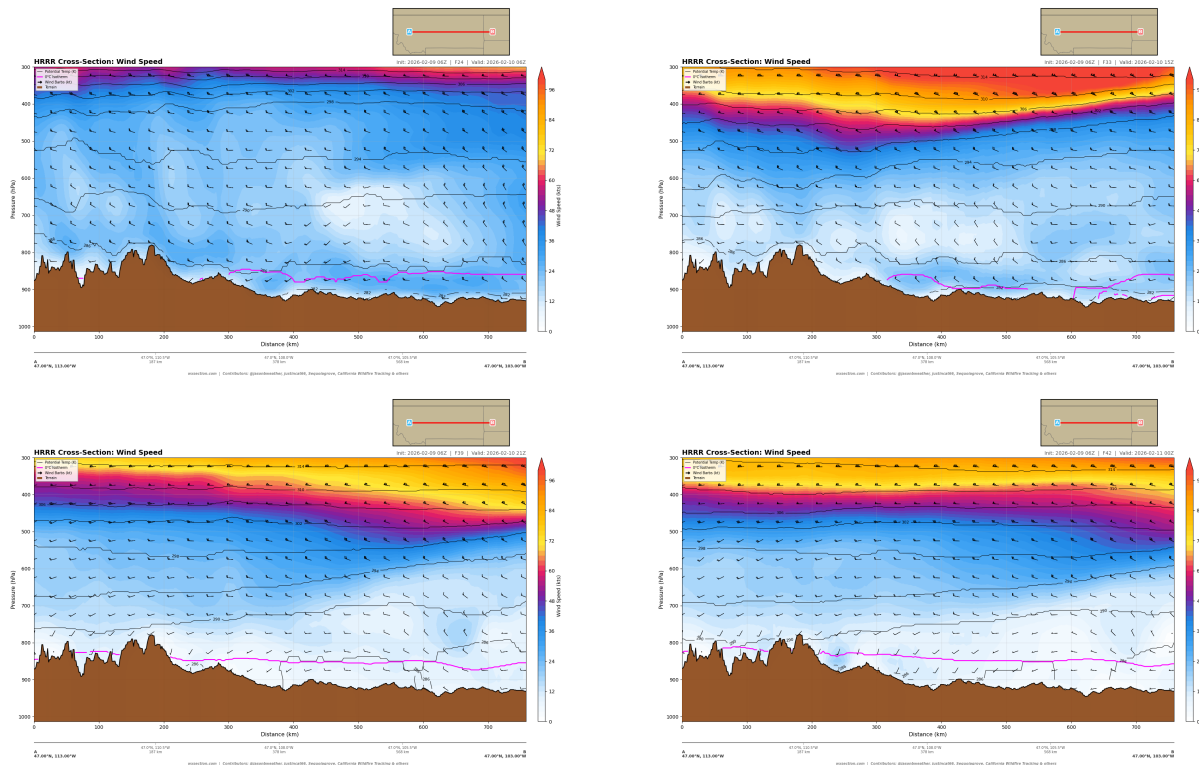


Figure 3: Temporal evolution of wind speed along the E–W Main transect from 06z February 10 (top left, FHR 24) through 15z (top right, FHR 33), 21z (bottom left, FHR 39), and 00z February 11 (bottom right, FHR 42). The upper-level jet strengthens and shifts eastward through the period while surface winds remain subdued.

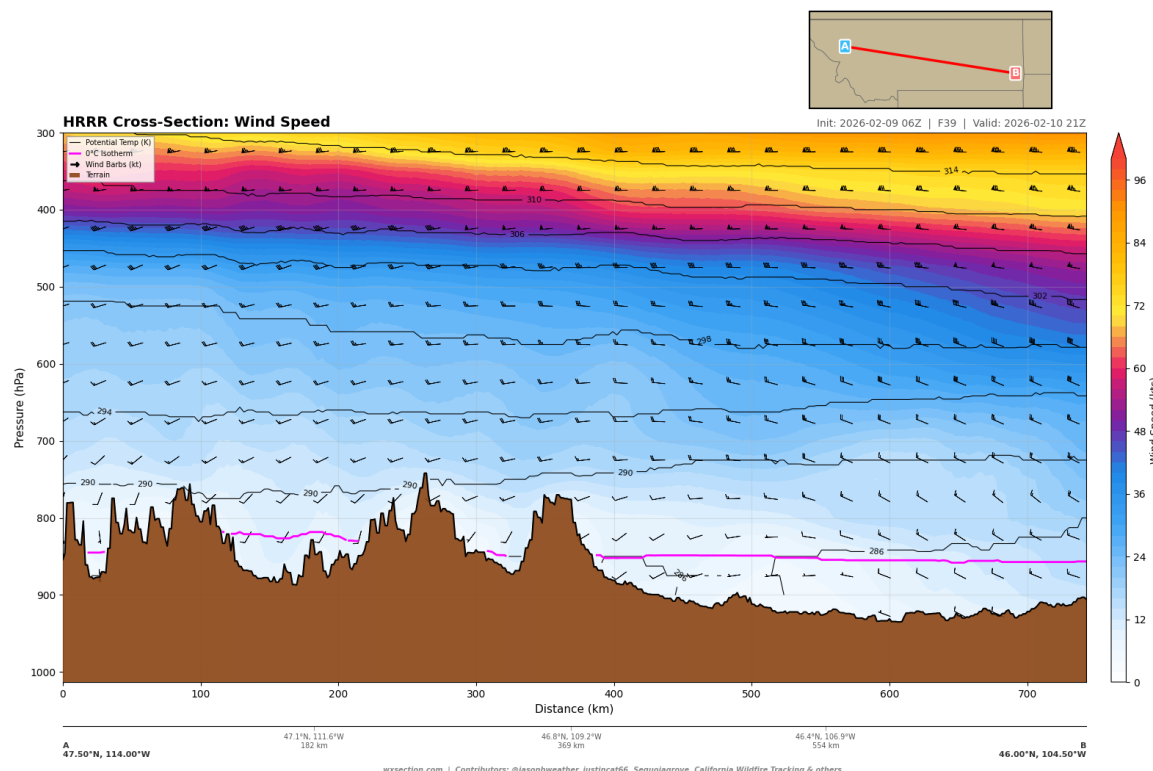


Figure 4: HRRR wind speed cross-section along the terrain-following NW-SE transect (47.5°N, 114°W to 46°N, 104.5°W) at 21z February 10, 2026. The transect captures the transition from the high Rockies to the Great Plains, showing terrain-modulated wind structures.

2.2. Humidity and Moisture Analysis

Surface Relative Humidity

The HRRR relative humidity cross-sections reveal an environment that is moderately dry at the surface but with markedly drier conditions aloft (Figure 5). Along the E–W Main transect at peak fire danger (21z, FHR 39), surface relative humidity ranges from 40.9% to 65.8% with a mean of 54.8%. Critically, **no grid points along this transect fall below the 15% or even 20% RH threshold at the surface**, and the minimum surface RH of 40.9% occurs near 112°W on the lee side of the Continental Divide. While these surface values are well above critical fire weather thresholds, the moderate dryness across the western half of the transect (RH 40–50%) combined with other factors warrants continued monitoring.

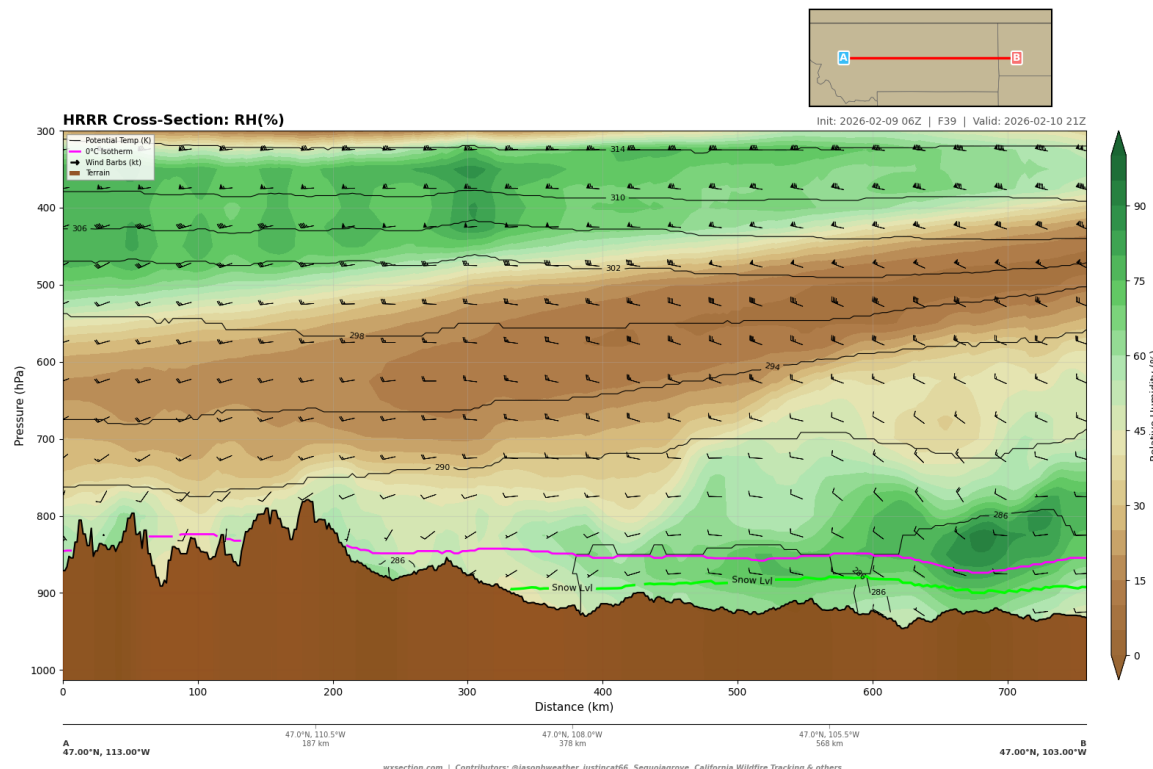


Figure 5: HRRR relative humidity cross-section along the E–W Main transect at 21z February 10, 2026 (FHR 39). Green shading indicates higher humidity; brown tones indicate drier air. The dashed contours mark key RH thresholds. Note the pronounced dry layer between 650–500 hPa with values below 20%.

Elevated Dry Layer and Entrainment Potential

The most significant moisture feature is the deep dry layer extending from approximately 700 hPa to 500 hPa. At 700 hPa, 21 of 252 grid points (8.3%) exhibit RH below 20%, with a minimum of 19.0%. The drying intensifies dramatically with altitude: at 650 hPa, 148 points (58.7%) fall below 20% RH with a minimum of 13.3%, and at 600 hPa, 146 points (57.9%) are below 20% with a minimum of just 10.4%. At 500 hPa, 118 points (46.8%) are below 20% with an extreme minimum of only 6.5% (Table 2).

This elevated dry layer is critically important for fire weather: as daytime convective mixing deepens the planetary boundary layer through peak heating, very dry air from the 700–600 hPa level can be entrained

Table 2: Relative humidity profile along the E–W Main transect at 21z February 10, 2026 (FHR 39).

Level (hPa)	Min (%)	Mean (%)	Max (%)	Points <20%
Surface (1013)	40.9	54.8	65.8	0
900	40.9	57.3	72.5	0
850	41.5	63.1	89.6	0
800	40.4	57.8	87.4	0
750	28.7	44.2	70.0	0
700	19.0	32.0	55.7	21
650	13.3	25.8	48.5	148
600	10.4	21.1	43.6	146
500	6.5	30.2	68.5	118

downward toward the surface. If the mixed layer top reaches 700 hPa (approximately 3 km AGL over the Montana plains), the resulting surface RH could drop substantially below the current HRRR surface forecast values. This mechanism is a well-documented pathway for rapid fire weather deterioration in the Northern Rockies.

Spatial Variability of Moisture

The column-mean RH analysis reveals a pronounced west-to-east moisture gradient. The driest column occurs near 112°W (lee of the Divide) with a mean tropospheric RH of 41.6%, while the moistest columns are in eastern Montana near 104°W (mean 71.9%). This gradient reflects the orographic drying effect of the Rocky Mountain front and the increasing distance from the Pacific moisture source.

The N–S transect along 108°W (Figure 6) reveals that the driest conditions extend across a broad latitudinal band from approximately 46°N to 48°N, centered on central Montana. The southern portion of the transect (northern Wyoming, 43–45°N) shows slightly higher terrain-level RH values due to the more complex orography of the Absaroka and Bighorn ranges producing localized upslope moisture.

Diurnal RH Evolution

The temporal progression of relative humidity (Figure 7) shows the expected diurnal cycle. At 06z (FHR 24, overnight), the surface layer maintains higher humidity under the nocturnal inversion, with the low-level moisture pool extending up to roughly 850 hPa. By 15z (FHR 33, 8 AM MST), surface heating begins to erode this moist boundary layer from below, and the mid-level dry layer begins to deepen. At 21z (FHR 39, peak heating), the boundary layer has mixed sufficiently to draw down some of the drier mid-level air, producing the observed surface RH minimum of 40.9%. By 00z February 11 (FHR 42), the boundary layer begins to restabilize, but the mid-level dry layer persists, indicating that the elevated dryness is a synoptic-scale feature rather than a diurnally forced one.

2.3. Temperature Structure and Stability

Surface Temperature Distribution

The HRRR temperature analysis at peak heating (21z, FHR 39) indicates surface temperatures ranging from 9.3°C (48.8°F) to 12.1°C (53.8°F) along the E–W Main transect, with a mean of 10.6°C (51.0°F). The warmest surface temperatures occur near 112°W on the lee side of the Continental Divide, consistent with chinook-type warming (Figure 8). While these temperatures are moderate for February in central

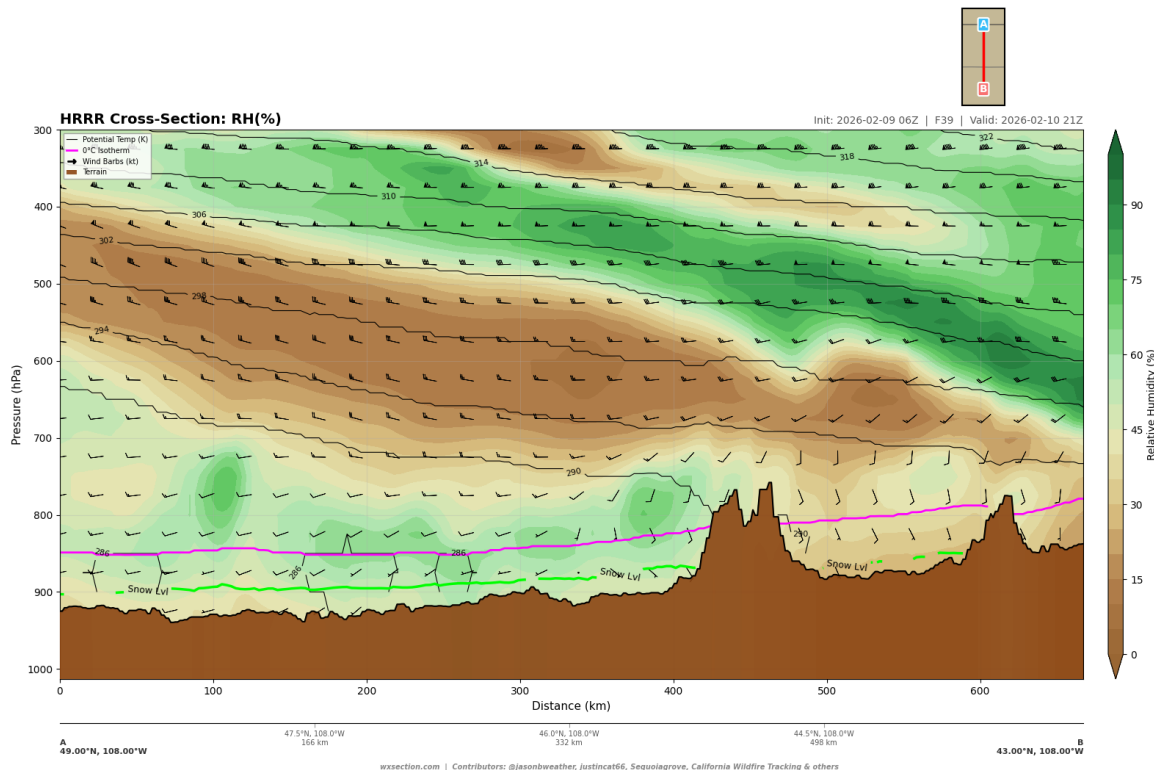


Figure 6: HRRR relative humidity cross-section along the N–S transect (49°N to 43°N , 108°W) at 21z February 10, 2026. The dry layer at 650–500 hPa is prominent across the full latitudinal extent, with the driest air at mid-levels near $46\text{--}47^{\circ}\text{N}$.

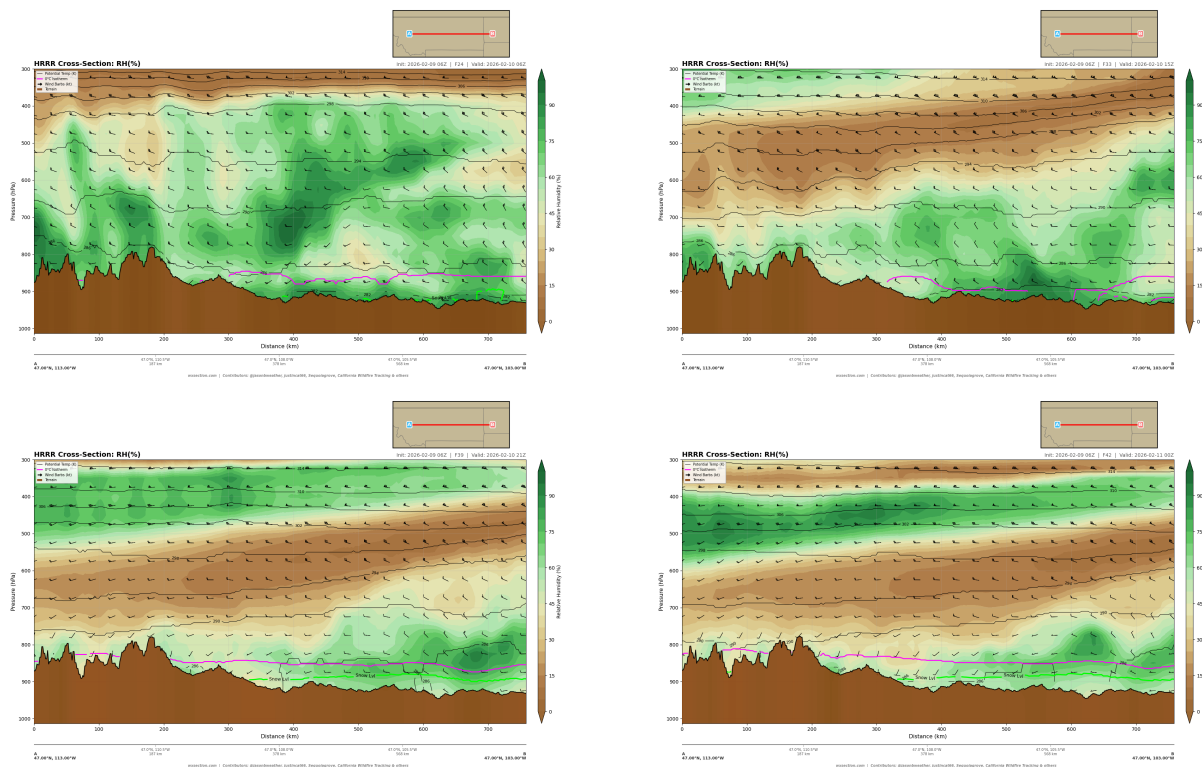


Figure 7: Temporal evolution of relative humidity along the E-W Main transect from 06z February 10 (top left) through 15z (top right), 21z (bottom left), and 00z February 11 (bottom right). The nocturnal moisture pool erodes through the day as boundary layer mixing entrains drier mid-level air toward the surface.

Montana—well above freezing and sufficient to support active fire behavior in cured fuels—they do not reach the extreme values associated with the most critical fire weather events.

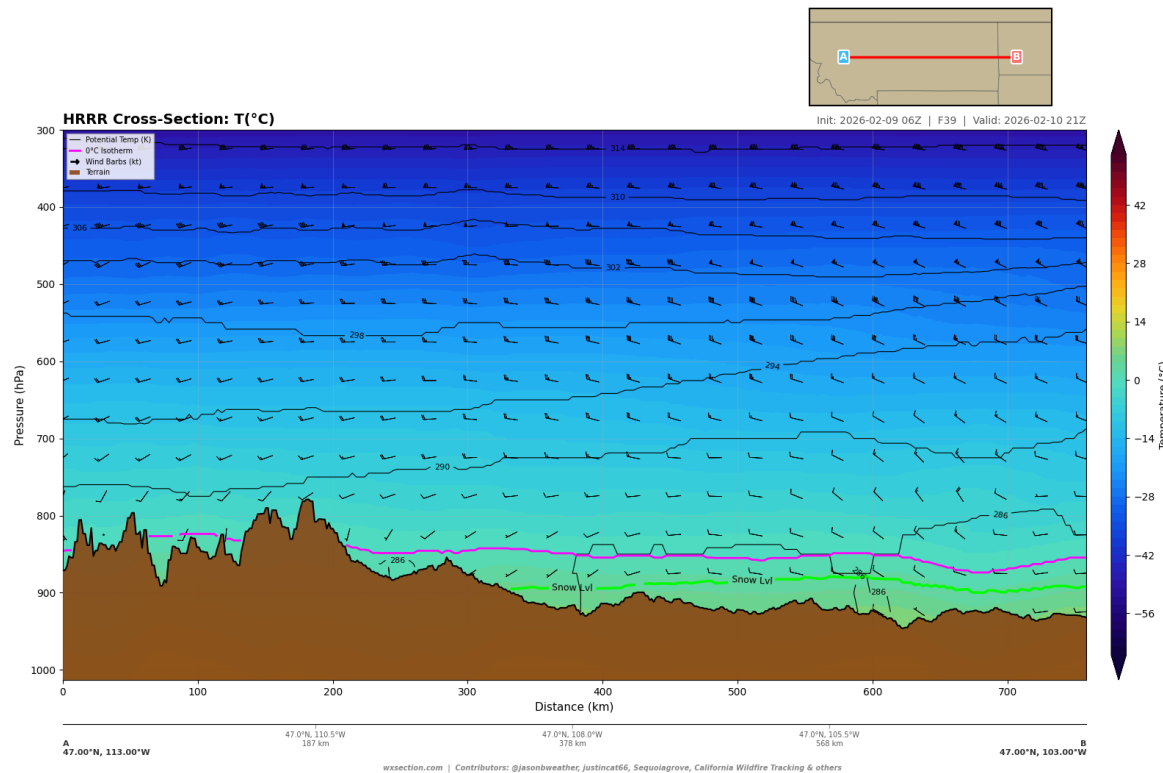


Figure 8: HRRR temperature cross-section along the E–W Main transect at 21z February 10, 2026 (FHR 39). Isotherms in °C. The 0°C isotherm (freezing level) is near 850 hPa over the western portion and slopes downward toward 900 hPa in the east. Note the warm surface anomaly near 112°W on the lee of the Continental Divide.

Vertical Temperature Profile

The vertical temperature structure reveals several key features. At 850 hPa, temperatures range from -1.9°C to 2.1°C , with above-freezing values confined to the western end of the transect where the terrain intersects this pressure level. The 700 hPa temperatures span -11.7°C to -8.4°C , and 500 hPa temperatures range from -28.5°C to -26.0°C (Table 3).

Table 3: Temperature profile along the E–W Main transect at 21z February 10, 2026.

Level	Min (°C)	Max (°C)	Range
Surface	9.3 (48.8°F)	12.1 (53.8°F)	2.8°C
850 hPa	-1.9	2.1	4.0°C
700 hPa	-11.7	-8.4	3.3°C
500 hPa	-28.5	-26.0	2.5°C

The N–S transect (Figure 9) shows a modest north-to-south temperature gradient at the surface, with the warmest conditions in the lower-elevation valleys of central Montana (near 46–47°N) and cooler temperatures at both ends of the transect—in the higher terrain of northern Wyoming (Absaroka/Bighorn ranges) and along the Canadian border.

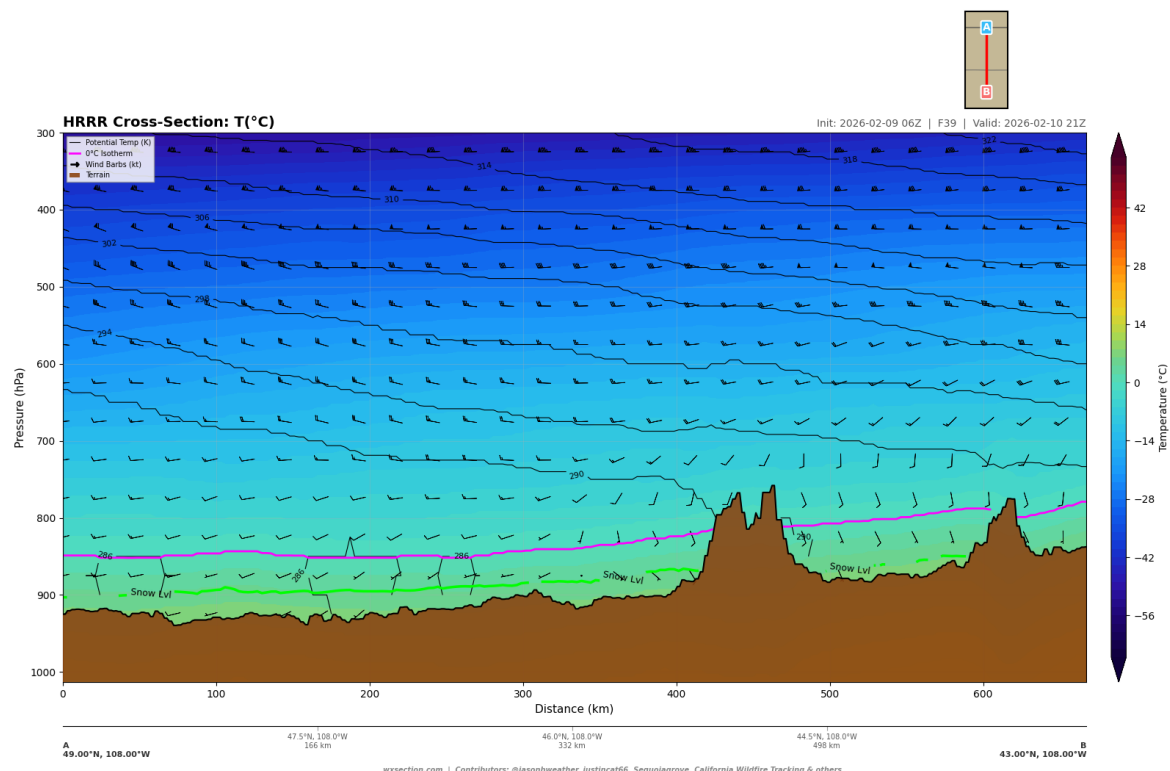


Figure 9: HRRR temperature cross-section along the N–S transect (49° N to 43° N, 108° W) at 21z February 10, 2026. The complex terrain of northern Wyoming (right side) elevates the surface into colder air, while the Montana plains (center) experience the warmest surface temperatures.

Lapse Rate and Atmospheric Stability

The lapse rate cross-sections (Figure 10) reveal near-dry-adiabatic conditions ($7\text{--}8\text{ }^{\circ}\text{C/km}$) in the lowest 1–2 km AGL across much of central Montana during peak heating, with steeper lapse rates ($>8\text{ }^{\circ}\text{C/km}$) developing in the surface layer over the plains east of the Divide. Along the terrain-following transect (Figure 11), lapse rates exceeding $8\text{ }^{\circ}\text{C/km}$ are observed near the surface over the eastern Montana grasslands, indicating the development of a superadiabatic surface layer. These steep near-surface lapse rates promote vigorous turbulent mixing and vertical transport of momentum, which can bring stronger winds from aloft down to the surface in gusts.

The 850–700 hPa layer lapse rate (computed from the temperature data: approximately $-1.9\text{ }^{\circ}\text{C}$ at 850 hPa to $-8.4\text{ }^{\circ}\text{C}$ at 700 hPa, a difference of $6.5\text{ }^{\circ}\text{C}$ over roughly 1.5 km) yields approximately $4.3\text{ }^{\circ}\text{C/km}$, which is conditionally stable. However, the surface-to-700 hPa lapse rate ($10.6\text{ }^{\circ}\text{C}$ at the surface to $-8.4\text{ }^{\circ}\text{C}$ at 700 hPa over roughly 3 km AGL) is approximately $6.3\text{ }^{\circ}\text{C/km}$, approaching moist adiabatic values and indicating a moderately unstable lower troposphere.

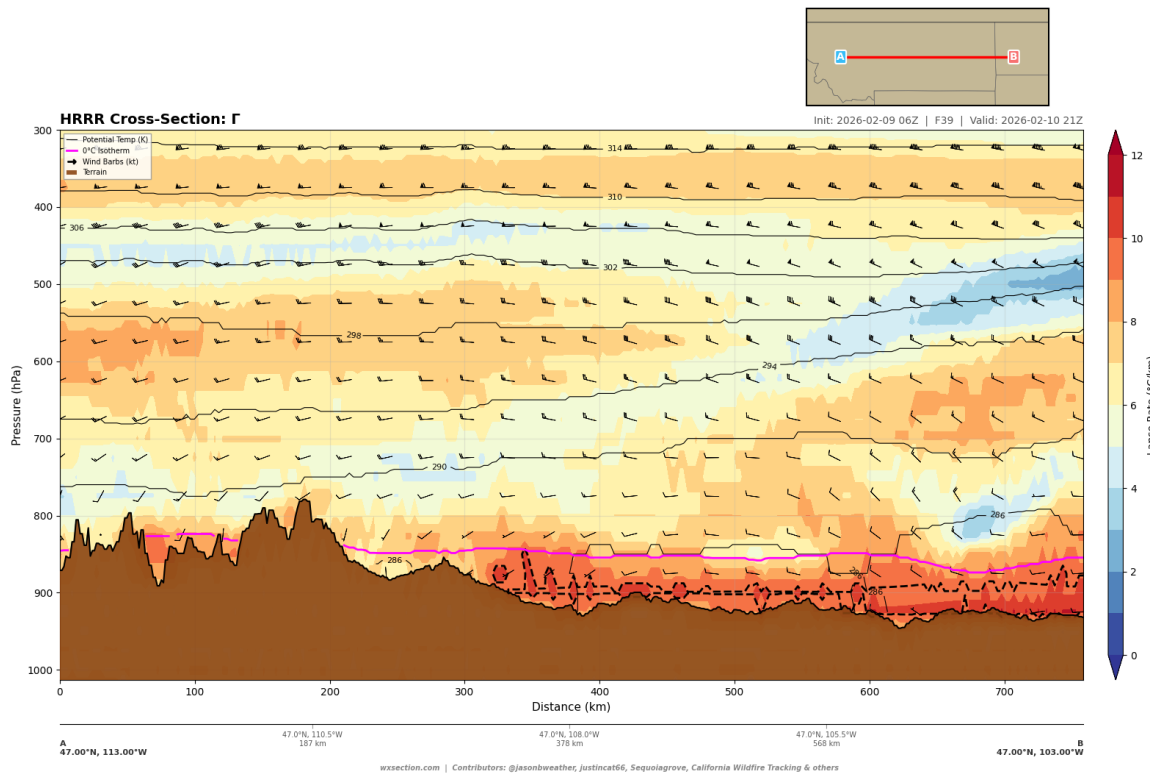


Figure 10: HRRR lapse rate cross-section along the E–W Main transect at 21z February 10, 2026. Values near or exceeding $8\text{ }^{\circ}\text{C/km}$ (warm colors, pink-red shading near the surface) indicate superadiabatic conditions promoting vigorous turbulent mixing and potential downward momentum transport.

2.4. Vertical Motion and Subsidence

Large-Scale Vertical Motion Pattern

The omega (vertical velocity) cross-sections reveal a complex pattern of vertical motion associated with mountain wave activity and synoptic-scale forcing (Figure 12). The most striking feature is the deep column

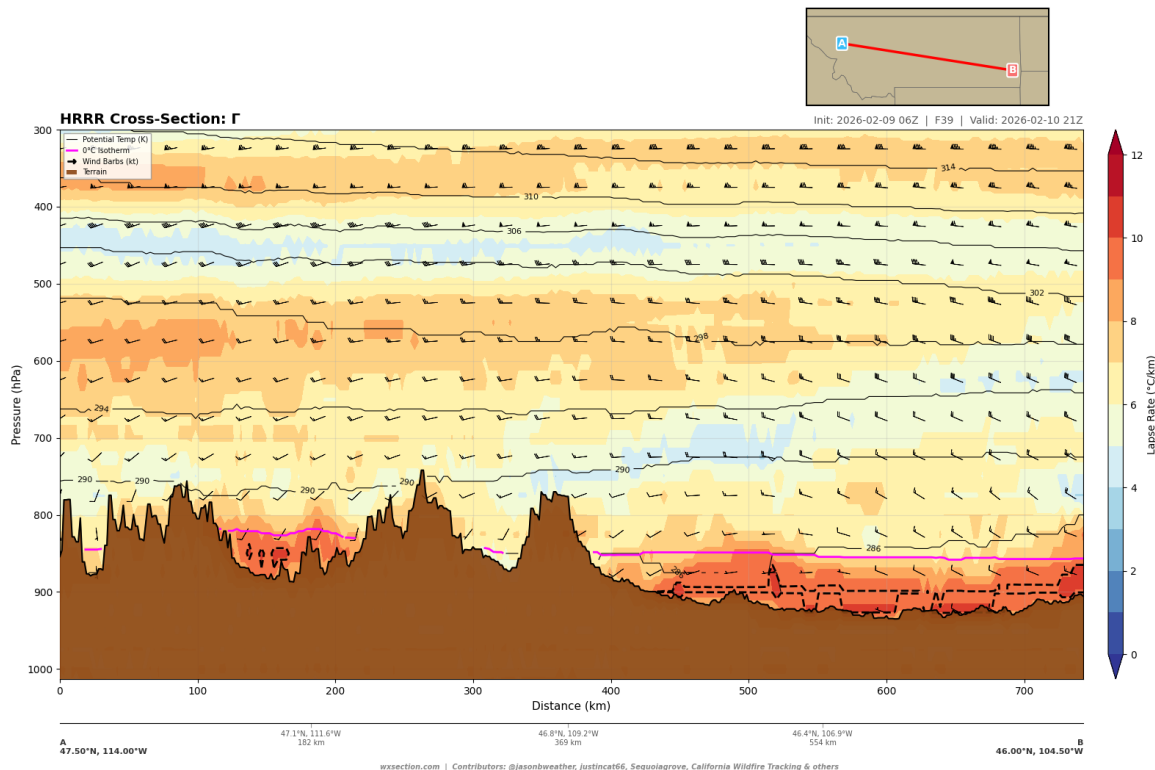


Figure 11: HRRR lapse rate cross-section along the terrain-following NW–SE transect at 21z February 10, 2026. Steep lapse rates ($> 8 ^{\circ}\text{C}/\text{km}$) are concentrated over the lower-elevation grasslands east of the Rocky Mountain front, where maximum surface heating occurs.

of alternating ascent and descent extending through the full troposphere, with the most vigorous vertical motions anchored to the terrain of the Rocky Mountain front. Strong upward motion (negative omega, blue shading) is evident over and immediately upstream of the Continental Divide, while compensating subsidence (positive omega, red shading) dominates the lee side.

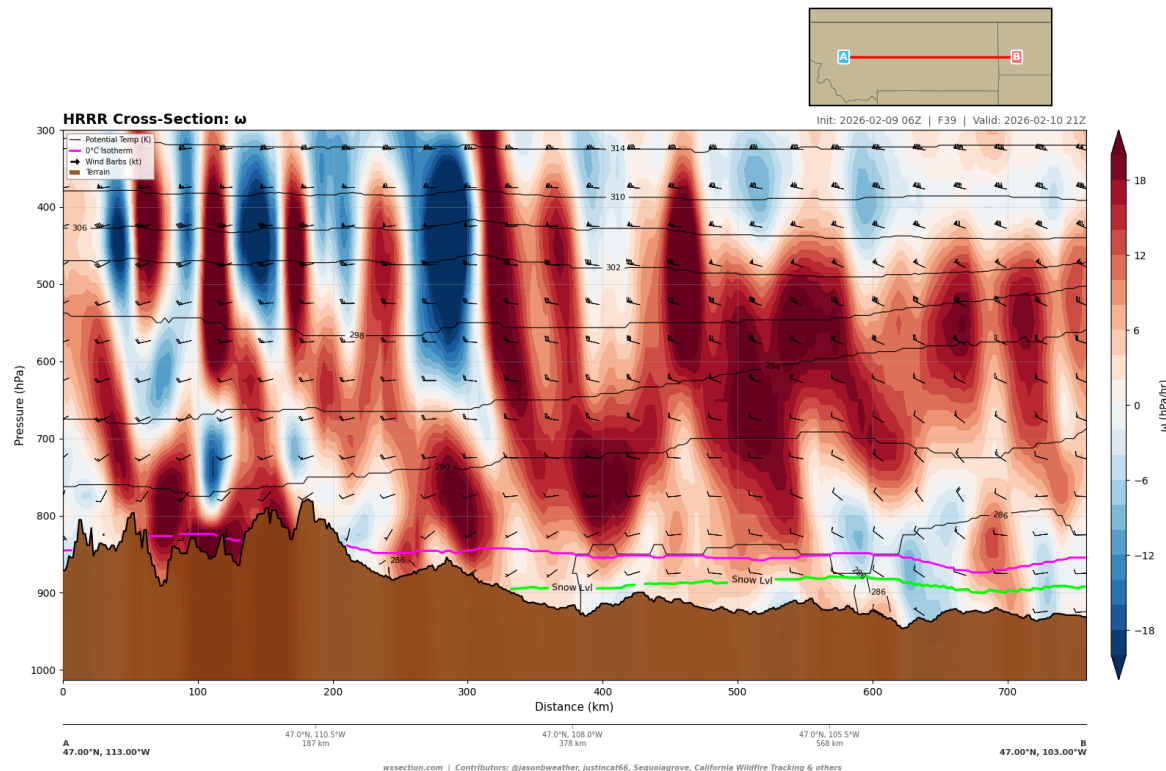


Figure 12: HRRR omega (vertical velocity) cross-section along the E–W Main transect at 21z February 10, 2026. Blue shading indicates upward motion; red shading indicates subsidence. The mountain wave pattern is prominent over the Rockies, with lee-side subsidence extending east to approximately 108°W. Convective-scale vertical velocities are visible in the boundary layer over the plains.

The terrain-following transect (Figure 13) provides the clearest view of the mountain wave structure. Deep subsidence extends from the mountaintops downstream for 200–300 km, with the sinking motion penetrating from 500 hPa all the way to the surface in some locations. This lee-side subsidence is a primary mechanism for transporting dry mid-level air toward the surface, and it explains the RH minimum observed near 112°W on the E–W Main transect. Gravity wave activity produces a series of rotor-like circulations in the 800–700 hPa layer, visible as alternating bands of ascent and descent downstream of the primary mountain barrier.

North–South Subsidence Variability

The N–S omega cross-section (Figure 14) reveals that the subsidence pattern varies substantially with latitude. The strongest subsidence at 108°W is concentrated between 46°N and 48°N—the latitude band where the terrain gradient between the Rockies and plains is steepest. South of 46°N, the higher and more continuous terrain of Wyoming produces a different wave response, with stronger low-level upward motion over the Absaroka and Wind River ranges but less organized subsidence over the basins. North of 48°N, the terrain becomes less abrupt and the wave response weakens, producing weaker subsidence.

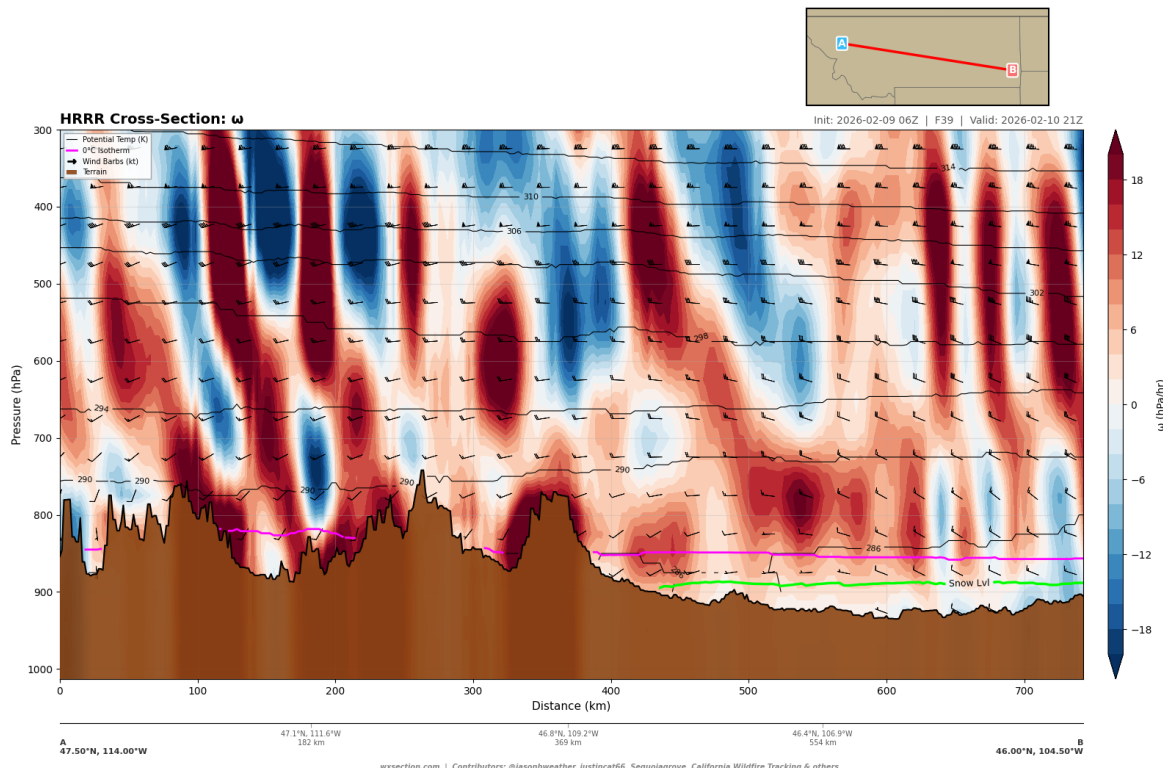


Figure 13: HRRR omega cross-section along the terrain-following NW–SE transect at 21z February 10, 2026. The mountain wave response to the westerly flow over the Rockies produces deep lee-side subsidence extending well into the Montana plains. Note the vertically propagating wave pattern with alternating ascent/descent cells.

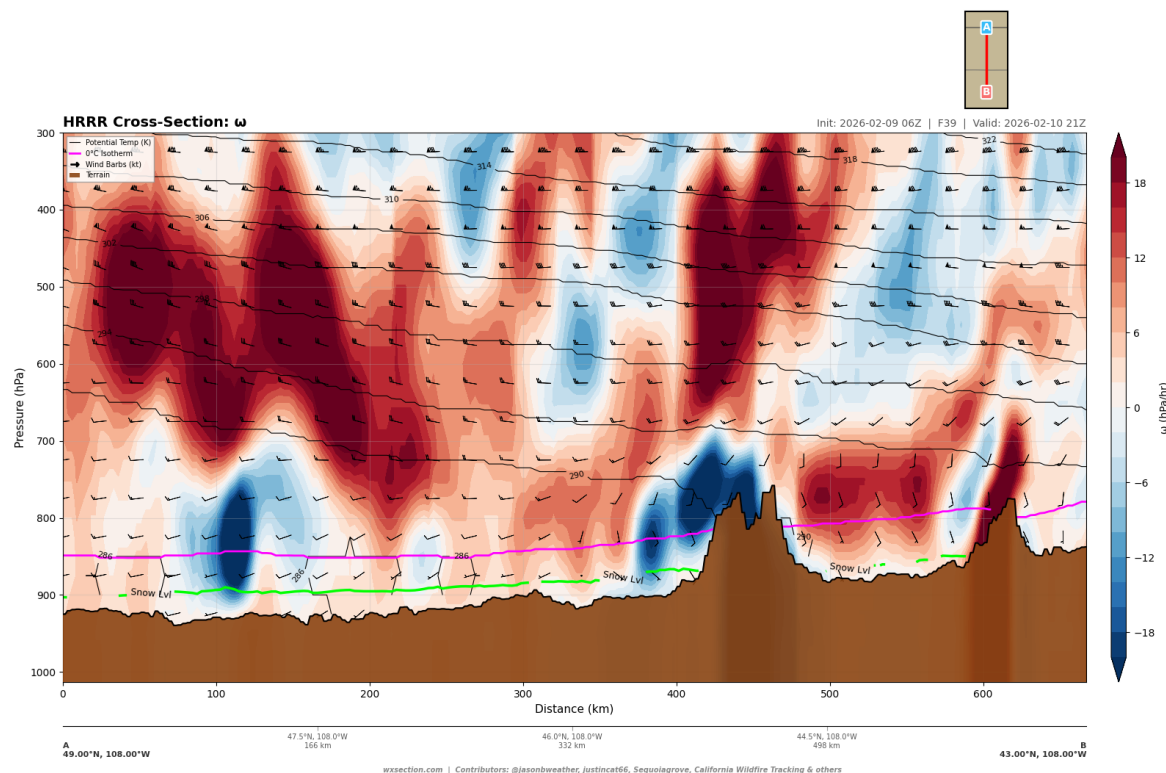


Figure 14: HRRR omega cross-section along the N–S transect (108°W) at 21z February 10, 2026. Vigorous ascent and descent are anchored to the complex terrain, with the strongest subsidence centered on the central Montana plains ($46\text{--}48^{\circ}\text{N}$).

The interplay between synoptic-scale subsidence (associated with the upper-level ridge/jet pattern) and terrain-forced subsidence (mountain waves) creates a reinforcing mechanism: synoptic descent deepens the dry layer aloft while terrain-forced descent transports this dry air toward the surface on the lee side. This coupling is a characteristic feature of Northern Rockies fire weather episodes, though in this case the surface moisture content remains sufficient to prevent extreme fire danger conditions at the surface.

2.5. Vapor Pressure Deficit and Fire Weather Composite

VPD Analysis

Vapor pressure deficit (VPD) integrates the combined effects of temperature and humidity into a single metric of atmospheric drying potential that is directly relevant to fuel moisture and fire behavior. Along the E-W Main transect at peak heating (Figure 15), surface VPD values range from 4.03 hPa to 8.35 hPa with a mean of 5.83 hPa. The maximum surface VPD of 8.35 hPa occurs at 112°W, coinciding with the lee-side location of warmest temperatures and lowest relative humidity.

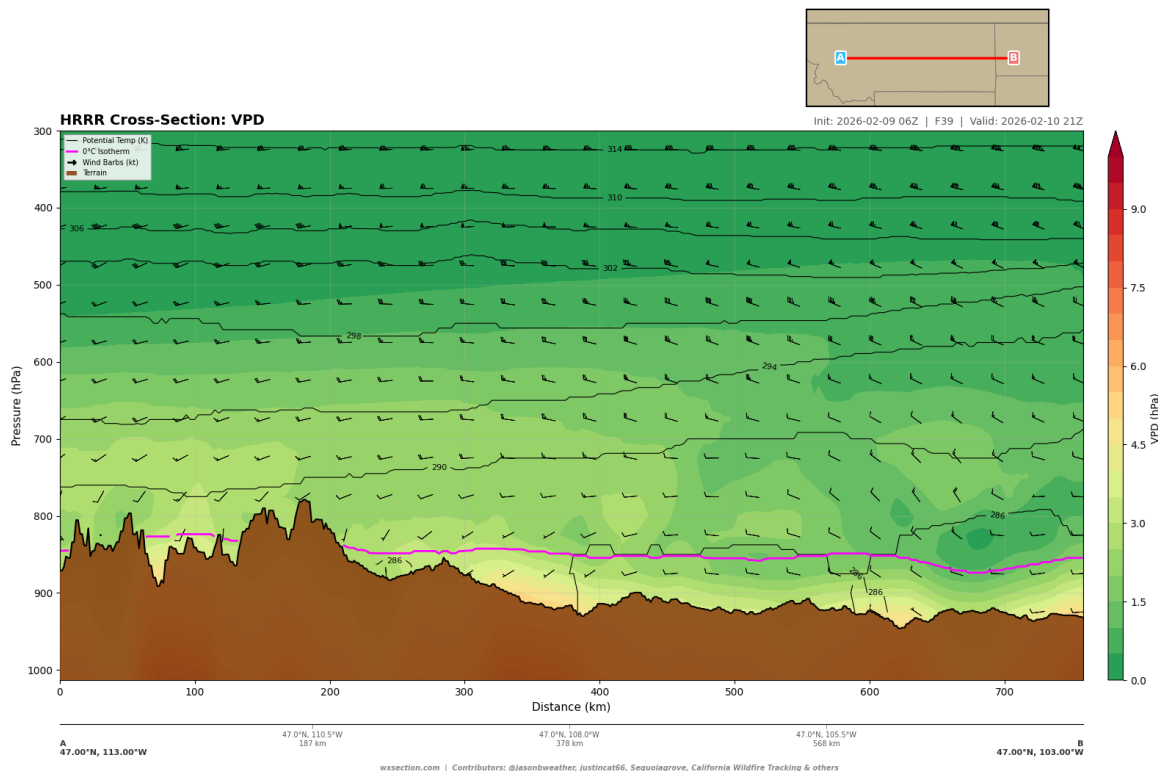


Figure 15: HRRR vapor pressure deficit cross-section along the E-W Main transect at 21z February 10, 2026. VPD values increase with height as temperature and humidity combine to produce a strong moisture gradient. The green shading indicates lower VPD (moister); yellows and browns indicate higher VPD (drier).

These surface VPD values are below the 20 hPa extreme threshold and the 15 hPa high-risk threshold—no grid points along the transect exceed either benchmark. However, the 850 hPa VPD reaches 4.16 hPa, and VPD values increase substantially in the mid-troposphere where the dry layer resides. The maximum low-level VPD (surface to 700 hPa) of 8.35 hPa, while elevated, indicates that the atmospheric demand for moisture is moderate. For the February time period, when fine fuels may have accumulated winter moisture, these VPD values suggest a limited but non-negligible potential for fire spread in receptive fuels, particularly

in south-facing exposures that have dried most rapidly.

Fire Weather Composite

The fire weather composite product integrates wind speed, RH, VPD, temperature, and lapse rate into a single visualization that highlights areas of coincident fire-critical conditions (Figure 16). At 21z on the E-W Main transect, the composite shows a predominantly warm-colored (elevated risk) pattern in the lower and middle troposphere, with the most intense fire weather signal in the 700–500 hPa layer where very low RH combines with stronger winds and steep lapse rates. The cross-hatched pattern in the composite indicates where multiple parameters simultaneously approach or exceed fire weather criteria.

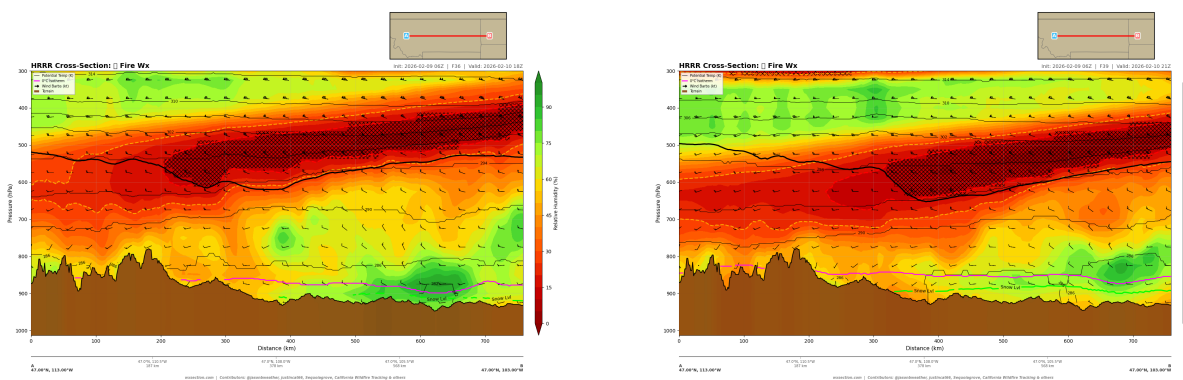


Figure 16: HRRR fire weather composite cross-sections along the E-W Main transect at 18z (left, FHR 36) and 21z (right, FHR 39). The composite integrates RH, wind, temperature, VPD, and lapse rate. Cross-hatching indicates areas where multiple parameters approach critical fire weather thresholds simultaneously. Note the intensification of the fire weather signal from 18z to 21z as boundary layer mixing deepens.

At the surface level, the fire weather composite shows a gradient from moderate risk in the western portion (lee of the Divide) to lower risk in the eastern portion where higher RH and lighter winds prevail. The critical observation is that while no single parameter reaches its critical threshold at the surface, the combination of moderate warmth (10–12°C), reduced RH (41–55%), steep lapse rates ($>7^{\circ}\text{C}/\text{km}$), and a deep reservoir of extremely dry air aloft (RH 6–13% at 600–500 hPa) creates a preconditioned environment. A modest increase in wind speed or additional surface heating could rapidly push conditions toward critical fire weather thresholds.

Multi-Transect Fire Weather Assessment

Comparison across all four transects at FHR 39 reveals spatial coherence in the fire weather pattern:

- **E-W Main (47°N):** Moderate surface fire weather risk, primarily driven by lee-side drying west of 108°W. Maximum risk is in the immediate lee of the Continental Divide near 112°W.
- **E-W Southern (45°N):** Similar pattern but with higher terrain intercepting the dry layer at lower altitudes. The fire weather composite (Figure 17) shows a slightly reduced surface risk compared to the main transect due to higher terrain-induced RH in the complex orography of southern Montana. However, valley floors between mountain ranges could experience locally enhanced drying.
- **N-S (108°W):** The fire weather signal is strongest in the 46–48°N latitude band (Figure 17), weakening both northward toward the Canadian border and southward into the Wyoming mountains. This confirms

that central Montana between the Rocky Mountain front and the Missouri River breaks is the primary area of concern.

- **Terrain (NW–SE):** The terrain transect (Figure 17) shows the fire weather risk increasing downstream along the Rocky Mountain front, with the most intense signal in the 200–500 km range east of the mountain crest where lee-side effects maximize.

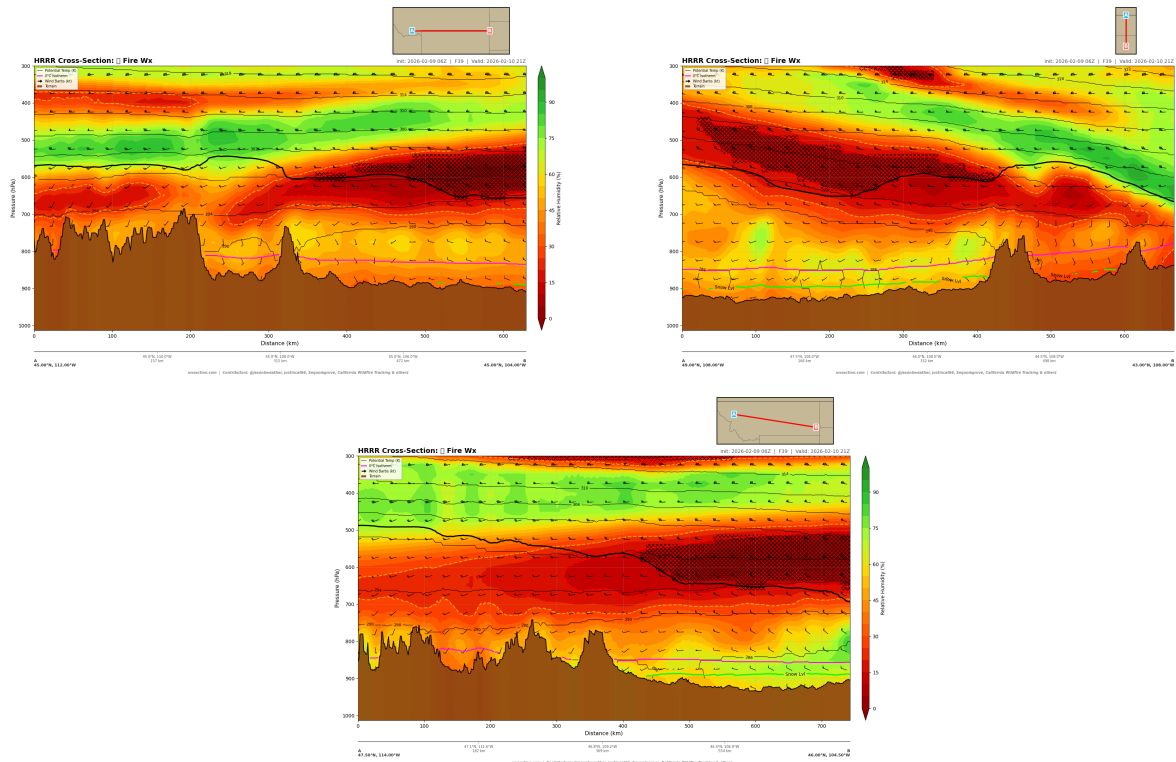


Figure 17: Fire weather composite cross-sections at 21z February 10 for the E–W Southern transect (top left), N–S transect (top right), and terrain-following transect (bottom). All three transects confirm the elevated mid-level fire weather signal with the surface risk concentrated in the lee of the Rocky Mountain front.

2.6. Summary and Fire Weather Assessment

The HRRR cross-section analysis for February 10, 2026 reveals an environment over the Northern Rockies that is *conditionally elevated* for fire weather but does not meet criteria for a classic critical fire weather event. The key findings are:

1. **Winds:** Surface winds remain well below critical thresholds (max 8.8 kt vs. 25 kt critical), though 700 hPa winds of 20.4 kt indicate potential for downward momentum transport during deep mixing events. The upper-level jet (100+ kt at 300 hPa) is positioned over eastern Montana but its direct surface impact is minimal.
2. **Humidity:** Surface RH remains above 40% across the entire transect—significantly above the 15% critical threshold. However, a deep reservoir of extremely dry air exists at 650–500 hPa (minimum RH 6.5%), and 58% of mid-level grid points have RH below 20%. This dry air mass could be entrained to the surface if mixing depth exceeds forecast expectations.

3. **Temperature:** Surface temperatures of 9–12°C (49–54°F) are above freezing and sufficient to support fire activity in dry fuels. Lee-side warming near the Continental Divide produces the warmest and driest surface conditions.
4. **VPD:** Surface VPD values of 4–8 hPa are moderate and well below the 20 hPa extreme threshold, indicating limited atmospheric drying demand on fuels.
5. **Vertical Motion:** Mountain wave-induced subsidence on the lee side of the Rockies transports dry mid-level air toward the surface, concentrated between 46–48°N. This terrain-forced subsidence reinforces the synoptic-scale descent.
6. **Lapse Rates:** Near-dry-adiabatic to superadiabatic lapse rates ($>8^{\circ}\text{C}/\text{km}$) develop in the surface layer during peak heating, promoting vigorous mixing that could bring drier and windier conditions from aloft to the surface.

The primary fire weather concern for February 10 is the juxtaposition of a deep, extremely dry layer aloft (especially 650–500 hPa) with steep lapse rates and mountain wave subsidence that could drive surface drying beyond what the standard model surface fields indicate. While the HRRR surface forecast does not show RH values approaching critical levels, forecasters should be aware that rapid deepening of the mixed layer—especially in the lee of the Continental Divide near 112°W—could produce brief periods of lower RH and gustier winds at the surface than the deterministic forecast suggests. This is most likely between 19z and 23z (12 PM to 4 PM MST) when surface heating is maximal.

The overall fire weather risk for the Northern Rockies on February 10, 2026 is assessed as **ELEVATED but SUB-CRITICAL**, with localized areas of enhanced concern in the immediate lee of the Rocky Mountain front across central Montana (approximately 112°W to 109°W, 46°N to 48°N). No Red Flag Warning criteria are met based on the HRRR deterministic forecast, but a Fire Weather Watch may be warranted for the lee-side areas if observations during the morning transition show lower humidity or stronger winds than forecast.

3. Four Corners Critical Area Analysis (Arizona–New Mexico–Colorado)

The Four Corners region of the American Southwest presents a uniquely challenging fire weather environment for 10 February 2026. Situated at the confluence of the Colorado Plateau, the Mogollon Rim, and the upper Rio Grande Valley, the complex terrain modulates wind flow, moisture transport, and vertical mixing in ways that amplify fire danger well beyond what synoptic-scale analysis alone would suggest. This section presents a detailed cross-section diagnosis of the HRRR 06z 09 February 2026 cycle across four carefully designed transects that sample the critical terrain features of this region.

Transect definitions:

- **E–W Main** (35.0°N, 113.0°W → 35.0°N, 105.0°W): 729 km east–west transect across central Arizona into central New Mexico, sampling the Mogollon Rim, the Tonto Basin, the White Mountains, and the Rio Grande Valley.
- **E–W Northern** (37.0°N, 112.0°W → 37.0°N, 105.0°W): 637 km transect across southern Utah/Colorado Plateau into the San Juan Mountains and the upper San Luis Valley.
- **N–S** (38.0°N, 109.0°W → 32.0°N, 109.0°W): 667 km meridional transect through the Four Corners point, from the La Sal Mountains of Utah south through the Arizona–New Mexico border country into the Chihuahuan Desert.

- **Mogollon Rim** (35.5°N , $112.5^{\circ}\text{W} \rightarrow 34.0^{\circ}\text{N}$, 108.0°W): 430 km northwest-to-southeast transect diagonally across the Mogollon Rim escarpment, capturing the dramatic 600–900 m terrain drop and its effects on downslope flow.

Seasonal context. Winter fire season in the Southwest is an increasingly recognized hazard. Unlike the traditional June pre-monsoon fire season driven by lightning ignitions in cured fine fuels, the February fire window is dominated by drought-stressed dormant grasslands and failed early green-up. La Niña-pattern winters suppress Pacific moisture transport into Arizona and New Mexico, leaving fine fuel moisture content anomalously low. The combination of dormant *C₄* grasses, sparse winter precipitation, and strong diurnal heating under clear skies creates a fire environment where wind-driven runs on grass and light brush fuels can produce rapid rates of spread despite modest temperatures.

3.1. Wind Field and Terrain Channeling

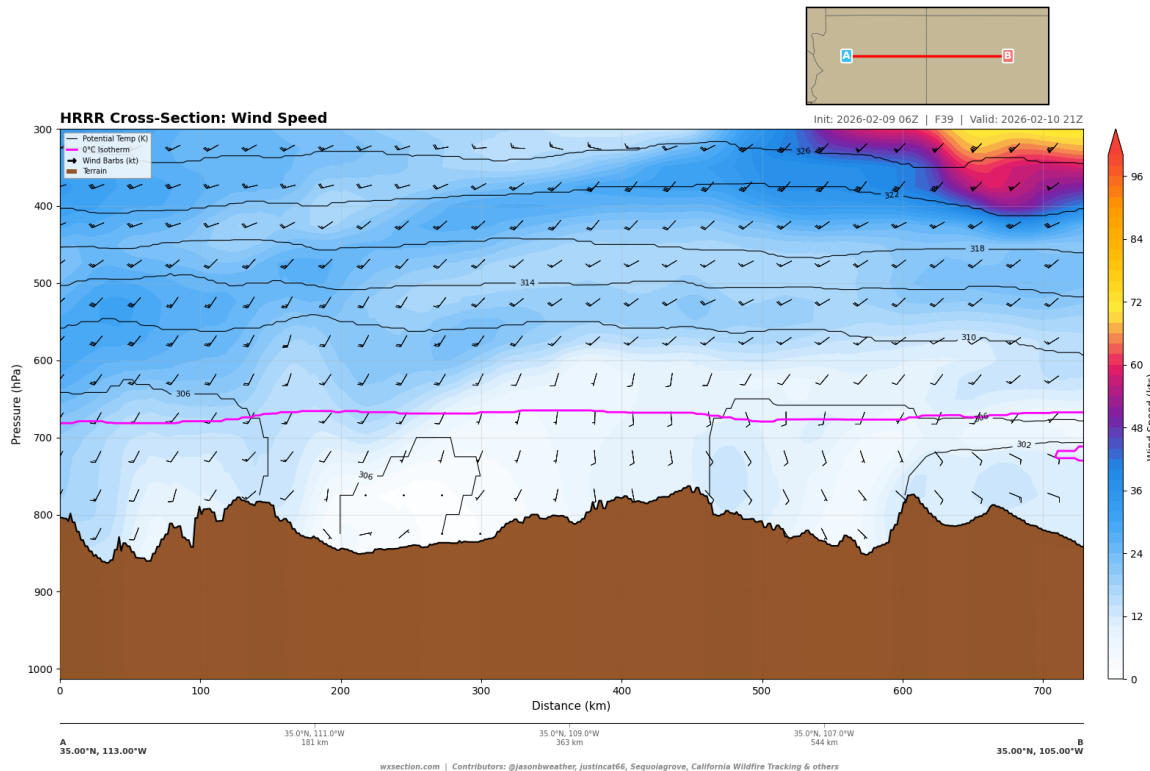


Figure 18: Wind speed cross-section along the E–W Main transect (35°N , $113^{\circ}\text{W} \rightarrow 105^{\circ}\text{W}$) valid 21z 10 Feb 2026 (FHR 39, 2 PM MST). Terrain is shaded brown; pink contour marks the freezing level. Wind barbs show flow direction and speed.

The wind analysis at peak heating (21z, 2 PM MST; Figure 18) reveals a moderate low-level wind regime across the E–W Main transect. Near-surface winds along the transect range from 0.6 to 17.3 kt, with a mean of 8.4 kt. The strongest near-surface winds (up to 17 kt) are found at the western end of the transect near the 800 hPa level, corresponding to the elevated terrain of the Hualapai Mountains and the transition from the Mojave Desert into the Colorado Plateau. The maximum wind speed below 700 hPa reaches 19.6 kt at the western terminus.

At the 700 hPa level—which lies near crest height for much of the Mogollon Rim—winds are stronger, ranging from 4.7 to 19.6 kt with a mean of 9.7 kt. The 750 hPa level shows similar values (2.3–18.3 kt, mean 9.3 kt). These speeds, while not individually reaching the 25 kt sustained threshold for Red Flag conditions, represent the ambient flow that can be locally amplified by terrain channeling.

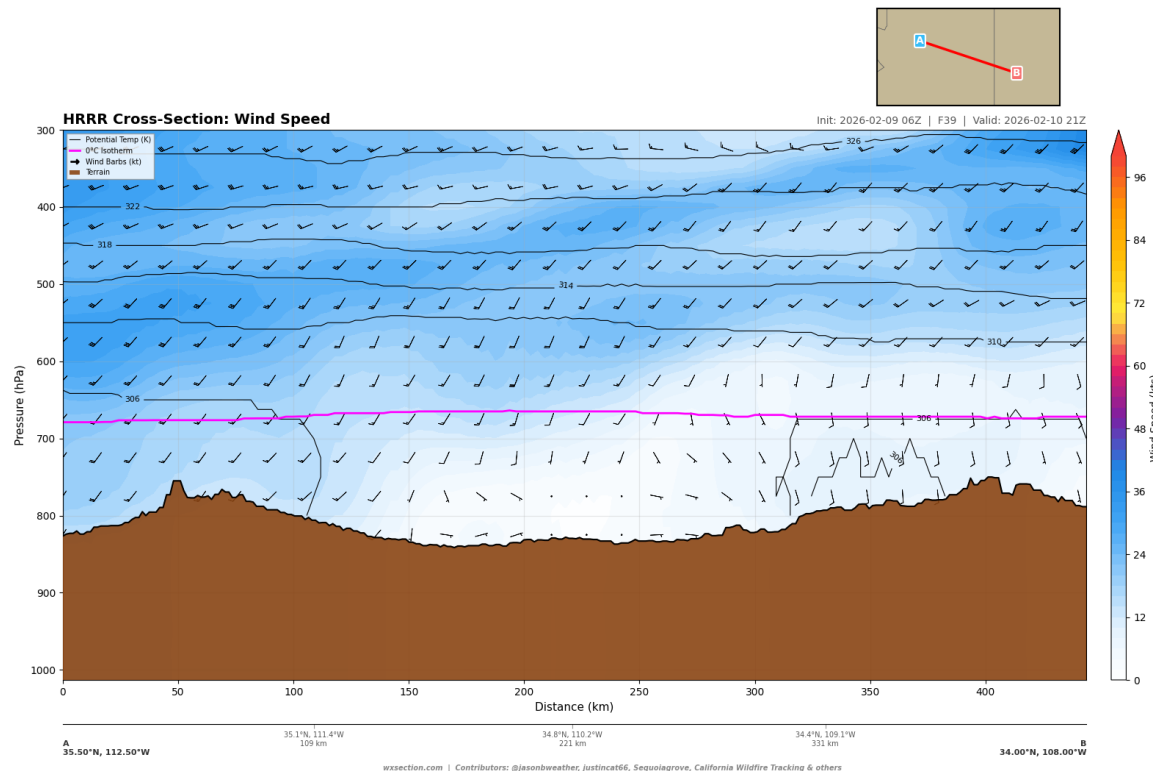


Figure 19: Wind speed cross-section along the Mogollon Rim transect ($35.5^{\circ}\text{N}, 112.5^{\circ}\text{W} \rightarrow 34.0^{\circ}\text{N}, 108.0^{\circ}\text{W}$) valid 21z 10 Feb (FHR 39). Note the terrain profile capturing the Rim escarpment.

The Mogollon Rim transect (Figure 19) reveals the terrain influence on the wind field. The Rim itself, rising to approximately 700 hPa equivalent pressure altitude, acts as a barrier to low-level flow. Winds accelerate along the Rim escarpment, where the terrain drops sharply from the Colorado Plateau (2300 m) to the Tonto Basin (600 m). This downslope acceleration zone is a well-known fire weather hazard for central Arizona communities like Payson, Pine, and Strawberry.

The N–S transect along 109°W (Figure 20) shows the meridional wind structure through the heart of the Four Corners region. Winds are generally light to moderate through the boundary layer, with the strongest low-level flow concentrated above the elevated terrain of the San Juan Basin and the Chuska Mountains. The complex terrain fragmentation of the flow field is evident, with wind speed varying significantly across short horizontal distances as the flow negotiates canyon systems and mesa edges.

The temporal evolution from overnight (Figure 21) through late afternoon (Figure 22) reveals the diurnal wind cycle. Overnight winds at 06z are relatively strong aloft with a modest low-level jet feature near the 700 hPa level, while surface winds are suppressed under the nocturnal inversion. By 21z (peak heating), turbulent mixing has coupled the boundary layer to the free atmosphere, transporting mid-level momentum to the surface. The wind field remains active through 00z (5 PM MST), indicating that the fire danger window extends through late afternoon.

Despite the moderate wind speeds, the 3% of near-surface points exceeding 15 kt—concentrated along

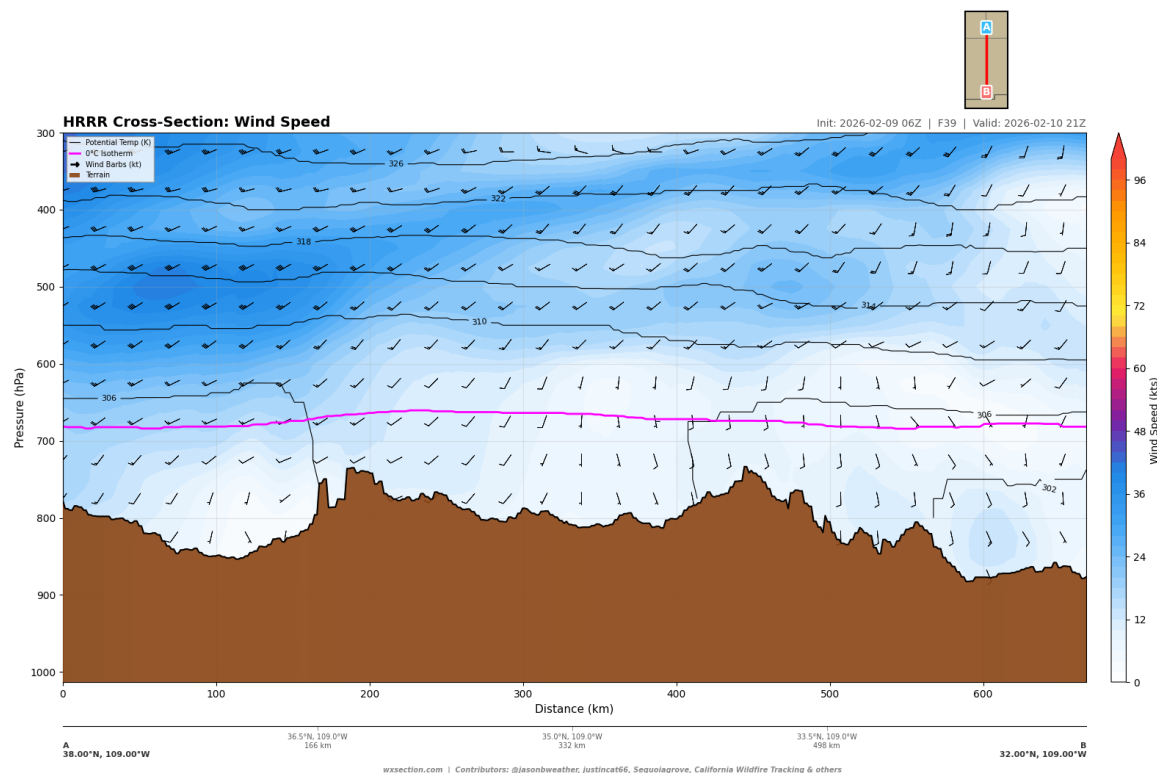


Figure 20: Wind speed cross-section along the N–S transect ($38^{\circ}\text{N} \rightarrow 32^{\circ}\text{N}$ at 109°W) valid 21z 10 Feb (FHR 39). This meridional transect crosses the La Sal Mountains, the Four Corners area, and extends south into the Chihuahuan borderlands.

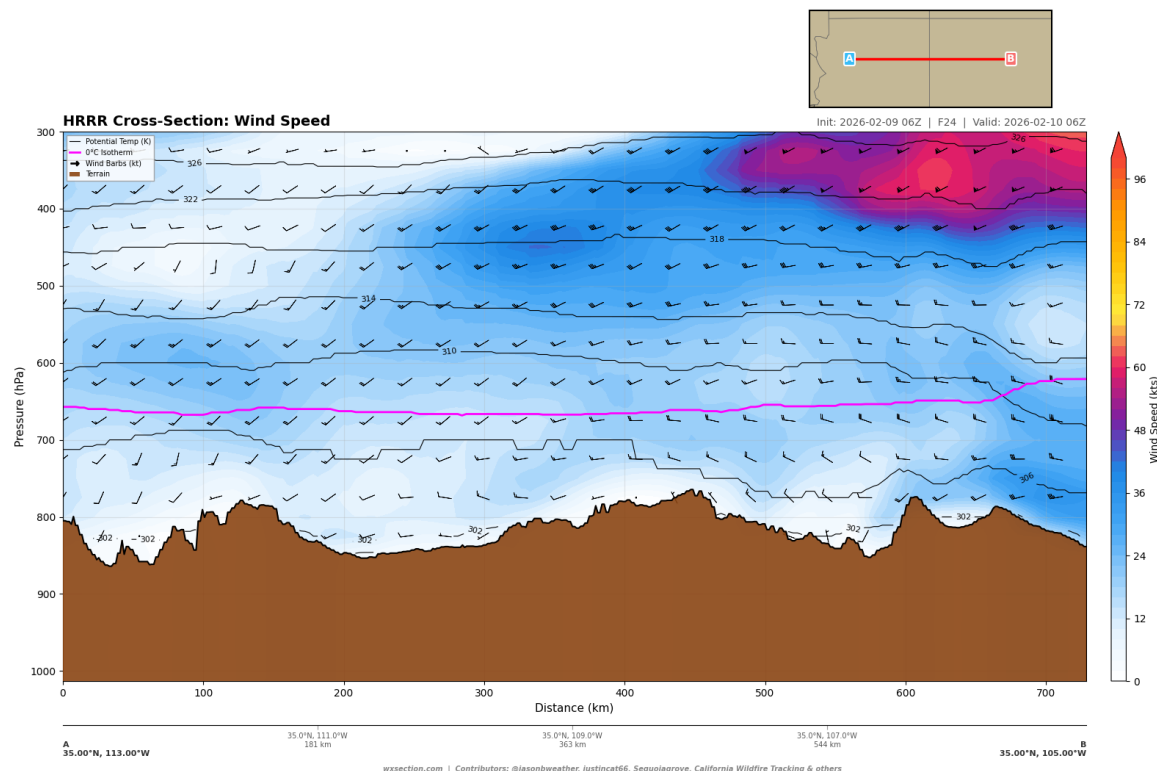


Figure 21: Wind speed temporal reference: E–W Main transect at 06z 10 Feb (FHR 24, overnight). Note the quiescent overnight boundary layer with light surface winds and a developing low-level jet.

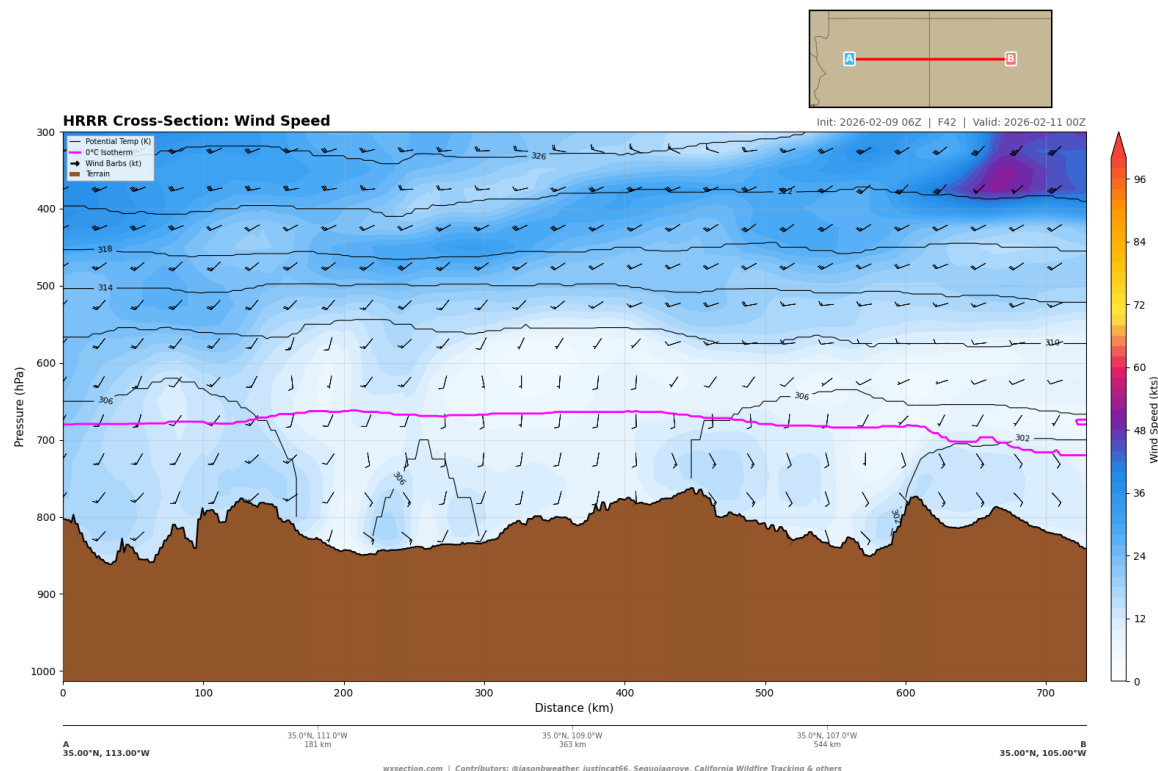


Figure 22: Wind speed at 00z 11 Feb (FHR 42, late afternoon 5 PM MST). Winds remain elevated through the end of the afternoon heating cycle.

elevated terrain crests and ridges—represent the locations most vulnerable to wind-driven fire spread. The absence of sustained winds above 25 kt suggests that this event does not meet the traditional Red Flag wind threshold; however, when combined with the extremely low humidity discussed in the following subsection, even these moderate winds are operationally significant.

3.2. Humidity Analysis

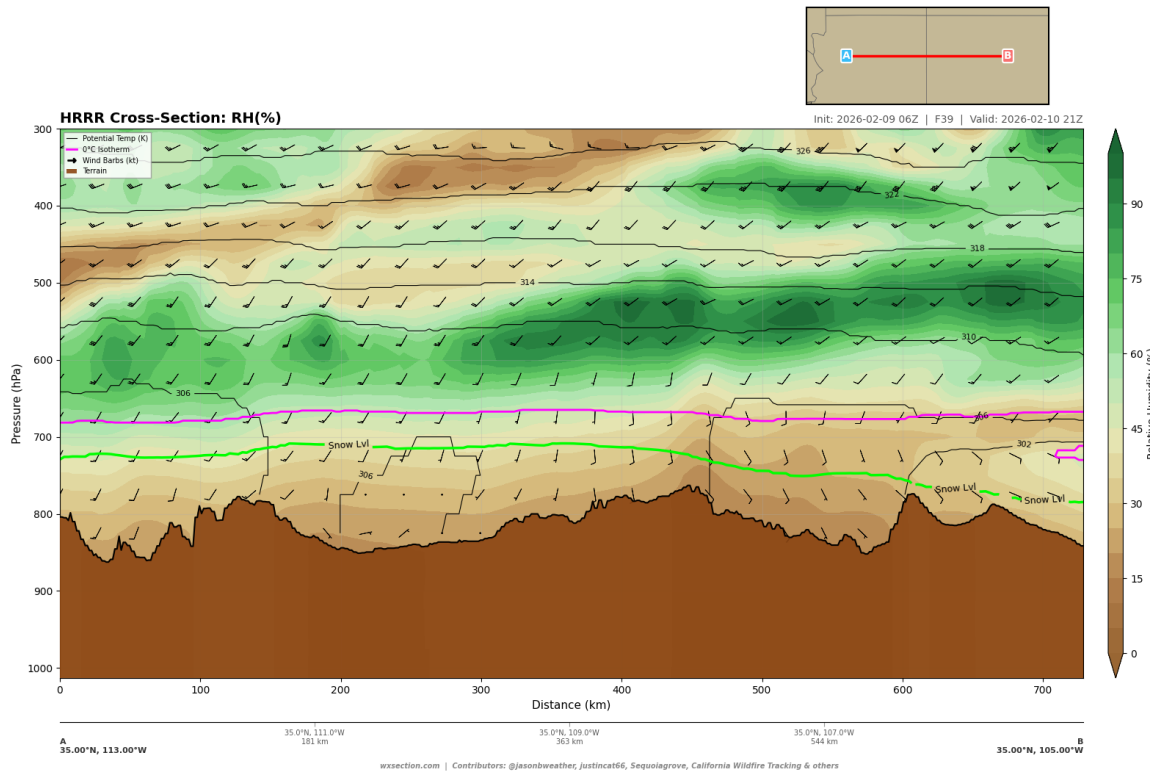


Figure 23: Relative humidity (%) along the E–W Main transect valid 21z 10 Feb (FHR 39). Green contour marks the freezing level; brown shading is terrain. The entire low-level atmosphere is extremely dry.

The humidity analysis is the most concerning element of this forecast. At 21z (2 PM MST), the E–W Main transect (Figure 23) reveals a profoundly dry atmosphere across the entire 729 km cross-section. Near-surface relative humidity ranges from 15.3% to 32.7%, with a transect mean of just 23.0%. The driest air at the surface is found in eastern New Mexico near 107.9°W (the eastern flanks of the Manzano and Sandia Mountains), where RH approaches the critical 15% threshold at 15.3%.

The 850 hPa level shows RH values of 15.4–29.5% (mean 21.9%), indicating that the dryness extends well into the elevated boundary layer rather than being confined to a shallow surface layer. At 700 hPa, RH recovers somewhat to 25.3–54.0% (mean 38.1%), but even at this level the atmosphere remains far drier than climatological norms.

The E–W Northern transect at 37°N (Figure 24) shows a similar pattern across southern Colorado, though with slightly higher RH values driven by higher terrain and cooler temperatures. Even here, the boundary layer remains critically dry, with RH values in the 20–35% range across the San Juan Basin and the lower elevations of the Colorado Plateau. The San Juan Mountains provide a modest moisture source through orographic uplift, but this effect is confined to above 600 hPa and does not extend downward into the fire-critical boundary layer.

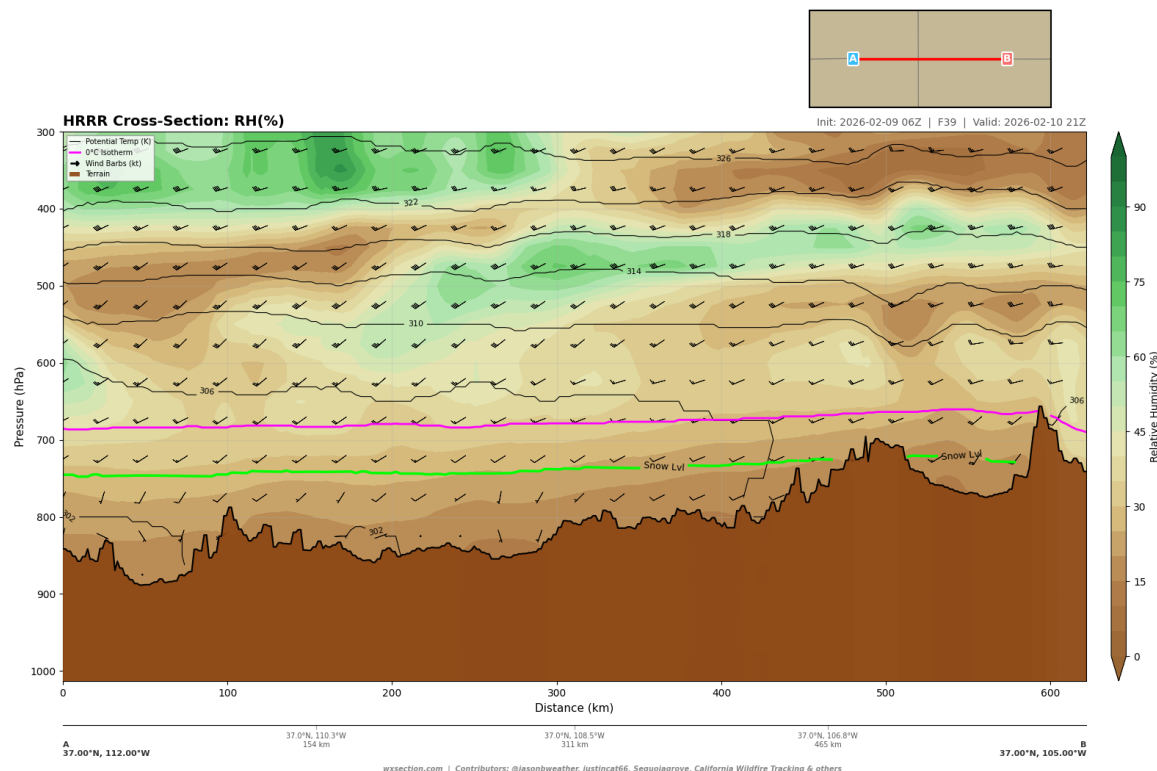


Figure 24: Relative humidity along the E–W Northern transect ($37^{\circ}\text{N}, 112^{\circ}\text{W} \rightarrow 37.00^{\circ}\text{N}, 105.00^{\circ}\text{W}$) valid 21z 10 Feb (FHR 39). Southern Colorado and the San Juan Mountains show slightly higher RH values but remain critically dry.

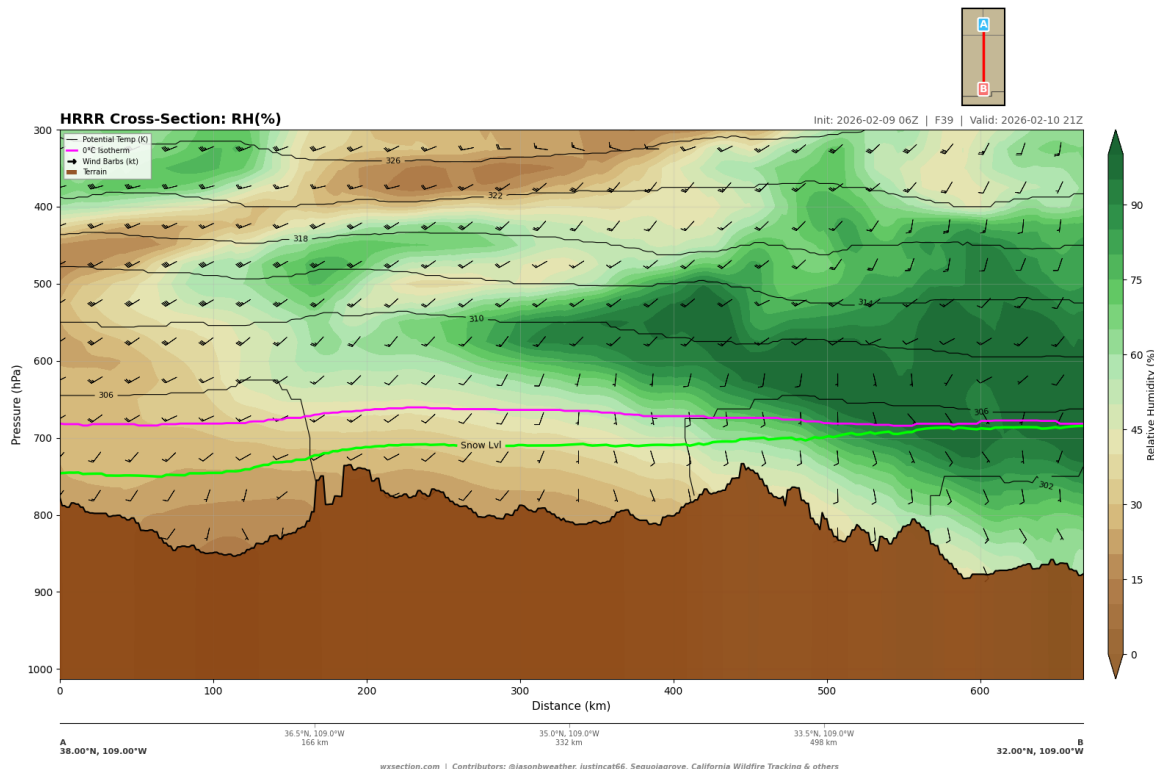


Figure 25: Relative humidity along the N–S transect ($38^{\circ}\text{N} \rightarrow 32^{\circ}\text{N}$ at 109°W) valid 21z 10 Feb (FHR 39). The low-level dry layer is deepest over the southern Chihuahuan terrain.

The N–S transect (Figure 25) reveals the meridional gradient in moisture. Moving southward from the La Sal Mountains of Utah through the Four Corners into southern New Mexico, the boundary layer becomes progressively drier. The deepest dry layer—with RH values below 25% extending from the surface through 700 hPa—is found over the lower-elevation terrain south of 34°N. This deep dry layer is a hallmark of the subsidence-driven aridification discussed in Section 3.4.

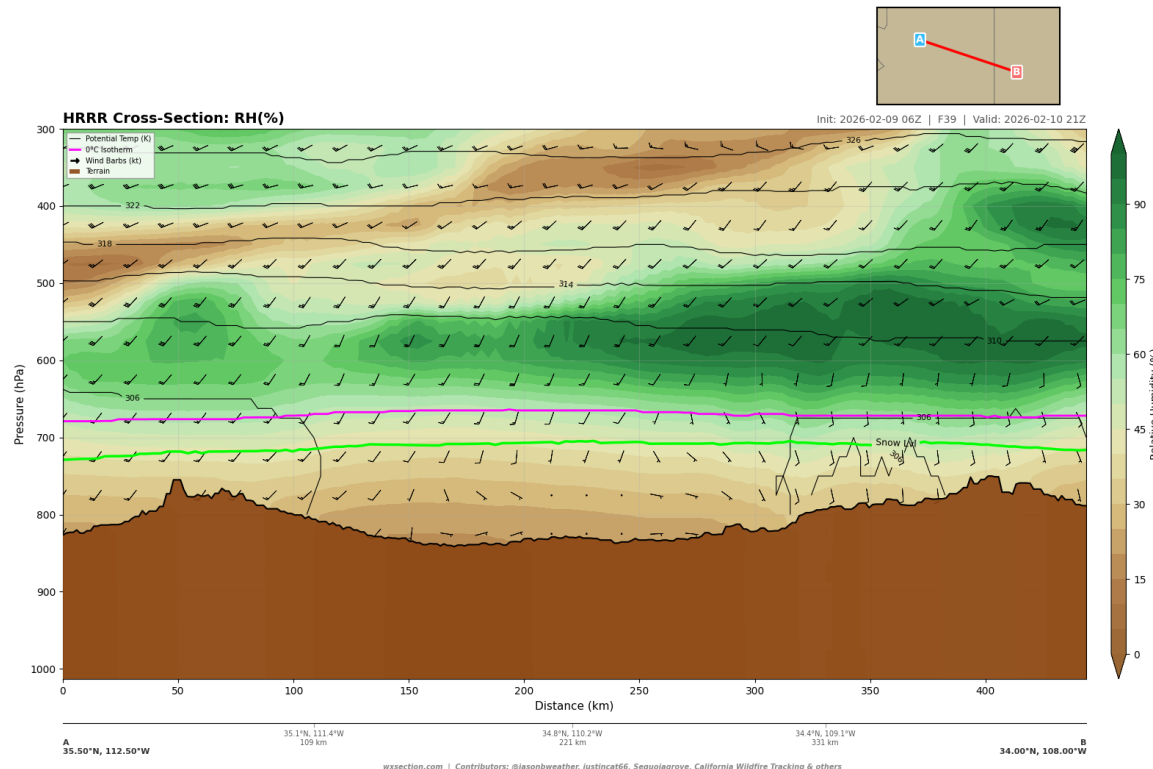


Figure 26: Relative humidity along the Mogollon Rim transect valid 21z 10 Feb (FHR 39). The sharp terrain drop of the Rim creates a distinctive moisture gradient.

The Mogollon Rim transect (Figure 26) highlights a terrain-driven moisture contrast. Above the Rim, at approximately 700 hPa, a moister layer (30–50% RH) is maintained by the higher terrain intercepting ambient moisture. Below the Rim, the Tonto Basin and lower Sonoran Desert fringe show dramatically drier conditions. This moisture gradient enhances downslope drying when winds transport Rim-top air into the lower terrain.

The diurnal humidity cycle (Figures 27 and 28) shows a striking feature: even during the overnight recovery period at 06z, near-surface RH barely recovers above 40%. In a well-watered environment, nocturnal cooling would produce recovery to 70–90%. The absence of meaningful overnight recovery indicates that the soil moisture reservoir is severely depleted and that dry air advection from the subsiding free atmosphere overwhelms radiative cooling. By late afternoon (00z), RH has returned to the 15–25% range, indicating that the fire danger window is both deep and prolonged.

Key finding: While the 15% RH threshold is only barely reached at the driest surface point (15.3% at 107.9°W), the *depth* and *spatial extent* of the dry layer—with mean near-surface RH of 23% and 850 hPa mean RH of 22%—is the more significant metric. The entire boundary layer, from the surface through at least the 700 hPa level, is critically dry. This deep dry layer means that any fire producing a convection column will entrain dry air at all levels, promoting extreme spotting distances and drying of fuels well ahead of the

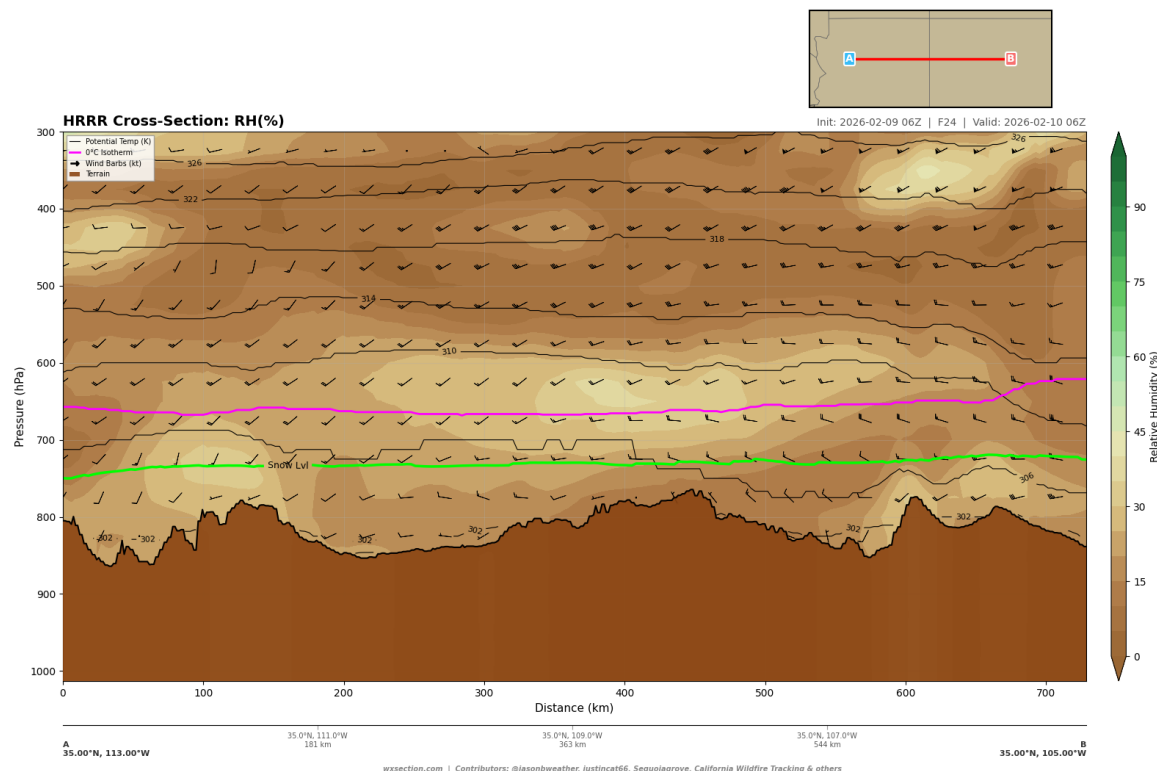


Figure 27: Relative humidity temporal evolution: E–W Main transect at 06z 10 Feb (FHR 24, overnight). The nocturnal inversion produces modest moisture recovery, but RH remains below 40% even during the overnight recovery period.

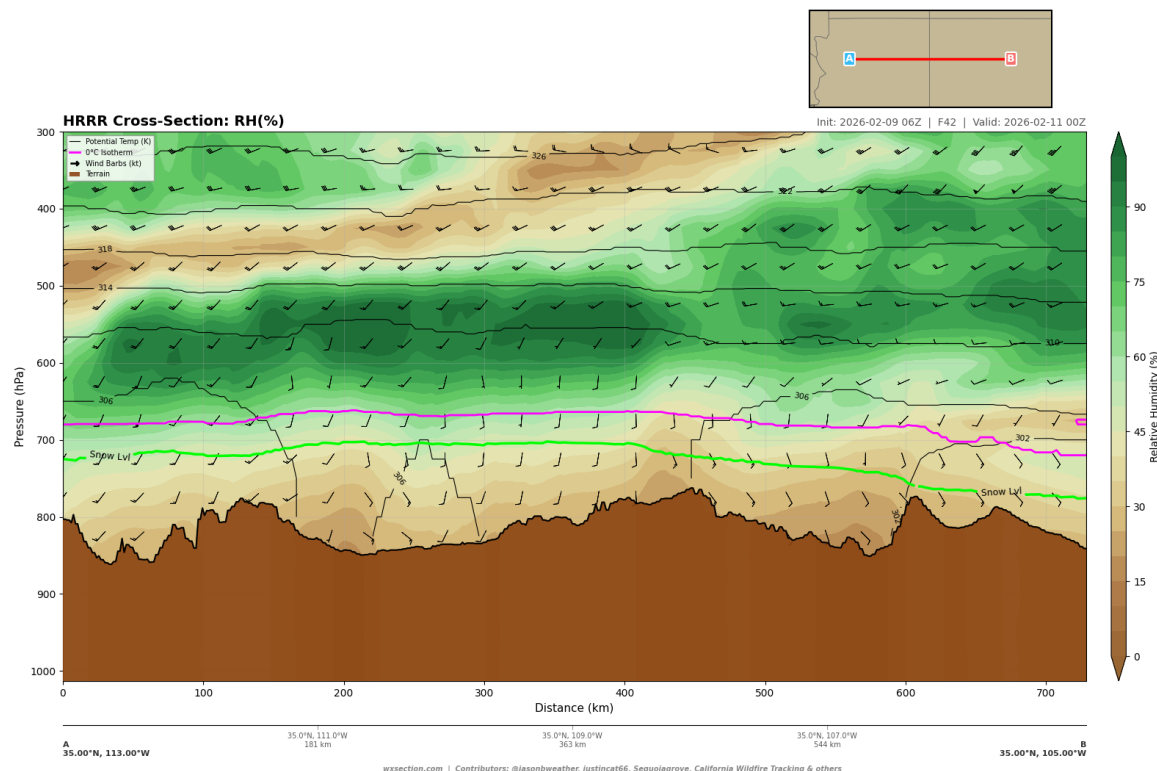


Figure 28: Relative humidity at 00z 11 Feb (FHR 42, late afternoon). Afternoon drying has driven RH to near-critical levels across most of the transect.

flame front.

3.3. Temperature Structure and Mixing Height

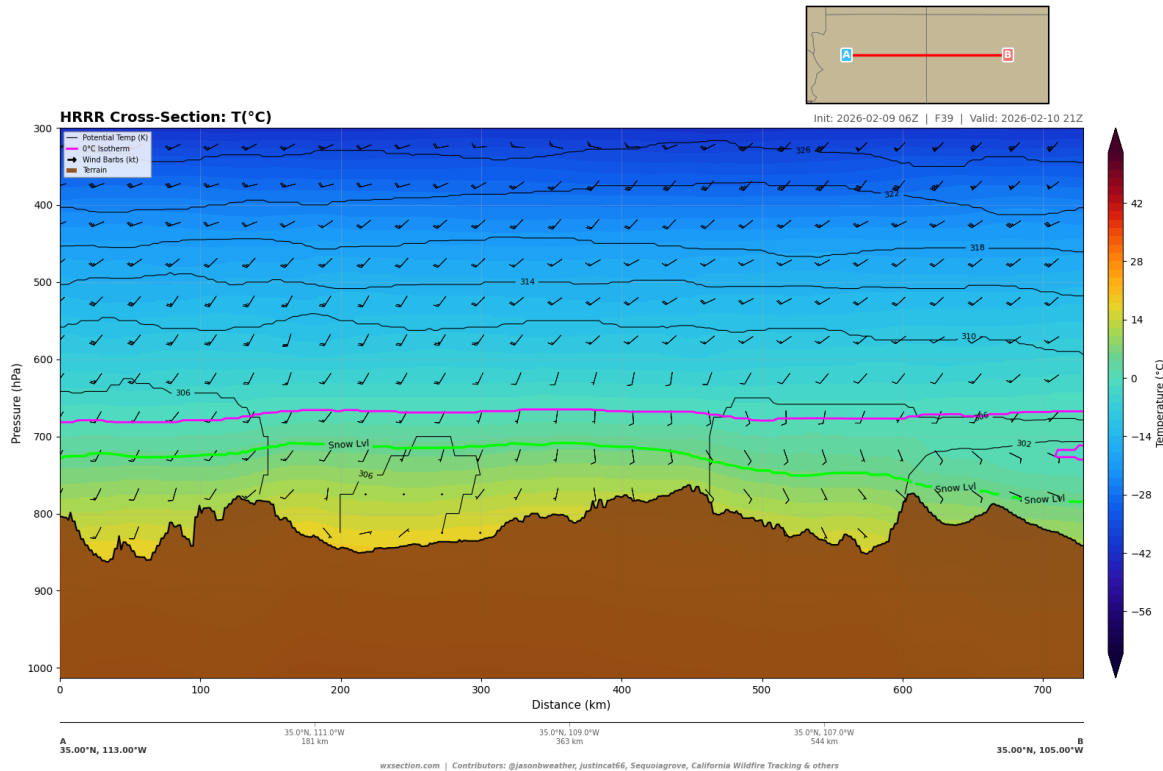


Figure 29: Temperature ($^{\circ}\text{C}$) along the E–W Main transect valid 21z 10 Feb (FHR 39). Isotherms show warm surface temperatures across the lower terrain. The freezing level (pink) is at approximately 700 hPa.

The temperature structure at 21z (Figure 29) reveals near-surface temperatures ranging from 4.6°C on the highest terrain to 18.9°C in the lower basins, with a mean of 12.9°C . These are moderate temperatures for February—warm enough to drive active boundary layer mixing but not extreme. The 850 hPa temperature of $11.1\text{--}19.4^{\circ}\text{C}$ (mean 16.4°C) indicates a well-mixed, nearly adiabatic layer from the surface to the terrain-top level.

The freezing level lies near 700 hPa (3000 m MSL), placing it above most of the fire-relevant terrain. The 700 hPa temperatures of $0.3\text{--}4.1^{\circ}\text{C}$ (mean 2.6°C) are notably warm for early February, contributing to the elevated snowline and dry fuel conditions at moderate elevations. At 500 hPa, temperatures of -14.7 to -16.4°C (mean -15.4°C) indicate a relatively warm mid-tropospheric environment.

The 700–500 hPa lapse rate is critically important for fire behavior. The temperature difference from 700 hPa (mean 2.6°C) to 500 hPa (mean -15.4°C) yields a mean mid-tropospheric lapse rate of approximately $6.5^{\circ}\text{C}/\text{km}$ —near the moist adiabatic rate but below the dry adiabatic rate. However, the surface-to-700 hPa layer is steeper, as confirmed by the lapse rate analysis below.

The lapse rate cross-section (Figure 31) reveals steep low-level lapse rates across the entire transect. Near-surface lapse rates of $8\text{--}10^{\circ}\text{C}/\text{km}$ (approaching the dry adiabatic rate of $9.8^{\circ}\text{C}/\text{km}$) dominate the lowest 100–150 hPa above the terrain. This indicates vigorous daytime convective mixing that extends the mixing height to approximately 650–600 hPa over the lower terrain.

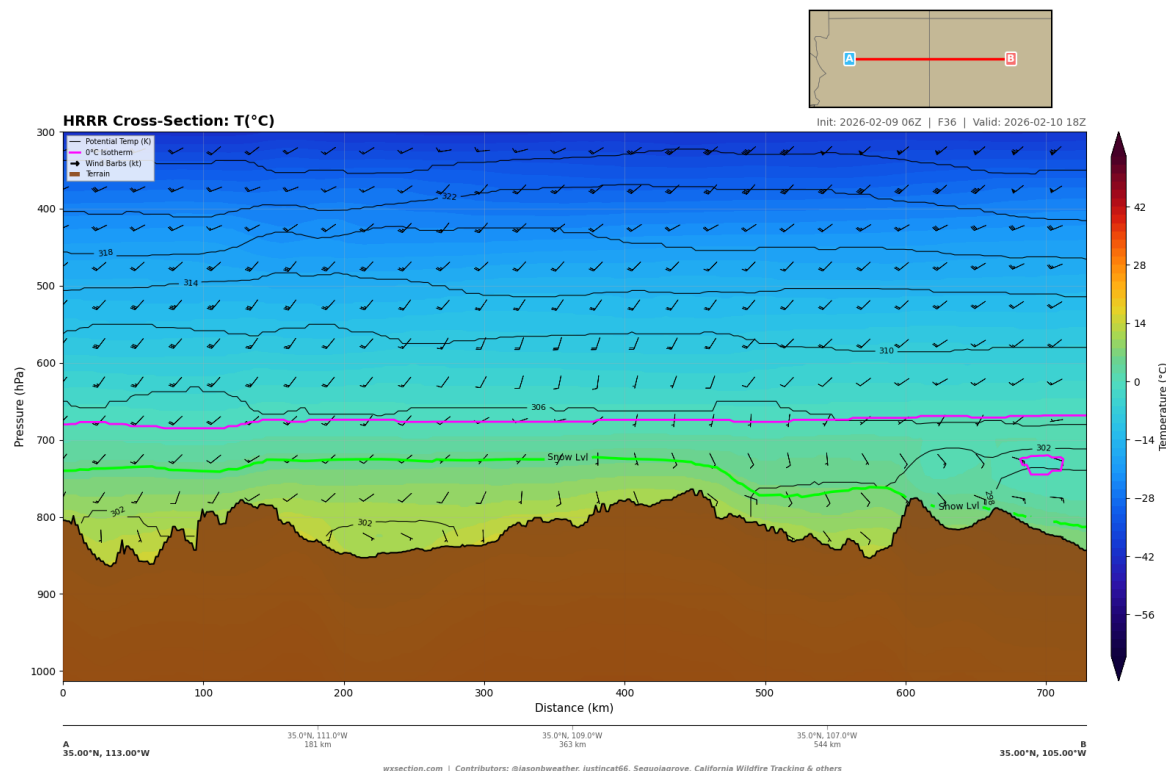


Figure 30: Temperature along the E–W Main transect at 18z 10 Feb (FHR 36, late morning). Comparison with Figure 29 shows the 3-hour temperature rise during peak heating.

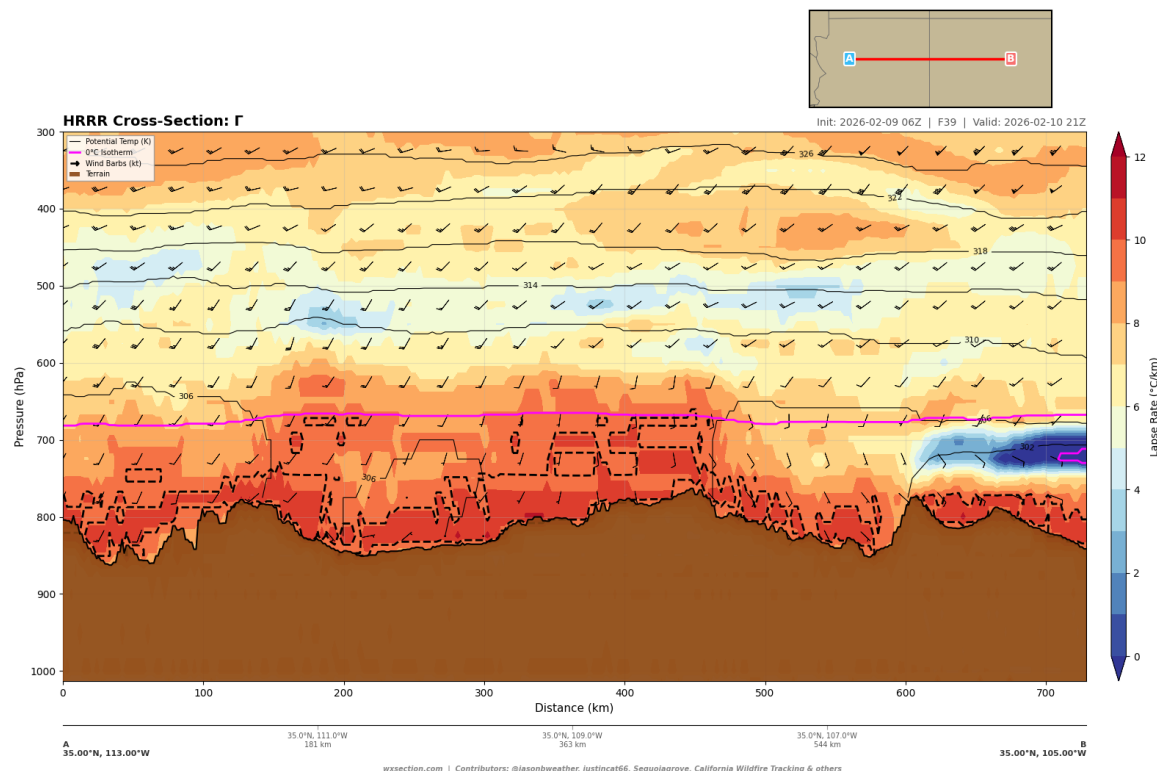


Figure 31: Lapse rate ($^{\circ}\text{C}/\text{km}$) along the E–W Main transect valid 21z 10 Feb (FHR 39). Warm colors (reds) indicate steep (unstable) lapse rates exceeding $8^{\circ}\text{C}/\text{km}$. Hatching marks regions approaching or exceeding the dry adiabatic rate.

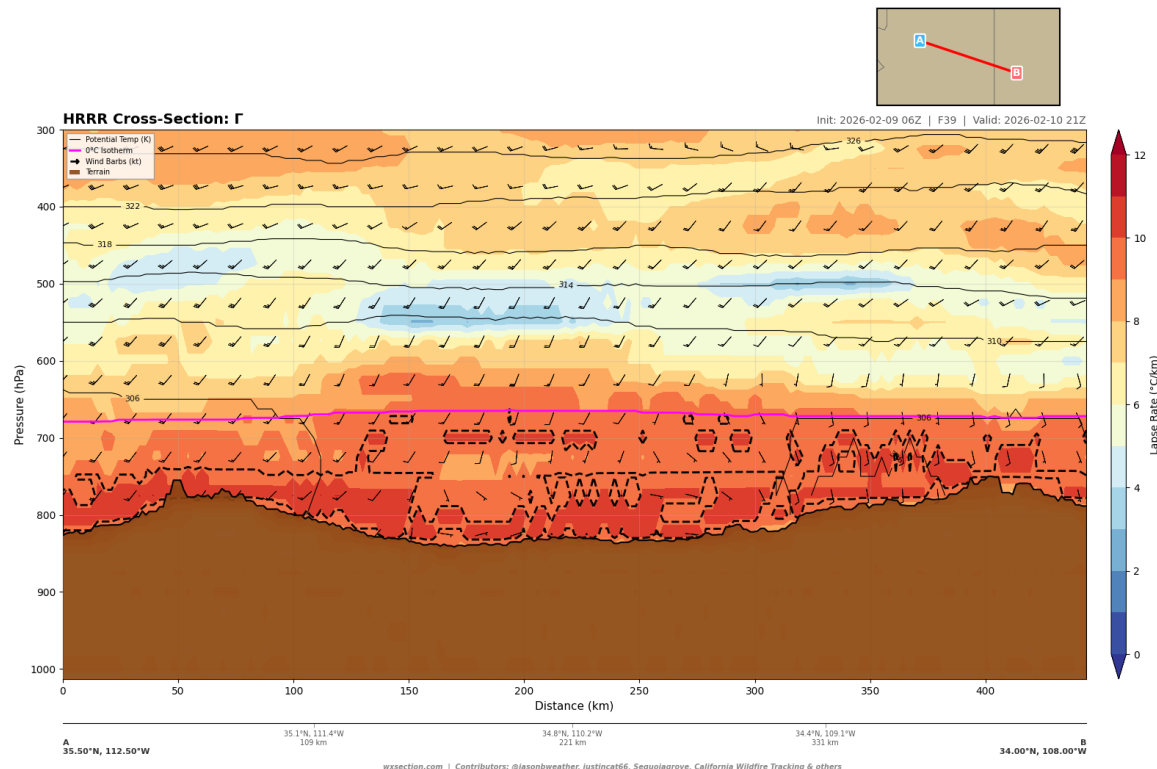


Figure 32: Lapse rate along the Mogollon Rim transect valid 21z 10 Feb (FHR 39). The Rim terrain enhances low-level lapse rates through terrain-amplified surface heating.

The Mogollon Rim lapse rate transect (Figure 32) shows enhanced instability along the Rim escarpment. The dark terrain of the Rim (ponderosa pine and mixed conifer) absorbs solar radiation efficiently, producing steep surface lapse rates. The combination of steep lapse rates and the terrain drop creates conditions favorable for downslope wind acceleration—a mechanism analogous to chinook/foehn development, though on a smaller scale.

The deep mixing layer (surface to 600 hPa, roughly 3 km AGL over the basins) has critical fire weather implications. First, it ensures that dry mid-level air is continuously entrained to the surface through convective eddies. Second, it creates conditions favorable for erratic fire behavior through plume-dominated convection. Any fire that develops a convection column within this unstable layer will exhibit rapid vertical development, producing strong and unpredictable surface inflow winds.

3.4. Vertical Motion and Subsidence

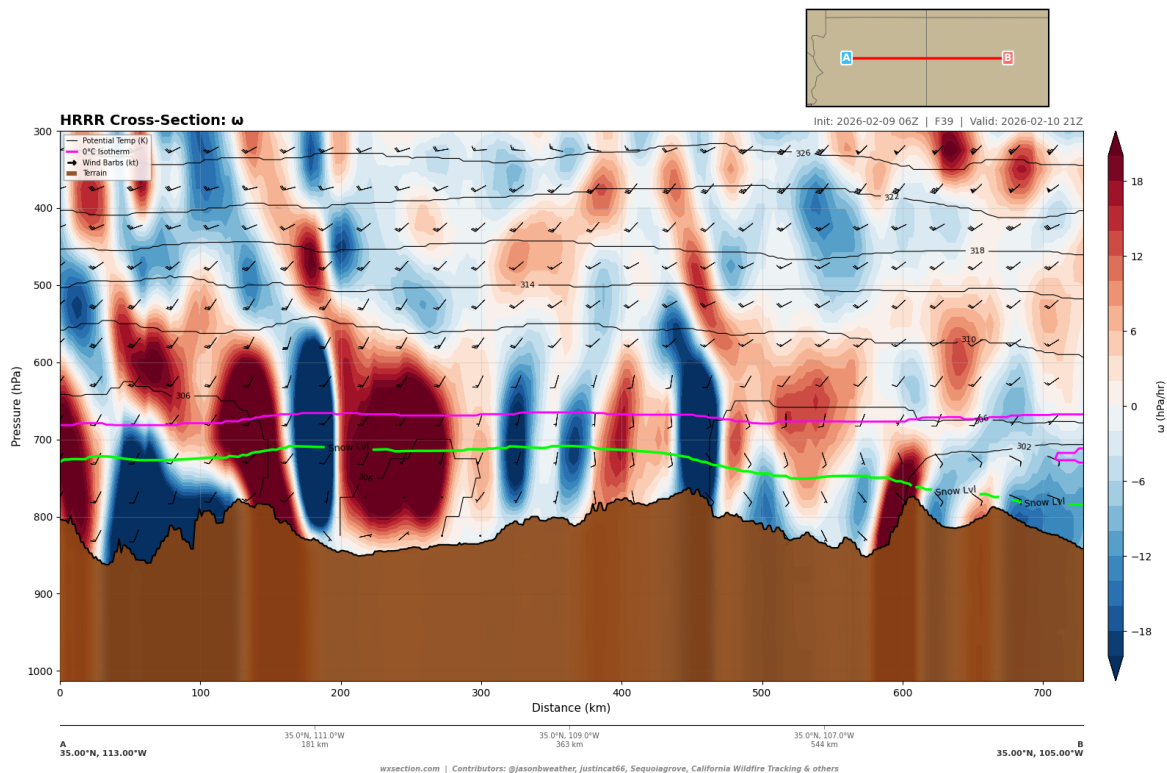


Figure 33: Vertical velocity (ω , Pa/s) along the E–W Main transect valid 21z 10 Feb (FHR 39). Blue/purple shading indicates strong upward motion (negative ω); red/brown indicates subsidence (positive ω). Mountain-wave signatures are prominent.

The vertical motion field at 21z (Figure 33) reveals a rich pattern of terrain-forced vertical motion. Strong upward motion (blue/purple, negative ω) is concentrated in several distinct columns, reaching from the terrain surface through the mid-troposphere to above 500 hPa. These updraft columns are spaced roughly 50–100 km apart and correspond to the major terrain ridges along the transect.

Between the updraft columns, compensating subsidence (red/warm colors) is clearly visible. This mountain-wave pattern is characteristic of the Colorado Plateau's mesa-and-canyon topography, where the flow alternately ascends terrain obstacles and descends in their lee. The subsidence between terrain features is a critical drying mechanism: descending air warms adiabatically and its relative humidity decreases

dramatically. This terrain-driven subsidence supplements the synoptic-scale subsidence to produce the extreme dryness documented in Section 3.2.

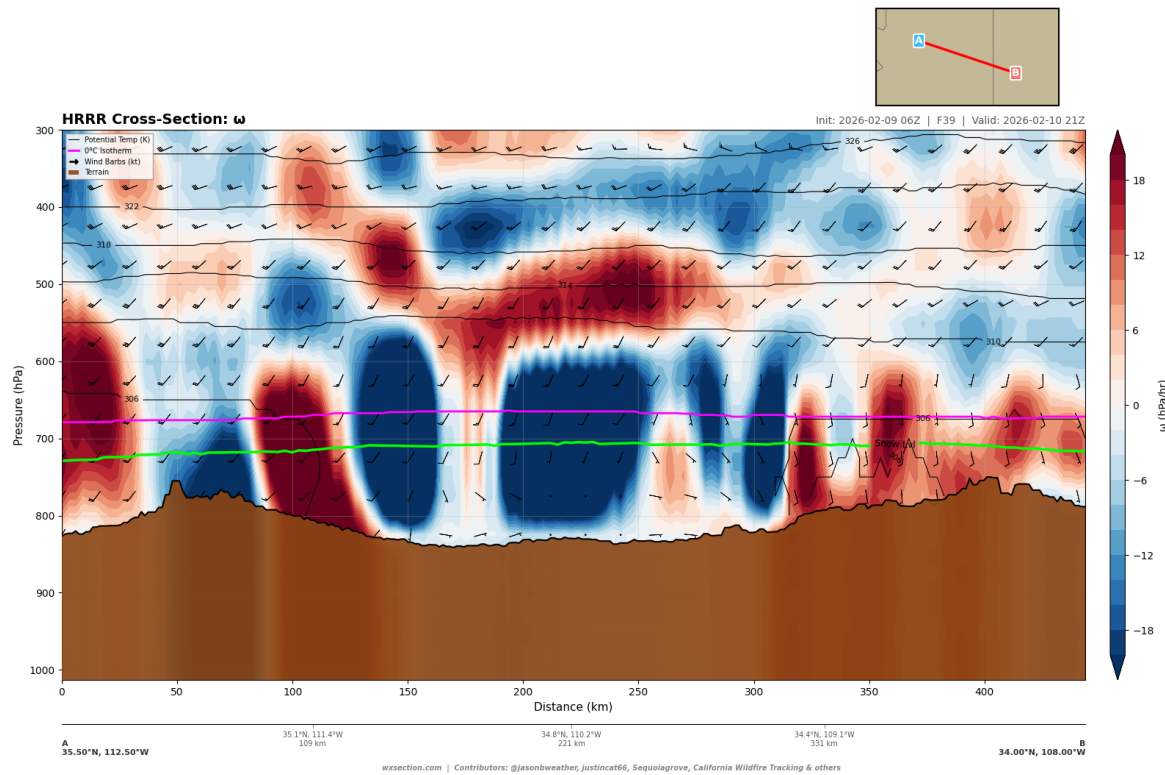


Figure 34: Vertical velocity along the Mogollon Rim transect valid 21z 10 Feb (FHR 39). The dramatic terrain discontinuity of the Rim produces an intense mountain-wave response with strong ascent/descent couplets.

The Mogollon Rim transect (Figure 34) shows the most dramatic vertical motion signatures. The Rim's abrupt topographic discontinuity—a 600–900 m escarpment over less than 10 km horizontal distance—generates an intense mountain wave. Strong ascent on the windward (northwest) side of the Rim is followed by equally strong lee-side descent. These mountain-wave signatures extend vertically through the entire troposphere, well above 500 hPa, indicating a strong wave response.

The lee-side subsidence below the Rim is particularly concerning for fire weather. Air descending from 650–700 hPa to the Tonto Basin floor (950 hPa equivalent) experiences approximately 2500 m of descent, producing adiabatic warming of roughly 25°C and a dramatic reduction in RH. This downslope drying mechanism explains why the basins immediately below the Mogollon Rim are among the driest and most fire-prone locations in Arizona.

The N–S transect (Figure 35) confirms that terrain-forced vertical motion is a pervasive feature across the entire Four Corners region. The updraft/downdraft couplets extend from the La Sal Mountains in the north through the Chuska Mountains and into the Gila Wilderness of southern New Mexico. Both the northern and southern ends of the transect show large-scale subsidence in the free troposphere above 500 hPa, consistent with the synoptic-scale ridging discussed in the large-scale overview.

3.5. Vapor Pressure Deficit

Vapor pressure deficit (VPD) integrates the effects of both temperature and humidity into a single metric that directly relates to the evaporative demand on fuels. The VPD analysis at 21z (Figure 36) reveals an

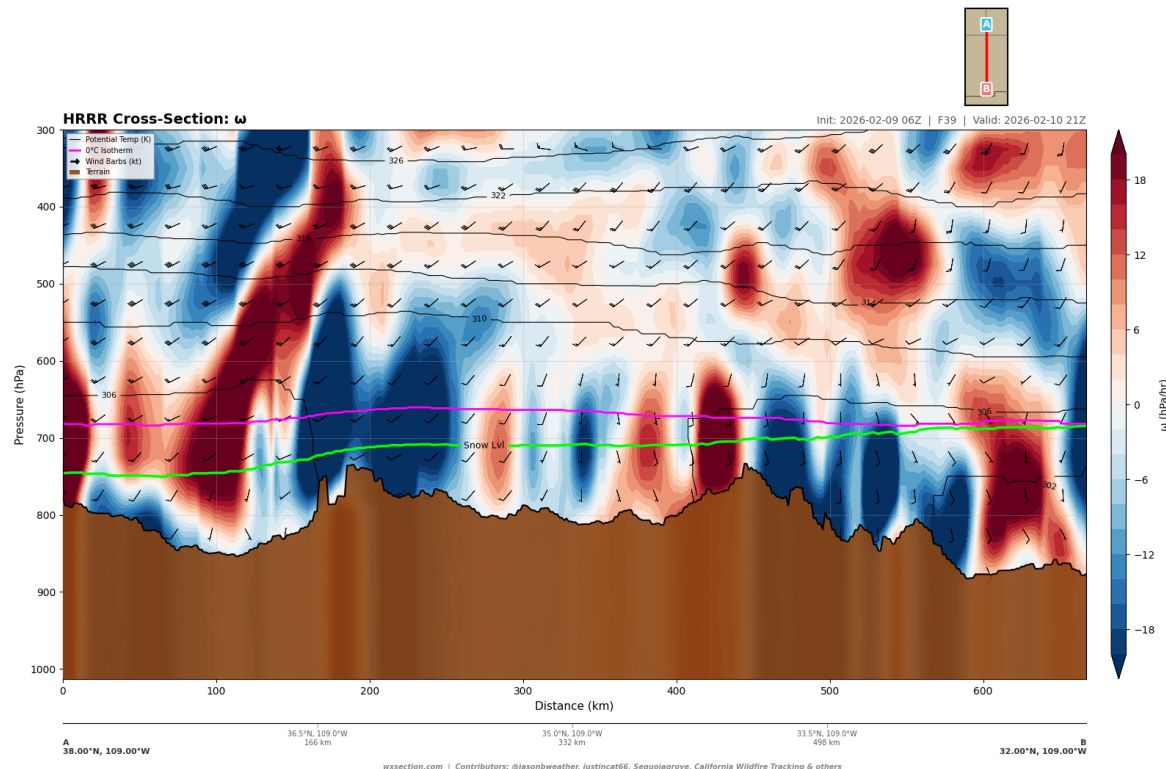


Figure 35: Vertical velocity along the N–S transect valid 21z 10 Feb (FHR 39). Terrain-driven vertical motion patterns are evident across the full meridional extent.

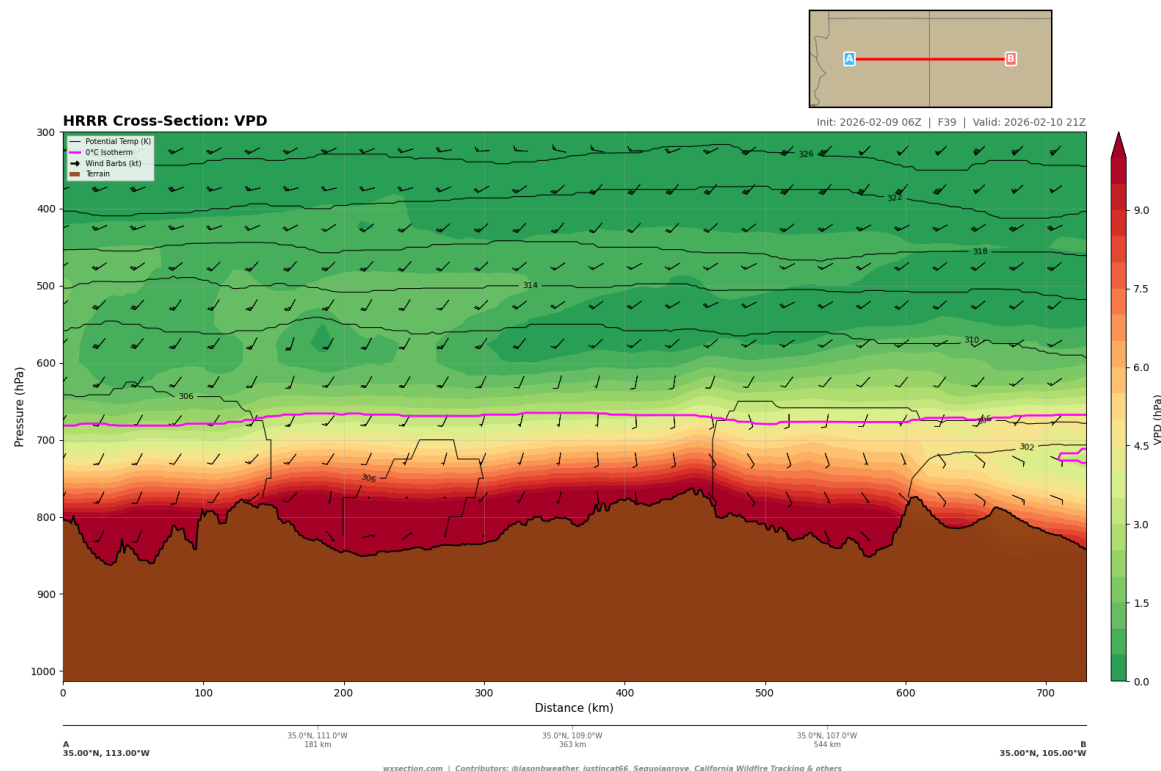


Figure 36: Vapor pressure deficit (VPD, hPa) along the E–W Main transect valid 21z 10 Feb (FHR 39). Deep red shading indicates VPD exceeding the 13 hPa extreme fire danger threshold.

alarmingly dry atmosphere across the E–W Main transect.

Near-surface VPD values range from 5.9 to 17.8 hPa, with a transect mean of 11.8 hPa. The maximum VPD of 17.8 hPa is located at 110.7°W (approximately 212 km along the transect), in the vicinity of the Tonto Basin below the Mogollon Rim. This value exceeds the 13 hPa extreme fire danger threshold by 37%. In total, 39% of near-surface grid points along the transect exceed 13 hPa (94 of 242 points), and a remarkable 89% exceed 8 hPa (216 of 242 points).

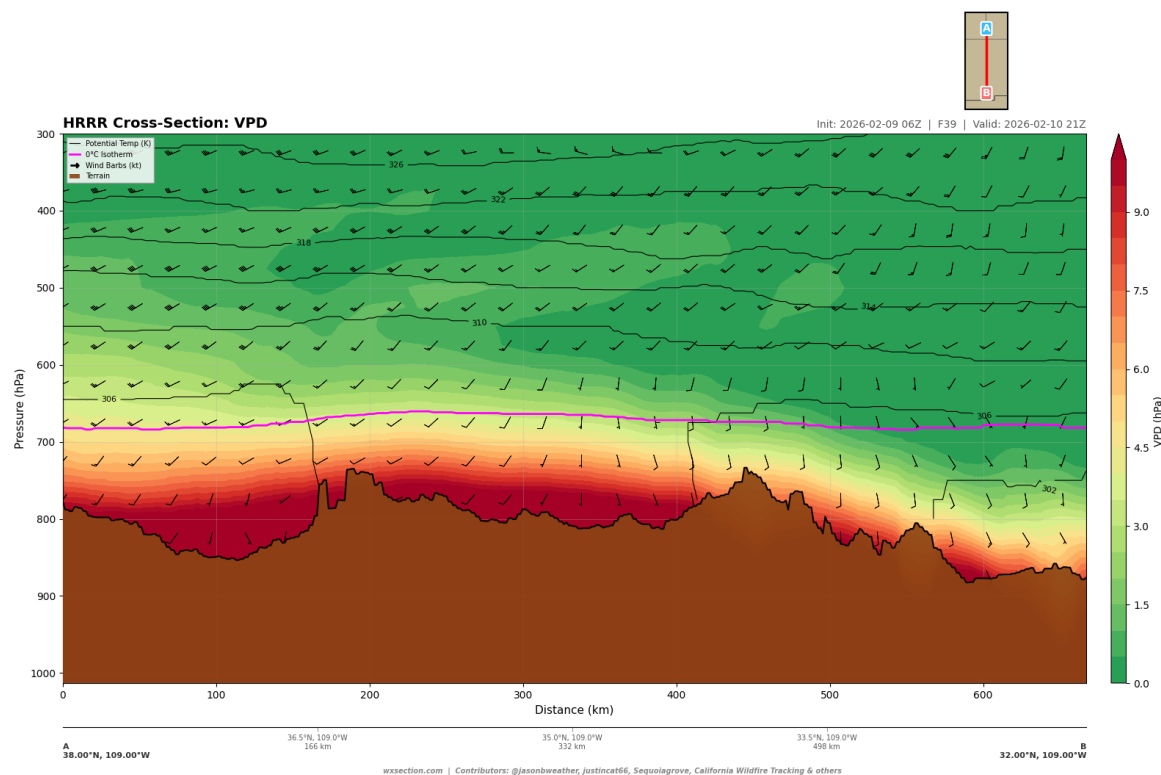


Figure 37: VPD along the N–S transect valid 21z 10 Feb (FHR 39). The highest VPD values are concentrated in the lower-elevation terrain of the southern portion of the transect.

The N–S transect VPD (Figure 37) shows a clear meridional gradient, with VPD increasing from north to south as temperatures rise and elevation decreases. The highest VPD values (exceeding 15 hPa) are found south of 34°N, where the terrain opens into the lower Gila and Chihuahuan Desert country.

The E–W Northern transect at 37°N (Figure 38) shows lower VPD values than the main transect, reflecting the cooler temperatures at higher latitude and elevation. However, near-surface VPD still broadly exceeds 8 hPa across the lower terrain west of the San Juan Mountains, indicating that fire weather concern extends well into southern Colorado.

The maximum VPD anywhere within the E–W Main cross-section reaches 32.7 hPa at elevated levels where warm temperatures combine with extremely low humidity. While this value occurs above the surface, it represents the desiccating potential of air that can be mixed to the surface through convective entrainment.

Key finding: The VPD analysis reveals that *extreme* atmospheric drying demand (>13 hPa) is not confined to isolated hot spots but covers nearly 40% of the 729 km E–W Main transect at the surface. This widespread extreme VPD, combined with the deep dry layer documented in the RH analysis, creates an atmospheric environment that will actively draw moisture from any fuels—including live fuels—at a rate that can produce critical fire weather conditions even with moderate winds.

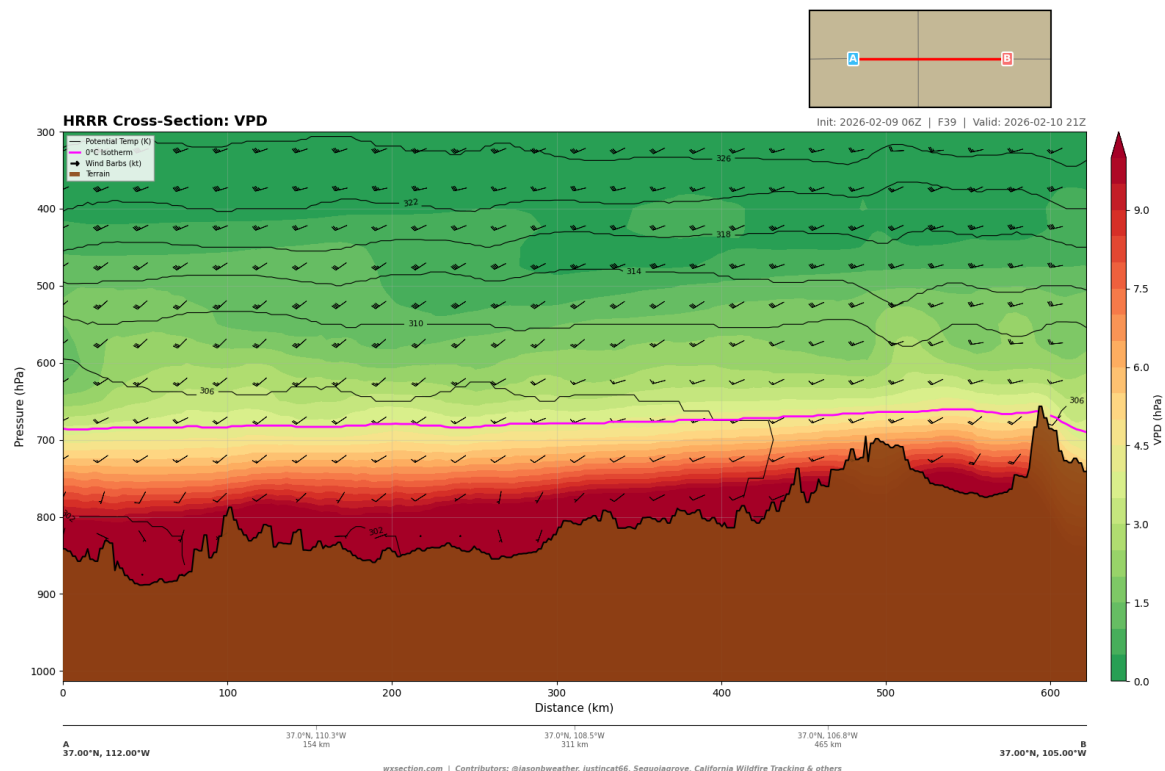


Figure 38: VPD along the E–W Northern transect (37°N) valid 21z 10 Feb (FHR 39). Lower temperatures at this latitude moderate VPD values slightly compared to the E–W Main transect.

3.6. Fire Weather Composite

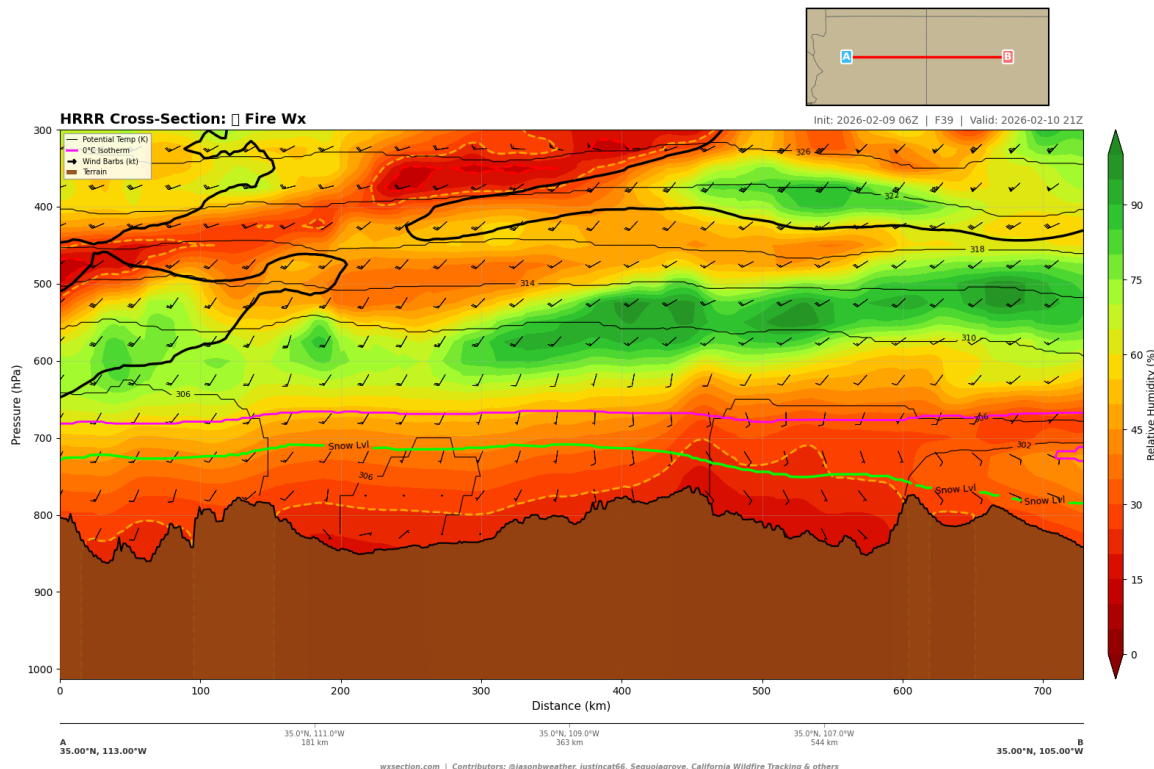


Figure 39: Fire weather composite along the E–W Main transect valid 21z 10 Feb (FHR 39, peak fire danger). Color shading integrates wind, humidity, and instability into a composite fire weather index. Deep red/orange indicates the highest fire danger.

The fire weather composite product (Figure 39) synthesizes wind speed, relative humidity, temperature, and instability into an integrated fire weather assessment. At 21z along the E–W Main transect, the composite shows elevated to critical fire weather conditions across essentially the entire cross-section. The surface and low-level atmosphere are uniformly shaded in warm colors (orange through red), indicating that no portion of this transect is exempt from fire weather concern.

The most extreme composite values are concentrated in three areas:

1. The central portion of the transect (approximately 200–350 km, near the AZ–NM border at 109°W), where the combination of moderate terrain elevation, strong VPD, and steep lapse rates produces the highest composite scores.
2. The Mogollon Rim transition zone, where downslope drying and wind acceleration compound the ambient fire danger.
3. The lower basins of central and western Arizona, where warm temperatures drive extreme VPD despite slightly higher RH values.

Comparison of the FHR 36 (18z, late morning; Figure 40) and FHR 39 (21z, early afternoon; Figure 39) composites reveals that fire danger is already elevated by late morning and intensifies through the early afternoon. The fire danger window on this day is expected to span from approximately 16z (9 AM MST) through at least 00z (5 PM MST)—a full 8-hour window of elevated conditions.

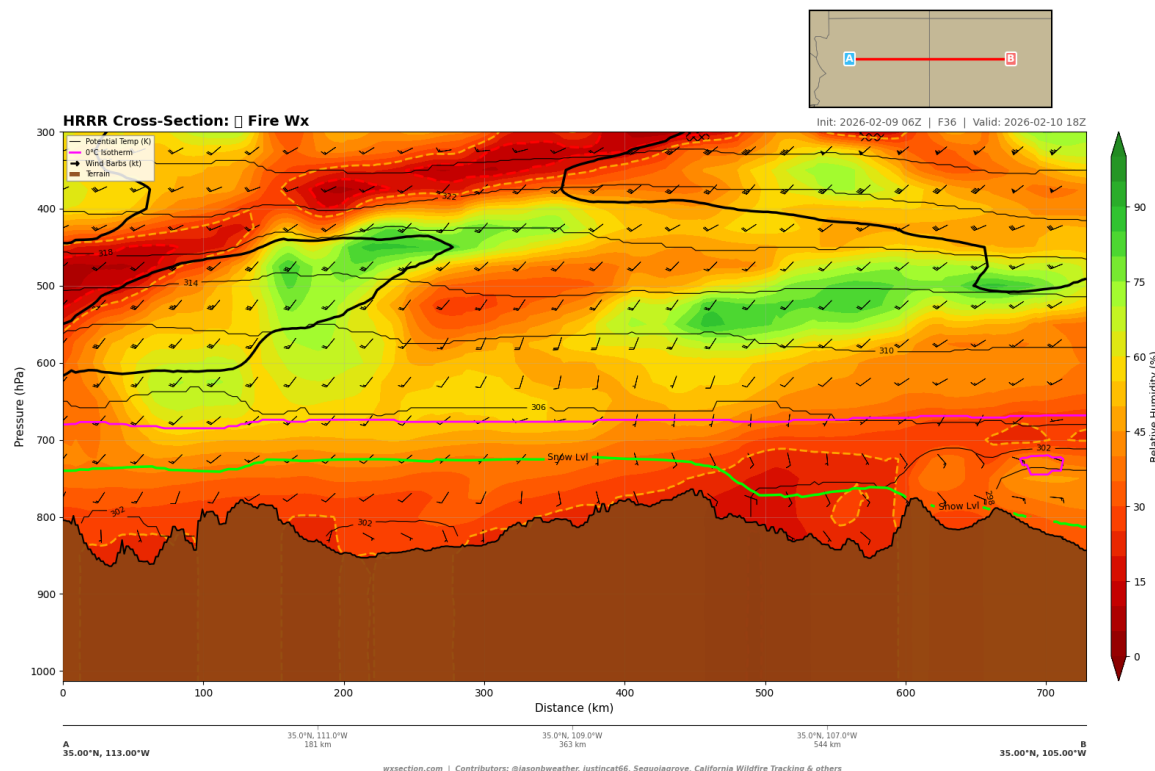


Figure 40: Fire weather composite along the E–W Main transect at 18z 10 Feb (FHR 36, late morning). Fire danger is already elevated by late morning, three hours before peak.

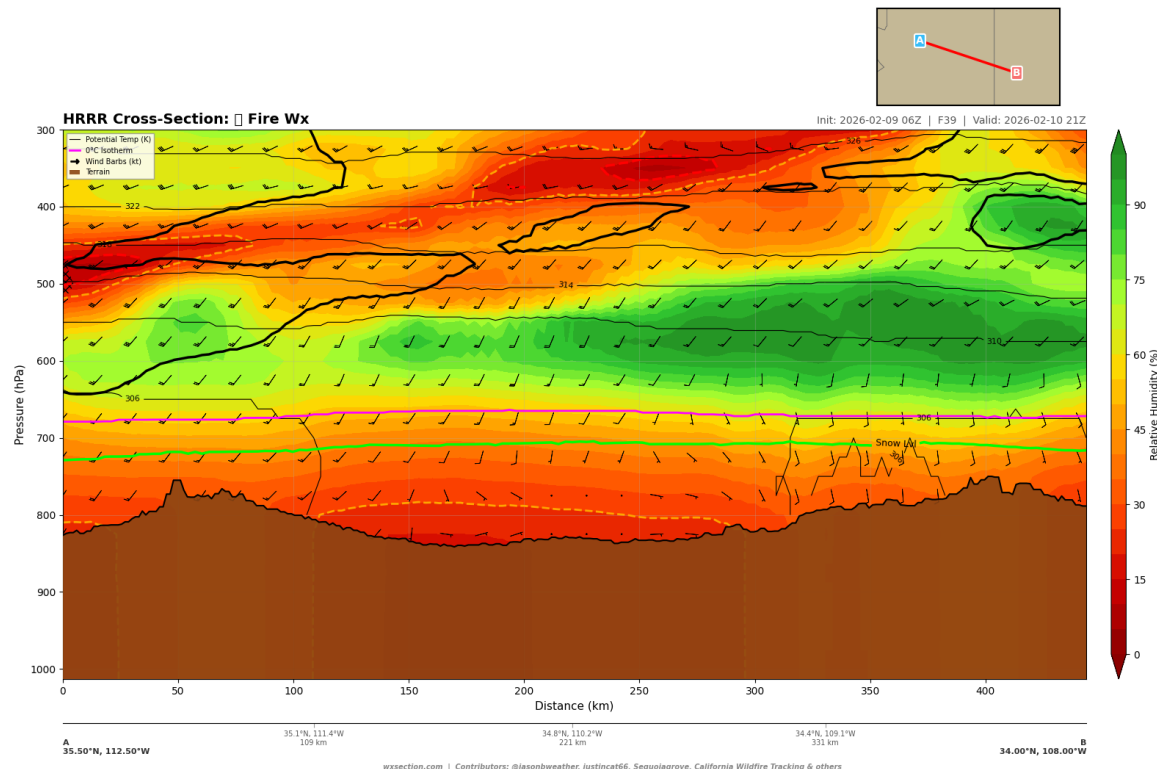


Figure 41: Fire weather composite along the Mogollon Rim transect valid 21z 10 Feb (FHR 39). The Rim escarpment and adjacent terrain show particularly high fire weather composite values.

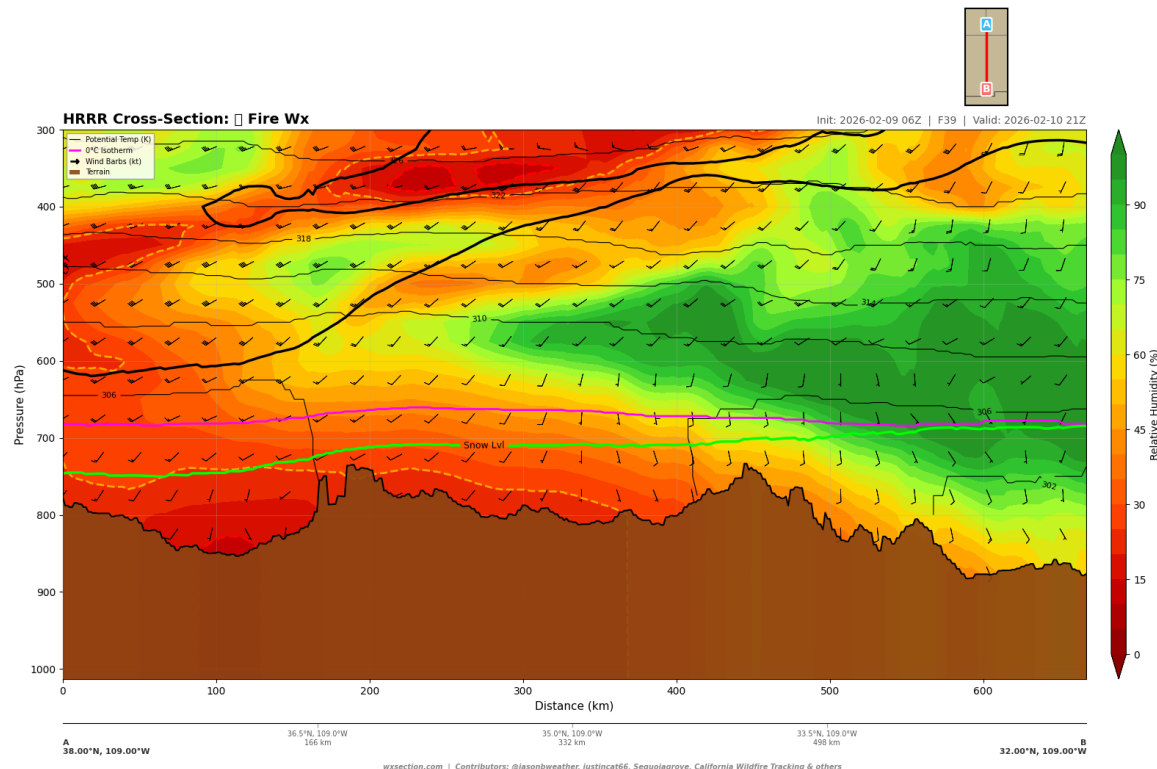


Figure 42: Fire weather composite along the N-S transect valid 21z 10 Feb (FHR 39). Fire danger increases from north to south as temperatures increase and elevation decreases.

The Mogollon Rim composite (Figure 41) confirms that the Rim country is one of the highest-concern areas within the Four Corners domain. The N–S composite (Figure 42) shows a clear meridional gradient, with the most intense fire weather conditions south of 35°N.

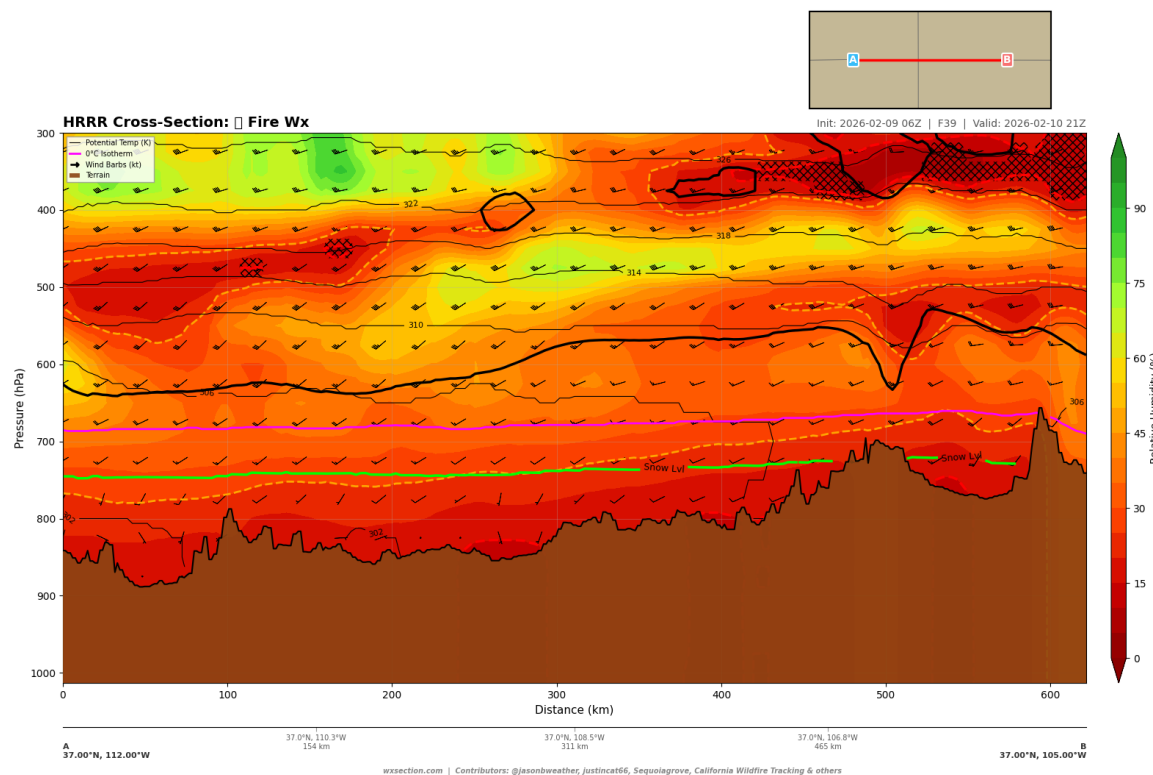


Figure 43: Fire weather composite along the E–W Northern transect (37°N) valid 21z 10 Feb (FHR 39). Southern Colorado and the San Juan Basin show moderately elevated fire weather conditions.

Even along the E–W Northern transect at 37°N (Figure 43), the fire weather composite shows elevated conditions across the Colorado Plateau and the San Juan Basin. The lower terrain between the San Juan Mountains and the La Plata Range displays orange shading, indicating that fire weather concern extends well into southern Colorado.

3.7. Summary and Risk Assessment

Table 4 summarizes the quantitative values extracted from the HRRR cross-section data at peak fire danger (21z 10 February 2026) along the E–W Main transect.

Risk assessment. The Four Corners region on 10 February 2026 presents a fire weather scenario that is *deceptively dangerous*. The moderate wind speeds (below traditional Red Flag thresholds) may tempt a downgrade in fire weather messaging, but the humidity and VPD analysis reveals conditions that are unambiguously critical:

1. **Deep, widespread dryness:** The entire boundary layer from surface to 700 hPa is critically dry, with mean RH values of 21–23% through the lowest 150 hPa. This is not a shallow surface dry layer that can be easily modified—it extends through the full depth of the afternoon mixed layer.
2. **Extreme VPD:** Nearly 40% of the E–W Main transect exceeds the 13 hPa extreme VPD threshold

Table 4: Fire weather parameter summary for the E–W Main transect (35°N , $113^{\circ}\text{W} \rightarrow 105^{\circ}\text{W}$) at 21z 10 Feb 2026 (FHR 39).

Parameter	Min	Max	Mean	Threshold
Near-surface wind (kt)	0.6	17.3	8.4	>25 sustained
850 hPa wind (kt)	0.7	13.7	7.5	—
700 hPa wind (kt)	4.7	19.6	9.7	—
Near-surface RH (%)	15.3	32.7	23.0	<15 critical
850 hPa RH (%)	15.4	29.5	21.9	—
700 hPa RH (%)	25.3	54.0	38.1	—
Near-surface temp ($^{\circ}\text{C}$)	4.6	18.9	12.9	—
700 hPa temp ($^{\circ}\text{C}$)	0.3	4.1	2.6	—
500 hPa temp ($^{\circ}\text{C}$)	-16.4	-14.7	-15.4	—
Near-surface VPD (hPa)	5.9	17.8	11.8	>13 extreme
VPD > 13 hPa coverage	39% of transect			—
VPD > 8 hPa coverage	89% of transect			—

at the surface, and 89% exceeds 8 hPa. The maximum VPD of 17.8 hPa indicates extraordinary atmospheric demand for moisture from fuels.

3. **Terrain amplification:** The Mogollon Rim, the Chuska Mountains, and the numerous mesas and canyons of the Colorado Plateau produce local wind acceleration, mountain-wave subsidence, and downslope drying that push conditions beyond what the ambient values suggest.
4. **Steep lapse rates:** Near-surface lapse rates approaching the dry adiabatic rate ($8\text{--}10^{\circ}\text{C/km}$) create an unstable boundary layer that promotes erratic fire behavior, rapid plume development, and transport of firebrands well ahead of the fire front.
5. **Failed overnight recovery:** The nocturnal humidity recovery to only 35–40% (vs. the typical 70–90%) indicates that dead fine fuels (1-hour and 10-hour) will not recover overnight, entering the next burning period with cumulative moisture deficits.
6. **Winter fire season dynamics:** The Southwest’s dormant grass fuels—cured but not yet replaced by green-up—respond rapidly to the extreme VPD and moderate winds. Grass fire rates of spread in these conditions can exceed 3 mph, allowing fires to make significant runs before suppression resources can respond.

The cross-section analysis supports maintaining elevated fire weather concern across the entire Four Corners domain, with the highest risk concentrated along the Mogollon Rim country of central Arizona, the AZ–NM border region near the White Mountains and Zuni Mountains, and the lower-elevation terrain of the San Juan Basin in northwest New Mexico. While sustained winds do not meet the 25 kt Red Flag criterion, the combination of extreme VPD, deep dry layer, and steep lapse rates warrants a “below criteria” Red Flag discussion emphasizing the non-wind components of the fire weather threat.

4. Synoptic-Scale Atmospheric Pattern

The large-scale atmospheric configuration on February 10, 2026, features a potent upper-level jet stream driving a progressive trough–ridge couplet across the western United States. HRRR cross-sections spanning from the Pacific Ocean to the Great Plains reveal the three-dimensional architecture of this pattern and its role

in generating critical fire weather conditions across the Interior West. The analysis that follows draws on five continental-scale transects (2,000–2,700 km each) at multiple forecast hours, providing an unprecedented vertical view of the synoptic forcing.

4.1. Upper-Level Flow and Jet Stream Configuration

The polar jet stream dominates the upper troposphere across the western CONUS on February 10. Along the 36°N east–west transect at 18Z (F36, peak heating), the jet core reaches **122.5 kt at 250 hPa** near 123°W—directly offshore of the central California coast (Figure 44). This places the left-exit region of the jet streak over the Great Basin and northern Arizona/New Mexico, a classic configuration for large-scale subsidence and surface pressure falls that enhance fire weather potential.

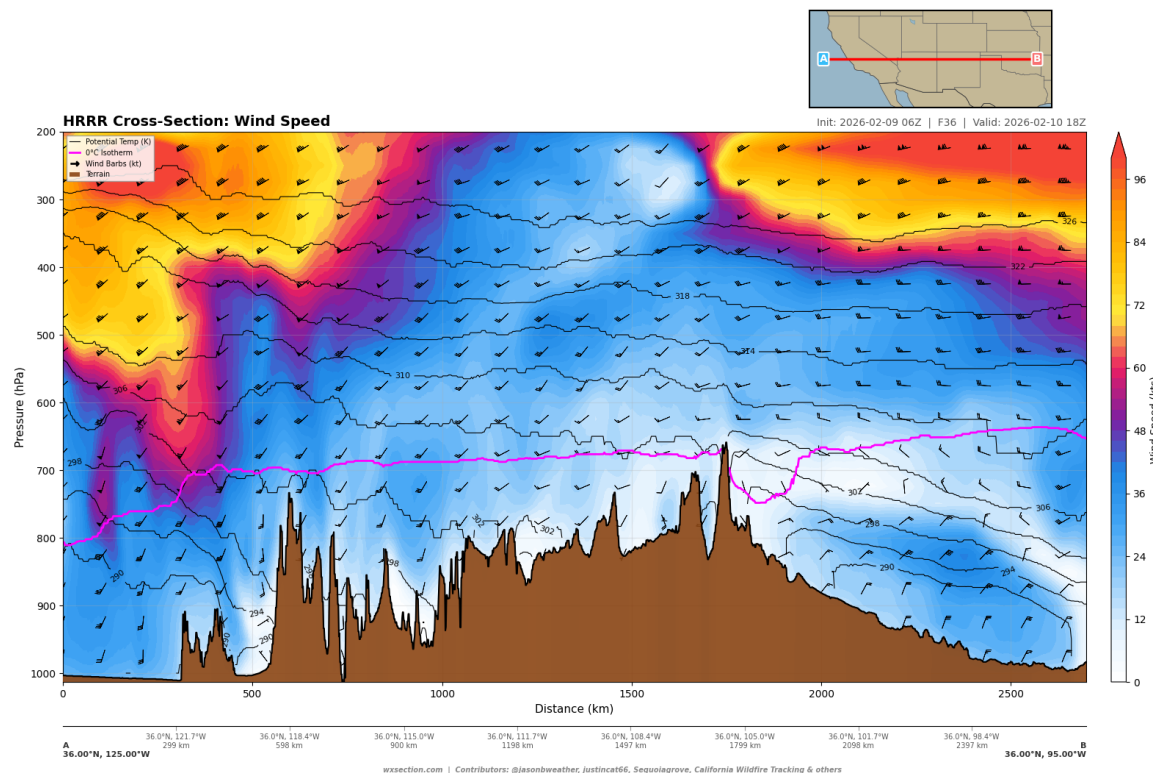


Figure 44: Wind speed cross-section along 36°N from the Pacific (125°W) to the southern Great Plains (95°W) at 18Z February 10 (F36). The jet core exceeds 120 kt at 250 hPa near the California coast. Note the secondary jet maximum near 96°W at 225 hPa (115 kt), indicating a split flow pattern. Low-level winds reach 55 kt at 700 hPa near 121°W.

A key feature of this jet configuration is the pronounced **wind speed minimum** over the Intermountain West between 115°W and 110°W. Along the southern transect, upper-level winds drop to just 62 kt at 200 hPa near 115°W and 67 kt at 150 hPa near 110°W, compared to 120+ kt on either flank. This reflects the ridge axis positioned over the Intermountain West, with deceleration in the upper-level flow as air traverses the ridge crest. A secondary jet maximum of 106–115 kt reappears at 225 hPa east of 100°W, indicating the entrance region of the downstream jet streak over the central Plains. This split-flow configuration channels divergent upper-level flow across the entire fire weather threat area.

The north–south transect along 110°W (Figure 45) reveals the jet stream's latitudinal position. The jet core lies at **44.3°N at 225 hPa with 118 kt**, centered over southern Montana. This is slightly south of the climatological mean jet position for early February, indicating an amplified trough–ridge pattern. The strong

wind speed gradient between the jet core and the lower latitudes (winds fall from 118 kt at 44°N to under 40 kt by 35°N) highlights a tight baroclinic zone that separates cold Canadian air from warmer subtropical air to the south.

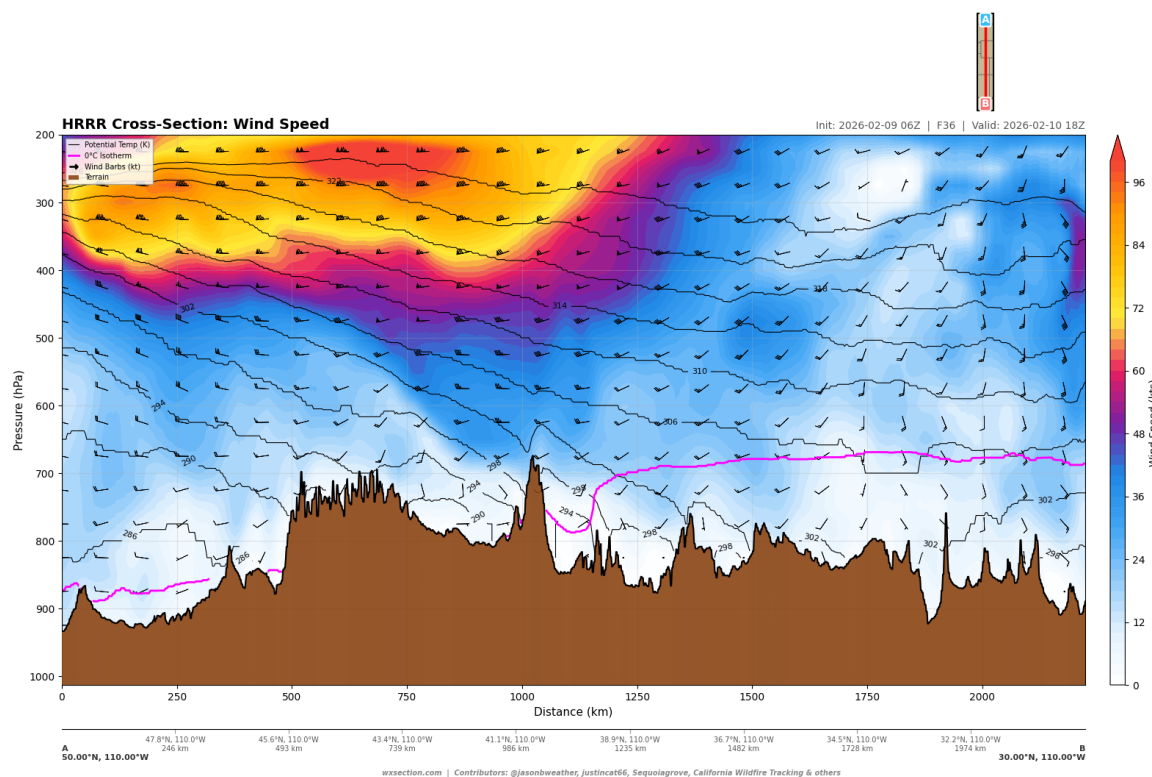


Figure 45: Wind speed cross-section along 110°W from southern Canada (50°N) to the US–Mexico border (30°N) at 18Z February 10. The polar jet core peaks at 118 kt near 44°N at 225 hPa. Low-level winds are modest (10–23 kt below 700 hPa) across the Rocky Mountain corridor.

The diagonal transect from 40°N, 125°W to 45°N, 100°W (Figure 46) captures the jet streak structure from its entrance region over the Pacific to the exit region over the northern Plains. This southwest-to-northeast slice reveals a broad, intense jet with speeds exceeding 80 kt through a deep layer (300–200 hPa) across the entire 2,000+ km transect. The highest winds (approaching 90 kt) tilt northeastward with height, consistent with warm advection and a developing trough east of the ridge axis.

The Pacific coastal transect (50°N to 30°N along 120°W; Figure 47) shows the upstream jet configuration. The jet core is displaced notably southward at the coast compared to the interior, with maximum winds centered near 37–40°N, reflecting the curvature of the jet around the base of the incoming Pacific trough. This configuration places the strongest upper-level forcing for ascent just offshore, with divergent flow (and thus subsidence) downstream across the interior West.

The northern east–west transect along 47°N (Figure 48) captures the polar jet in the heart of the baroclinic zone. The jet at this latitude is broader and extends farther east than the subtropical branch, with 60–80 kt winds spanning 1,500 km from the Pacific coast to the northern Rockies. This persistent upper-level flow contributes to sustained downslope wind events along the eastern slopes of the northern Rockies and creates the dynamic forcing necessary for mountain wave generation over Montana and Wyoming.

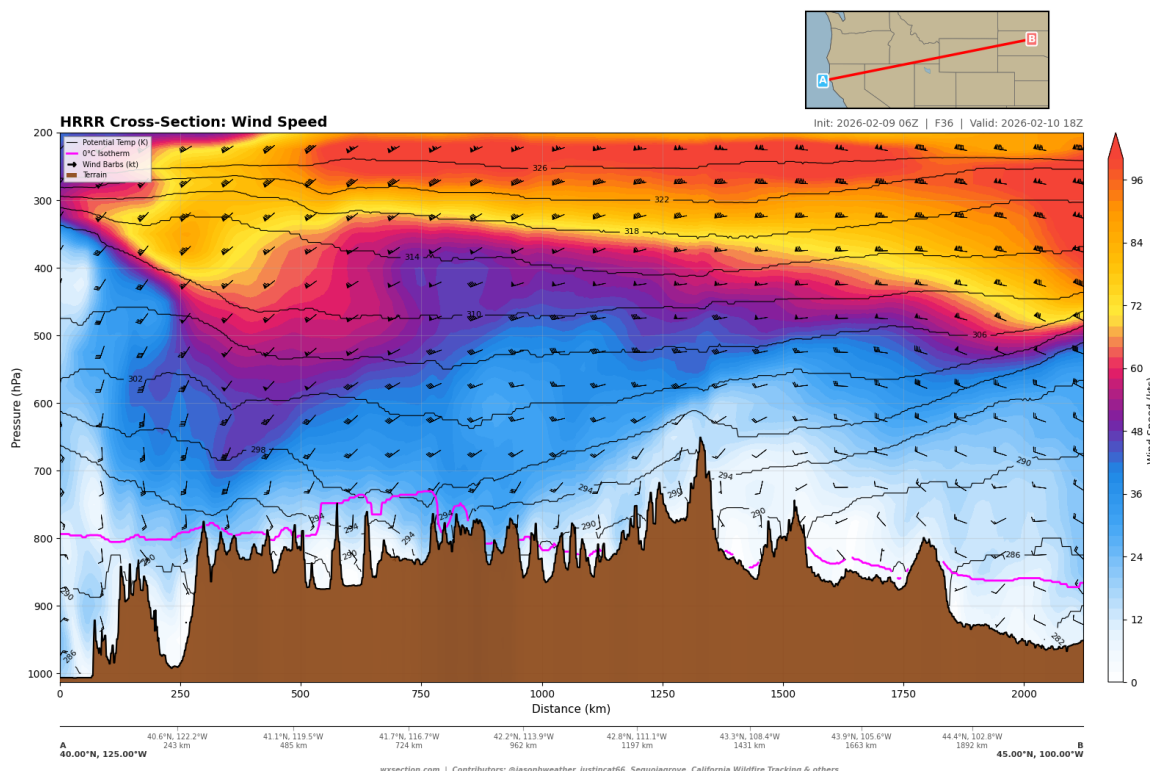


Figure 46: Wind speed along the diagonal transect (40°N , 125°W to 45°N , 100°W) at 18Z February 10. This SW–NE slice captures the full jet streak from Pacific entrance to Plains exit region. Sustained 80+ kt winds through a deep (300–200 hPa) layer drive large-scale forcing for subsidence downstream.

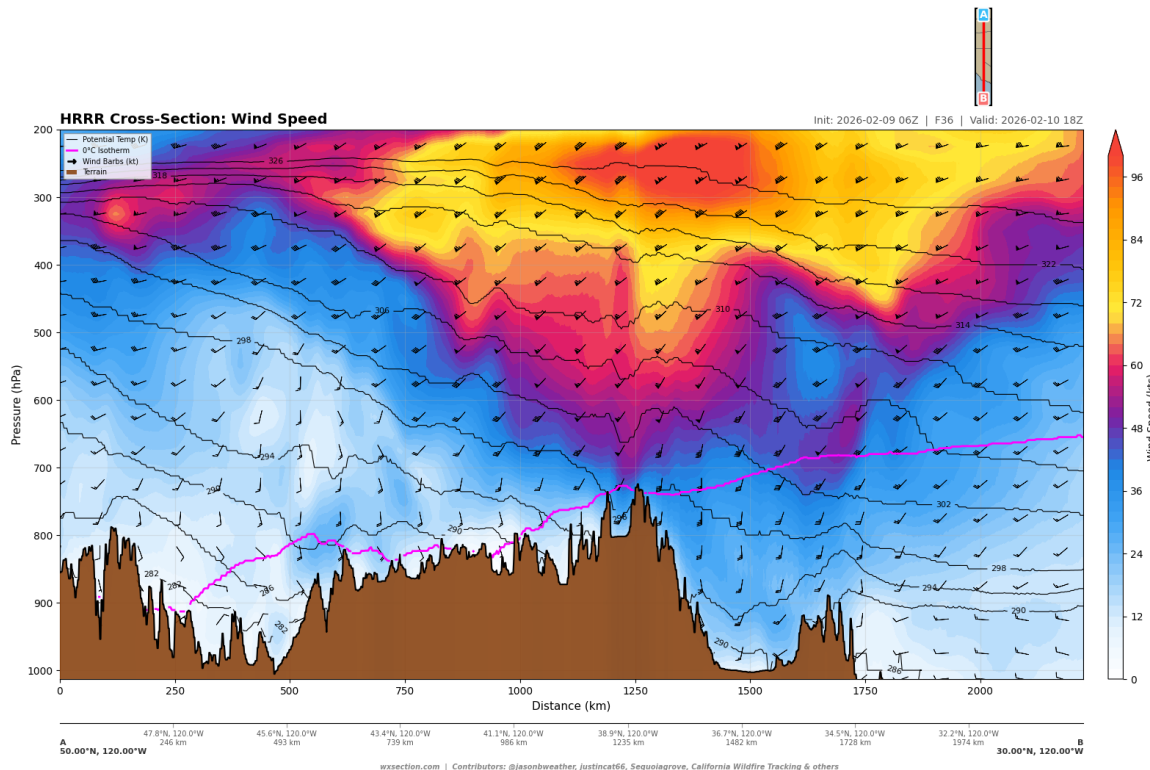


Figure 47: Wind speed cross-section along the Pacific coast (120°W , 50°N to 30°N) at 18Z February 10. The jet core sits near $37\text{--}40^{\circ}\text{N}$, with strong southwesterly flow impinging on the California coast. Low-level onshore flow is evident below 800 hPa.

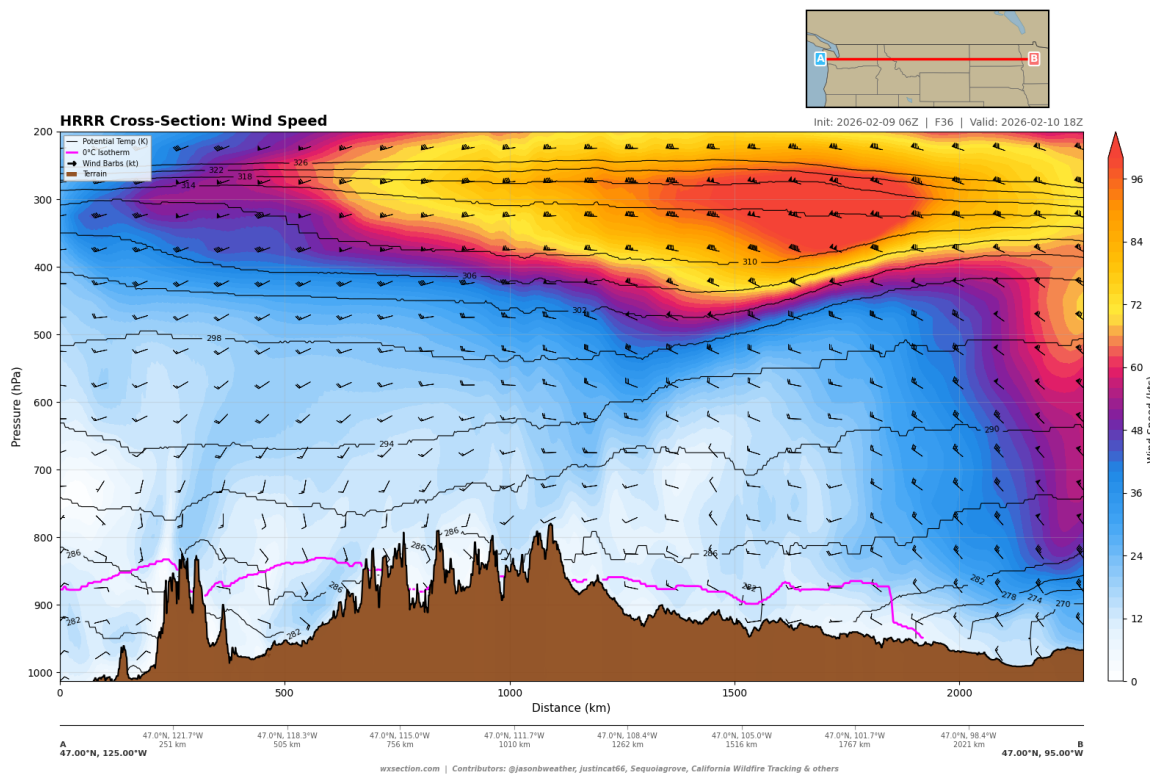


Figure 48: Wind speed cross-section along 47°N from the Pacific (125°W) to the northern Great Plains (95°W) at 18Z February 10. The polar jet is broad, with 60–80 kt winds extending across much of the northern tier.

4.2. Large-Scale Subsidence and the Western Ridge

The vertical motion field reveals the critical role of large-scale subsidence in creating fire weather conditions. Along the 36°N transect at 18Z (Figure 49), the omega field shows a striking east–west dipole. West of 120°W, vigorous ascending motion dominates the mid-troposphere, associated with the incoming Pacific trough and frontal forcing. The strongest ascent reaches -4.88 Pa s^{-1} (approximately $-17.6 \text{ hPa hr}^{-1}$) at 825 hPa near 123°W, indicating active precipitation processes along the California coast.

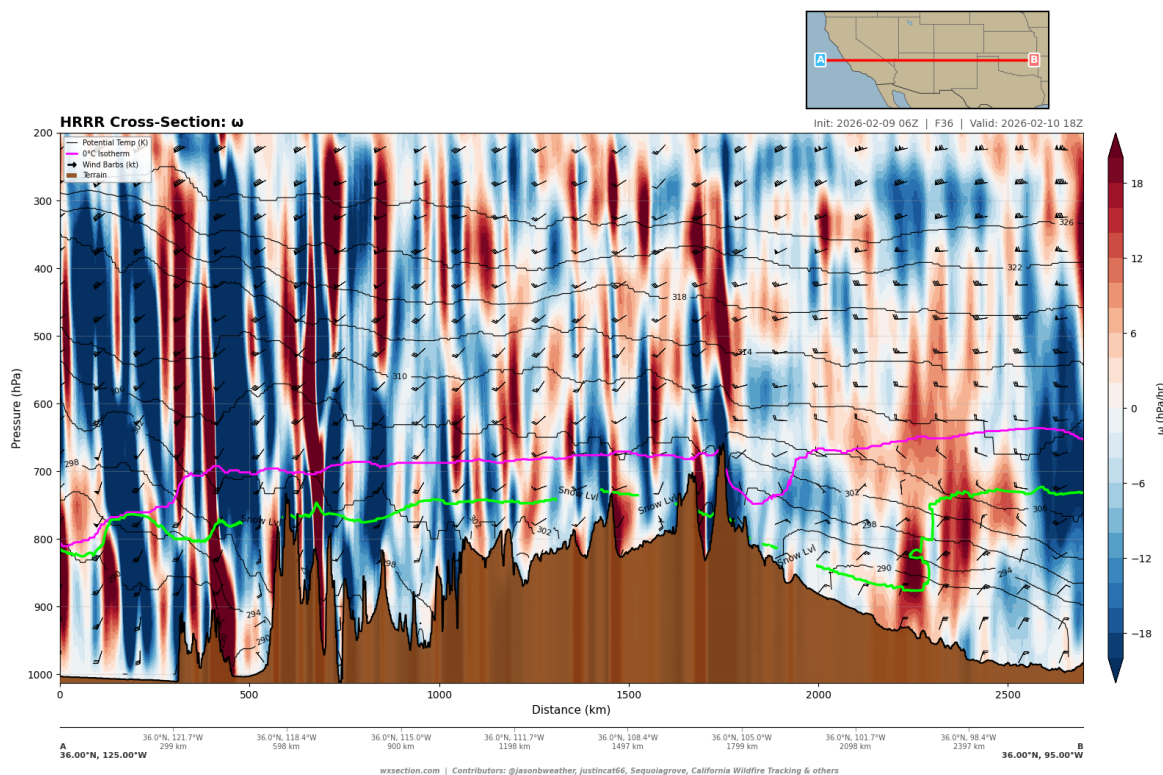


Figure 49: Vertical velocity (omega) cross-section along 36°N at 18Z February 10. Blue shading (negative omega) indicates ascent; red/warm shading (positive omega) indicates subsidence. Note the strong ascent near the coast and the broad region of mid-level subsidence east of 110°W. Gravity wave signatures are visible as alternating ascent/descent columns in the upper troposphere over terrain.

East of 115°W, the pattern reverses. Mid-level (500–700 hPa) average omega becomes positive (subsiding) across the Interior West: $+0.176 \text{ Pa s}^{-1}$ at 110°W, $+0.024 \text{ Pa s}^{-1}$ at 105°W, and $+0.305 \text{ Pa s}^{-1}$ at 100°W. While these area-averaged values appear modest, the cross-section reveals intense localized subsidence columns embedded within the broader pattern, particularly above terrain features where orographic gravity waves produce organized downward motion extending through the full tropospheric depth. The maximum subsidence along the southern transect reaches $+2.77 \text{ Pa s}^{-1}$ at 950 hPa near 120°W, associated with downslope flow on the lee side of the Coast Ranges.

The north–south omega transect along 110°W (Figure 50) reveals the latitudinal structure of the subsidence pattern. Mid-level subsidence is most pronounced at higher latitudes (47–49°N), where values reach $+0.225$ to $+0.385 \text{ Pa s}^{-1}$ averaged through the 500–700 hPa layer. This is consistent with the ridge axis position and the post-trough subsidence that characterizes downslope wind events along the Montana/Wyoming front ranges. At lower latitudes (33–35°N), weak ascent prevails in the mid-levels, suggesting that the fire weather threat in the Southwest arises more from dry air advection and thermal mechanisms than from dynamic

subsidence.

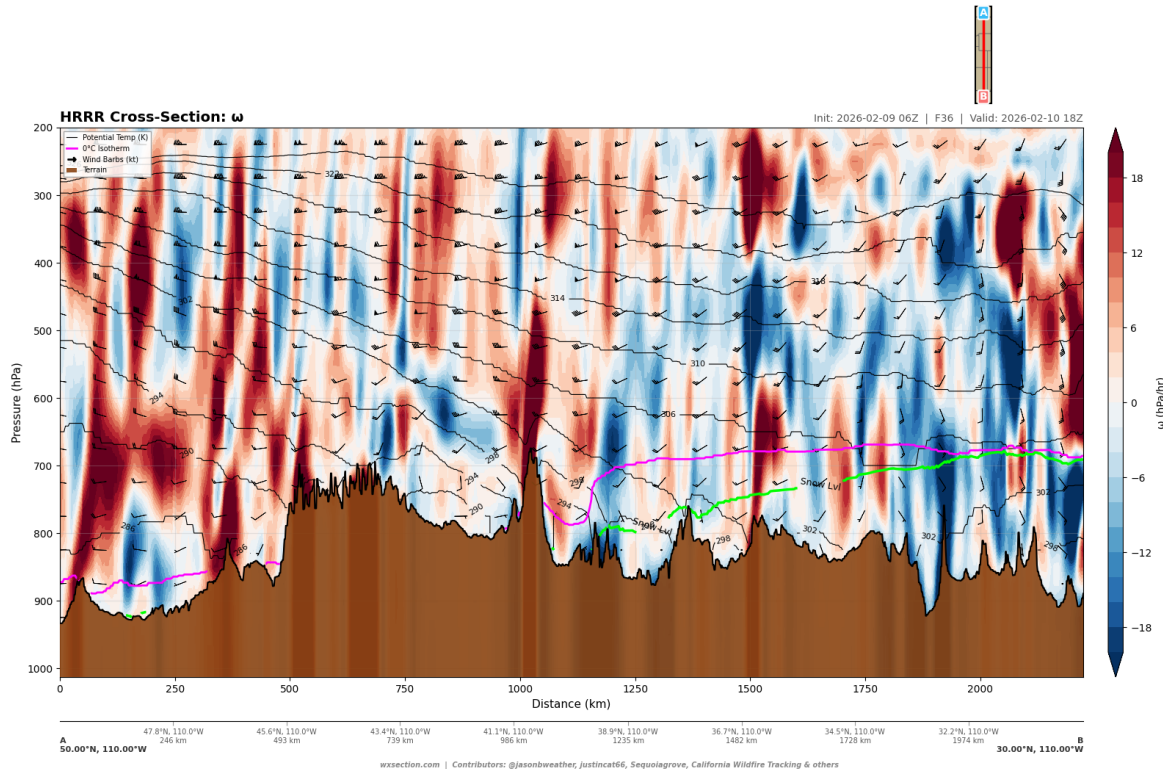


Figure 50: Vertical velocity (omega) cross-section along 110°W at 18Z February 10. Mid-level subsidence dominates the northern tier ($47\text{--}50^{\circ}\text{N}$), while weak ascent characterizes the southern latitudes. The omega field is heavily modulated by orographic gravity waves across the Rocky Mountain terrain.

The diagonal transect omega field (Figure 51) provides a particularly compelling view of the subsidence pattern. This slice from the Pacific coast to the northern Plains crosses the ridge axis at an oblique angle, revealing the transition from vigorous coastal ascent to deep subsidence in the lee of the Cascades and northern Rockies. The alternating columns of ascent and descent in the upper troposphere (above 500 hPa) are gravity wave signatures forced by the strong cross-mountain flow, which transport momentum and energy downward from the jet stream to the surface—a key mechanism for generating severe downslope windstorms.

4.3. Moisture Distribution and Dry Air Intrusion

The relative humidity cross-sections reveal a deep dry air mass entrenched across the Interior West, sharply contrasting with moist Pacific air along the coast. At 18Z along 36°N (Figure 52), the moisture distribution shows three distinct regimes:

1. **Moist Pacific air west of 121°W :** Average RH below 500 hPa exceeds 55%, with values reaching 90% in the lower troposphere near the coast. This moisture is associated with the approaching Pacific trough.
2. **Transition zone ($121\text{--}116^{\circ}\text{W}$):** A sharp drying gradient occurs across the California Coast Ranges and into the Great Basin, with average RH dropping from 55% to 25% over just 400 km. This is the critical fire weather boundary.

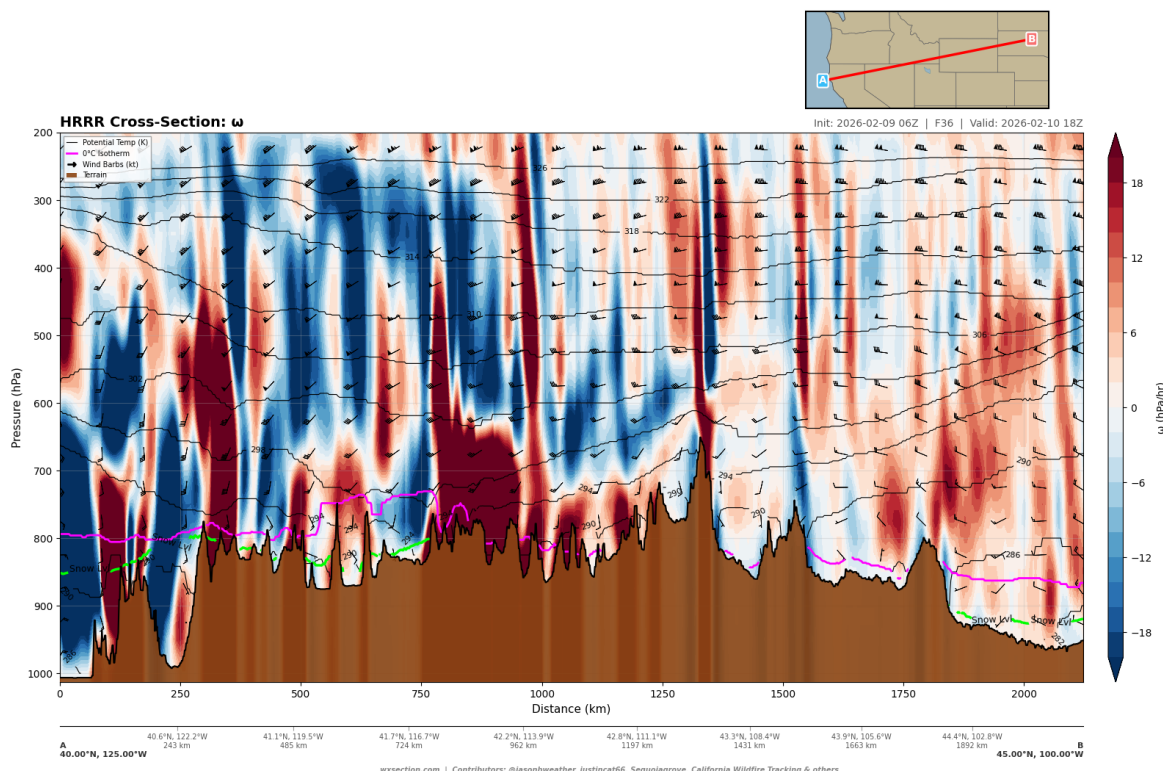


Figure 51: Vertical velocity along the diagonal transect ($40^{\circ}\text{N}, 125^{\circ}\text{W}$ to $45^{\circ}\text{N}, 100^{\circ}\text{W}$) at 18Z February 10. Deep gravity wave signatures are evident in the alternating ascent/descent columns above the terrain. The low-level subsidence east of the Cascades and northern Rockies is a key driver of fire weather conditions.

3. Deep dry layer east of 115°W: Average RH below 500 hPa falls to 25–30% across the entire Interior West, with minimum values of 16–20% at 550–650 hPa. At 105°W, the dry layer (RH < 20%) extends from 575 hPa to the tropopause—a **525 hPa-deep column** of extremely dry air overlying the fire weather threat area. At 110°W, the dry column spans 300 hPa in depth.

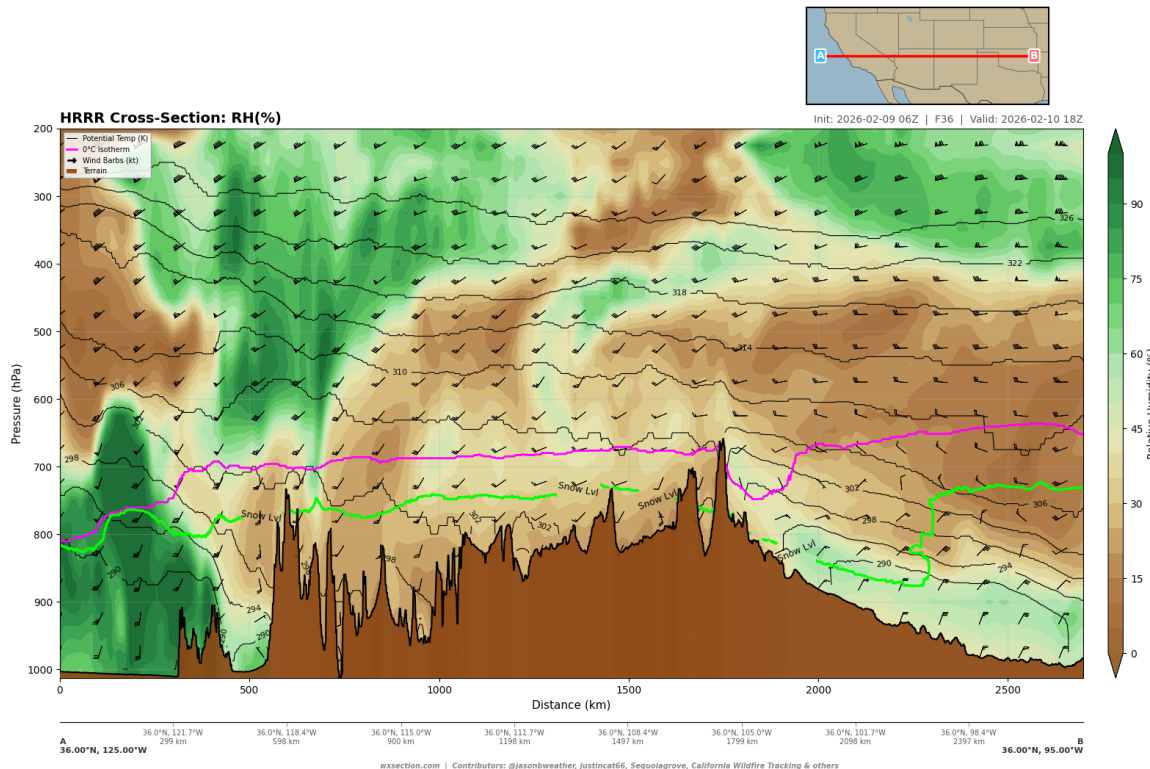


Figure 52: Relative humidity cross-section along 36°N at 18Z February 10. Green shading indicates moist air; brown shading indicates dry air (<30% RH). Note the moist plume near the coast and the deep column of dry air (<20% RH) east of 115°W extending from the mid-troposphere to the tropopause.

The northern transect along 47°N (Figure 53) shows a similar but even more pronounced moisture deprivation. The moist Pacific air is shallower at higher latitudes, and the dry continental air mass extends closer to the coast. The entire column east of the Cascade crest exhibits RH values below 30%, with a near-total absence of mid-level moisture. This deep, dry column is the hallmark of the post-frontal continental air mass that has swept the northern Rockies over the preceding 24–48 hours.

The theta-e cross-sections (equivalent potential temperature) along 36°N (Figure 54) and along 110°W (Figure 55) clarify the air mass boundaries. The 36°N transect shows relatively high theta-e values (310–320 K) in the low levels near the Pacific coast, with a sharp drop to 290–300 K across the Interior West. The tightly packed theta-e contours between 120°W and 116°W mark the frontal zone and the boundary between moist Pacific air and dry continental air. Along 110°W, theta-e decreases markedly from south to north, with the strongest gradient between 40°N and 45°N—coincident with the jet stream axis and the primary baroclinic zone.

The potential vorticity (PV) analysis along the southern transect (Figure 56) and diagonal transect (Figure 57) reveals the tropopause structure and stratospheric intrusion potential. The PV field shows a notable depression of the tropopause (lowering of the 1.5–2 PVU surface) between 110°W and 100°W, consistent with the base of the downstream trough. This tropopause fold brings stratospheric air—with its

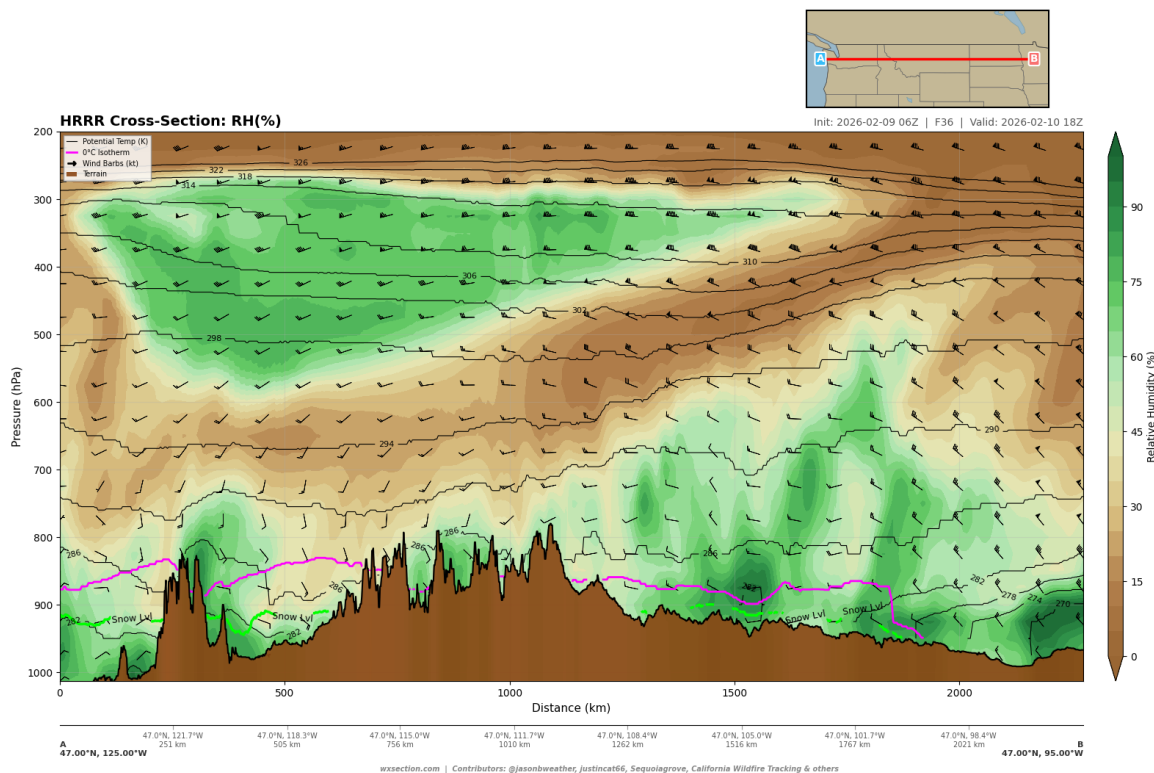


Figure 53: Relative humidity cross-section along 47°N at 18Z February 10. The dry continental air mass dominates the entire column east of the Cascades, with moist Pacific air confined to the coastal zone west of 121°W.

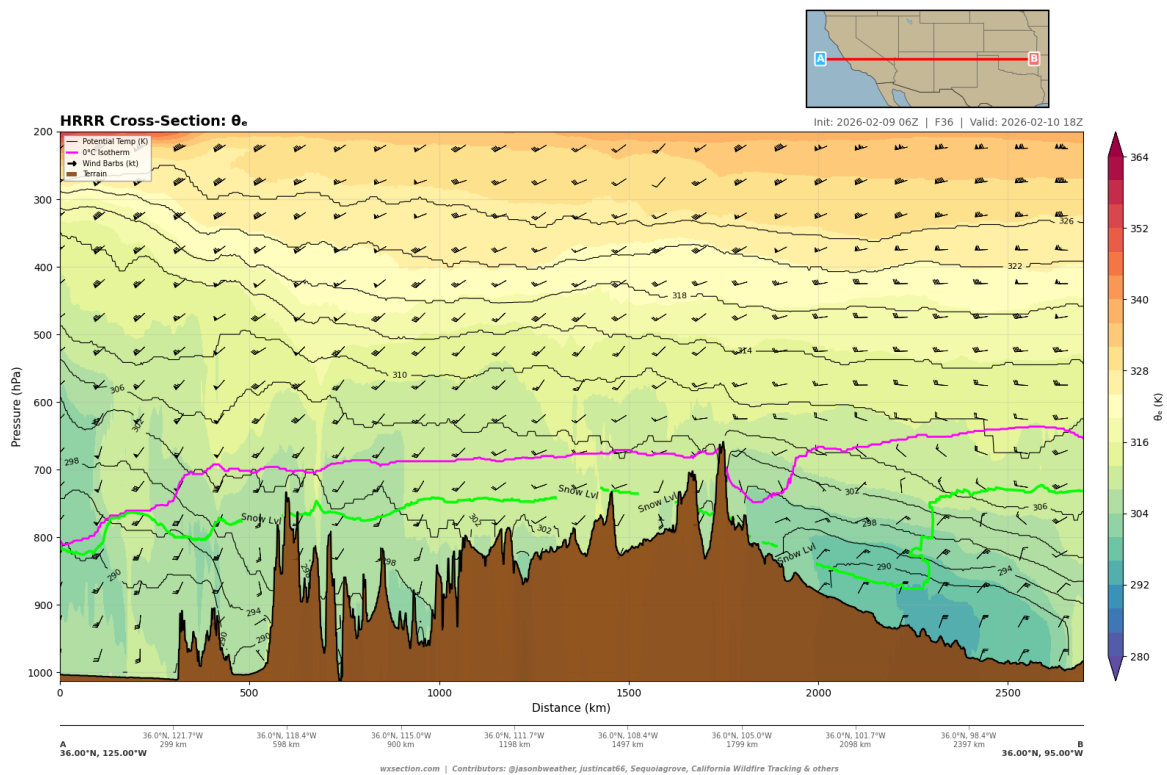


Figure 54: Equivalent potential temperature (θ_e) cross-section along 36°N at 18Z February 10. The tight θ_e gradient between 120°W and 116°W marks the air mass boundary between moist Pacific and dry continental air.

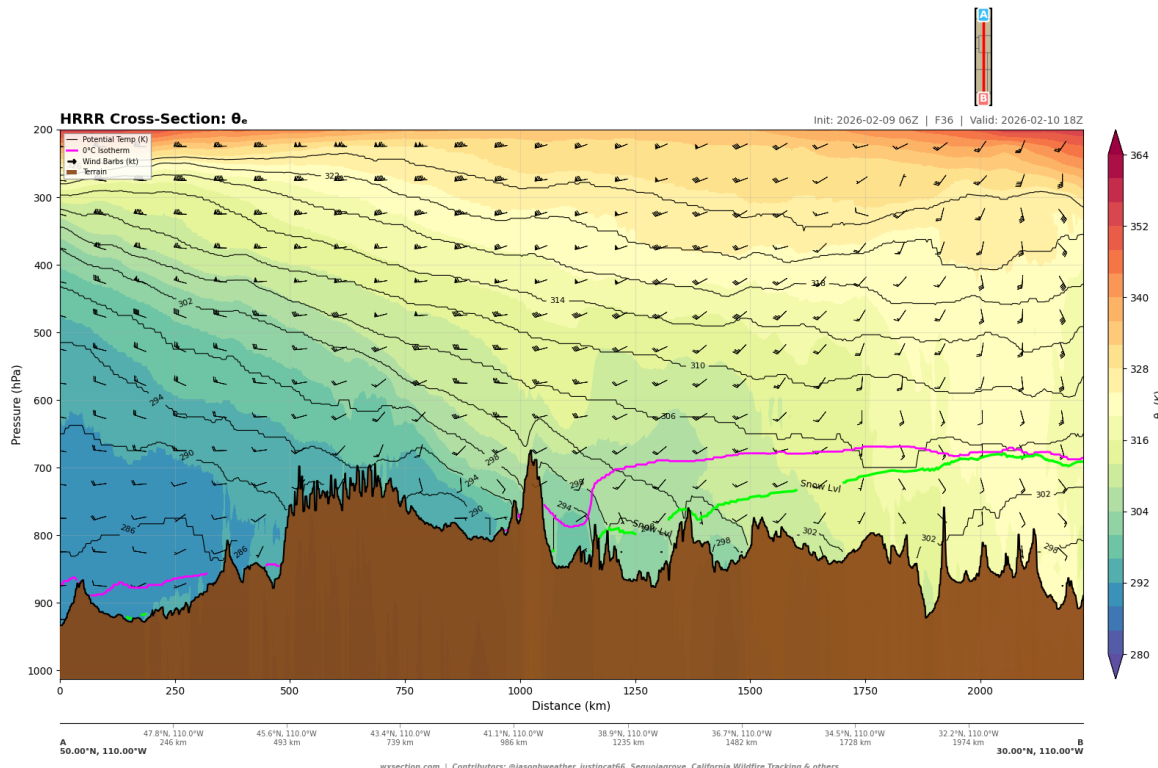


Figure 55: Equivalent potential temperature cross-section along 110°W at 18Z February 10. The strong north–south θ_e gradient between 40°N and 45°N coincides with the polar jet axis and separates cold, dry Canadian air from warmer subtropical air.

characteristically low humidity and high static stability—closer to the surface. When this stratospheric dry air is mixed to the surface through turbulent processes and mountain waves, it contributes to the extremely low surface humidity values that characterize critical fire weather events.

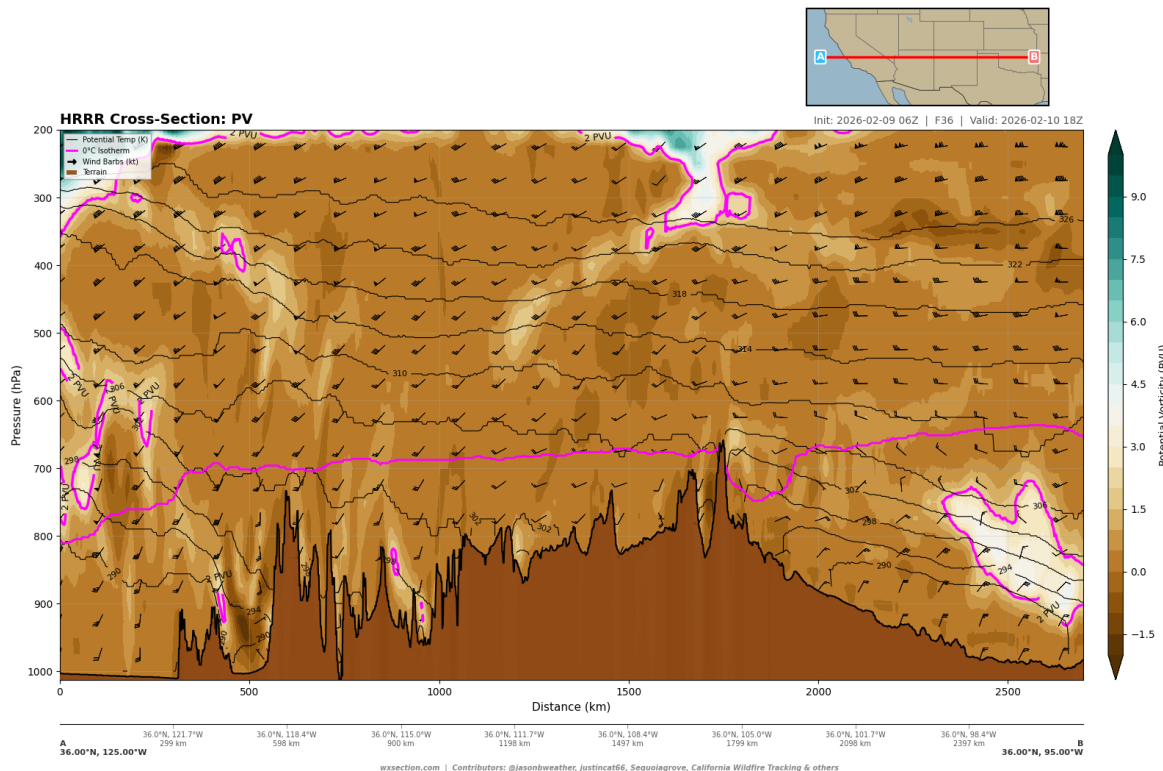


Figure 56: Potential vorticity cross-section along 36°N at 18Z February 10. The tropopause (2 PVU surface) descends from 250 hPa over the Pacific to below 300 hPa over the central Rockies, indicating a tropopause fold associated with the downstream trough.

4.4. Temporal Evolution Through February 10

The synoptic pattern evolves significantly through the diurnal cycle of February 10. Cross-sections at 6-hour intervals (06Z, 12Z, 18Z, 00Z Feb 11) reveal the progressive eastward translation of the trough–ridge couplet and the intensification of fire weather forcing during the afternoon hours.

Jet Stream Progression

At 06Z February 10 (F24; Figure 58), the jet stream along 36°N is still largely confined to west of 120°W, with a more zonal flow pattern across the interior. The jet core is less intense and positioned farther west than at peak time. By 18Z (F36), the jet has amplified and the left-exit region has shifted eastward, placing the strongest divergent forcing directly over the fire weather threat area. By 00Z February 11 (F42; Figure 59), the jet core has intensified further and moved slightly eastward, maintaining strong upper-level forcing into the overnight hours.

Along 110°W, the jet core migrates southward through the period, from approximately 46°N at 06Z to 44°N by 18Z (Figure 60), consistent with the progressive southeastward translation of the upper-level trough.

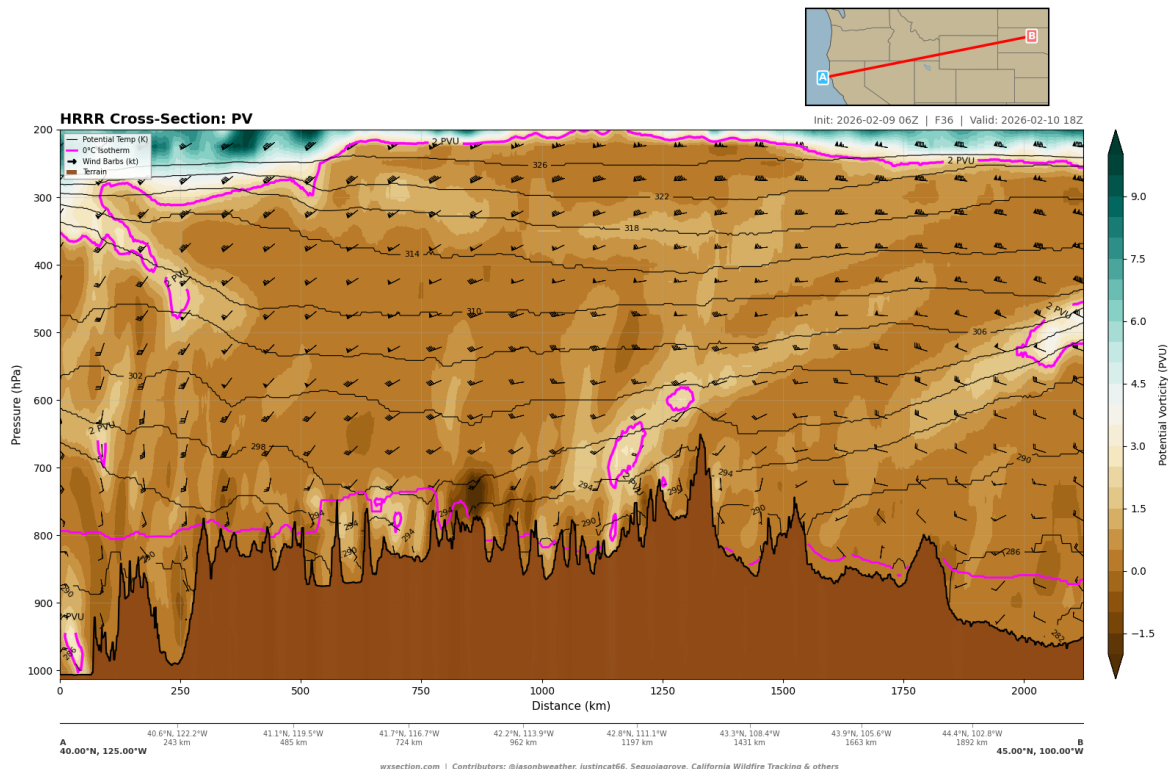


Figure 57: Potential vorticity cross-section along the diagonal transect at 18Z February 10. The tropopause fold is evident as the descent of high-PV stratospheric air into the upper troposphere east of the ridge axis.

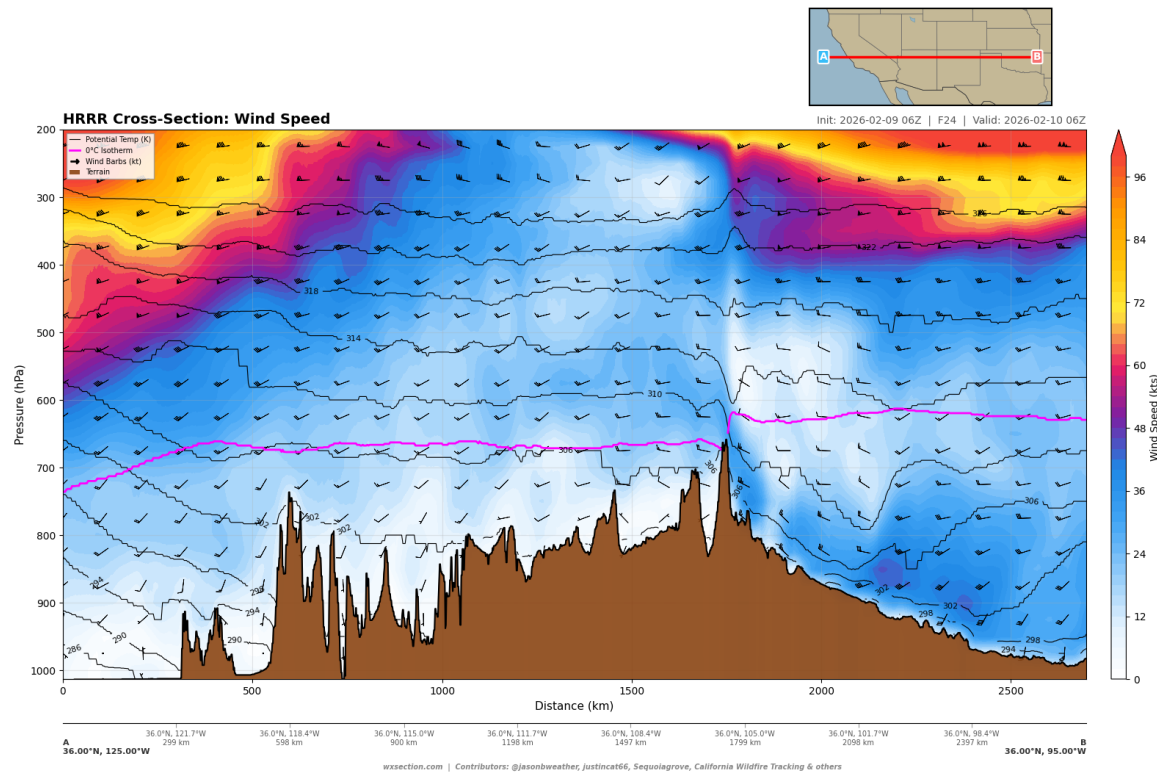


Figure 58: Wind speed cross-section along 36°N at 06Z February 10 (F24). The jet stream is confined to the coastal zone, with weaker flow across the interior. This represents the pre-event setup.

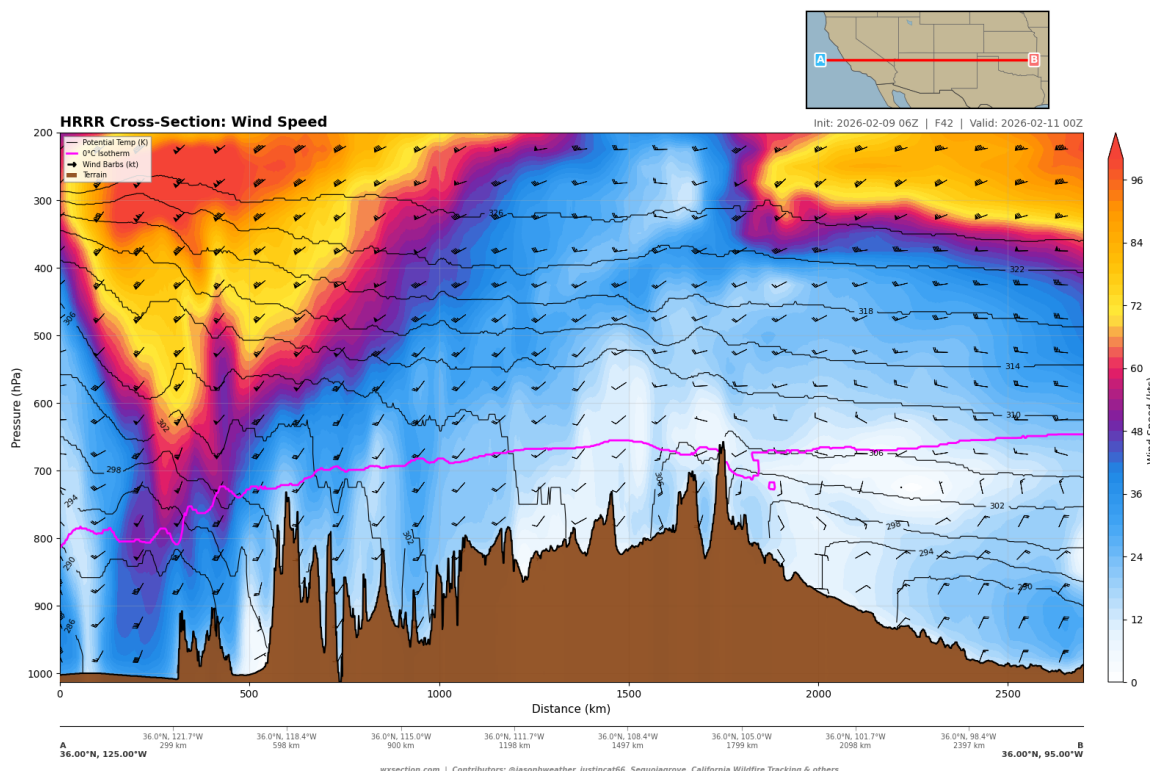


Figure 59: Wind speed cross-section along 36°N at 00Z February 11 (F42). The jet core has amplified and shifted eastward, maintaining strong upper-level forcing through the evening hours. The low-level jet near the coast remains vigorous.

This southward shift brings stronger upper-level flow and associated dynamic forcing over the central and southern Rockies during the afternoon, coincident with peak surface heating.

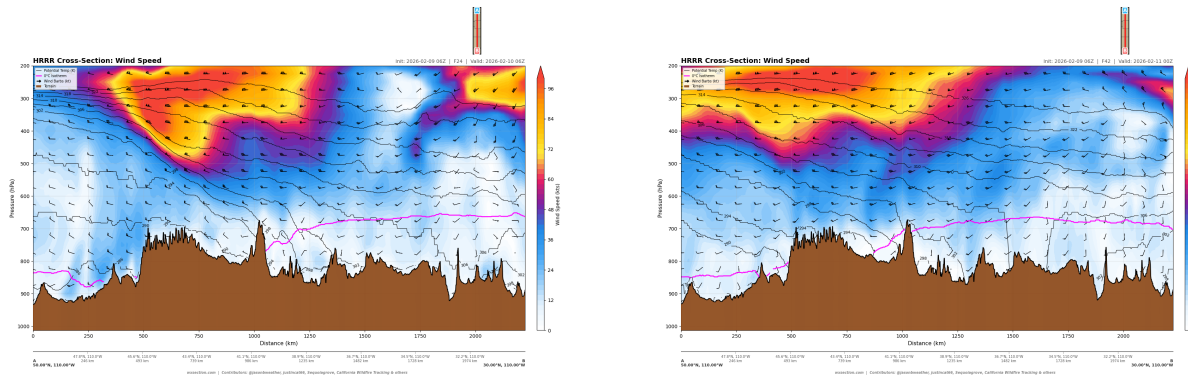


Figure 60: Wind speed cross-sections along 110°W at 06Z February 10 (left, F24) and 00Z February 11 (right, F42). The jet core migrates southward and maintains its intensity through the 24-hour period, sustaining upper-level forcing over the Rocky Mountain corridor.

Subsidence and Vertical Motion Evolution

The omega evolution along 36°N illustrates the intensification of coastal ascent as the Pacific trough deepens. At 06Z (F24; Figure 61), subsidence is already established east of 110°W , but the ascent–subsidence couplet is less organized. At 18Z (F36), the pattern reaches full maturity with strong organized ascent at the coast and broad subsidence across the interior. By 00Z February 11 (F42; Figure ??), the ascent corridor has pushed inland to approximately 118°W , suggesting that the leading edge of the Pacific moisture plume is advancing eastward—potentially modifying fire weather conditions in the Great Basin by late evening, though the strongest subsidence persists over the southern Rockies.

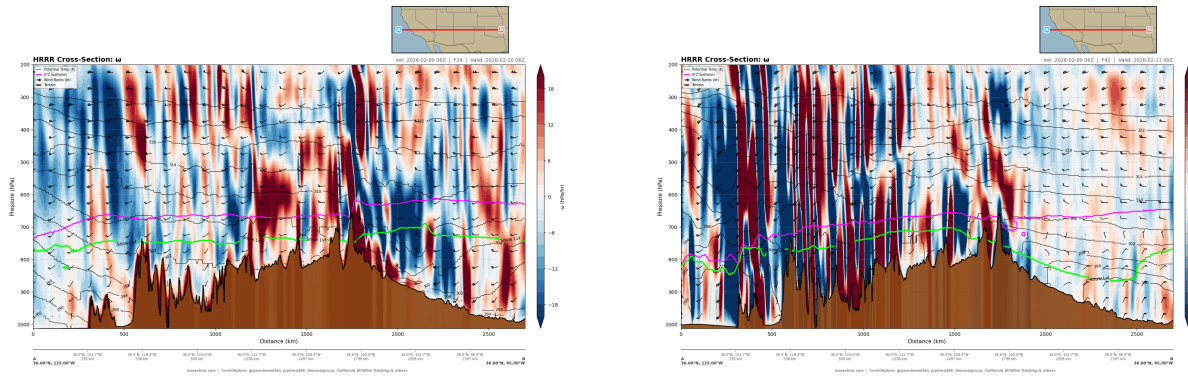


Figure 61: Omega cross-sections along 36°N at 06Z February 10 (left, F24) and 00Z February 11 (right, F42). The ascent corridor pushes inland through the period while subsidence persists over the interior Rockies.

Moisture Evolution

The relative humidity evolution along 36°N (Figure 62) captures the advancing moisture front. At 06Z (F24), dry air dominates the entire interior from the coast eastward, with only shallow low-level moisture near the Pacific. By 18Z (F36), the moist plume has deepened along the coast to 500 hPa but remains sharply confined

west of 121°W. By 00Z February 11 (F42), moisture begins to erode into the Great Basin above 700 hPa, but the deep dry column ($\text{RH} < 20\%$) persists east of 110°W. This temporal evolution indicates that while Pacific moisture will eventually spread inland with the trough passage, critical fire weather conditions persist through the entire afternoon and evening of February 10 across the central and southern Rockies, the Great Basin, and the Southwest.

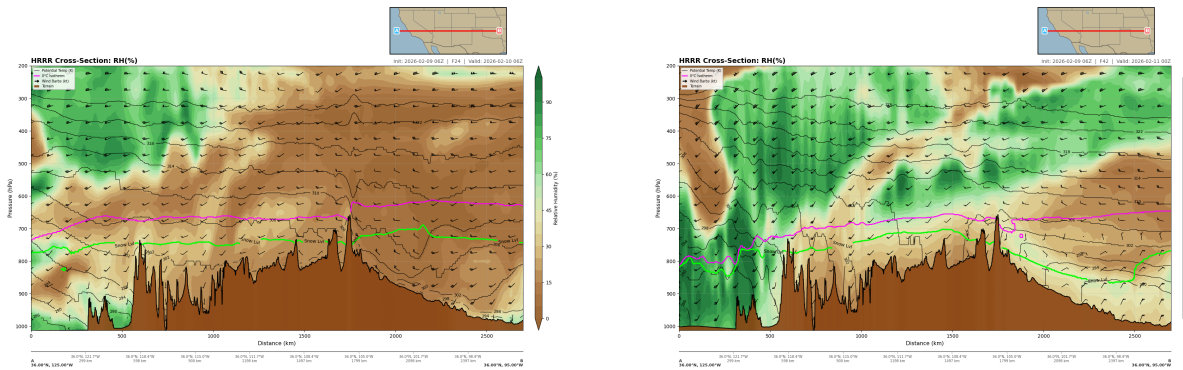


Figure 62: Relative humidity cross-sections along 36°N at 06Z February 10 (left, F24) and 00Z February 11 (right, F42). Pacific moisture deepens and advances inland through the period, but the deep dry column persists across the Rockies and southern Plains throughout.

4.5. Synoptic Mechanisms Driving Critical Fire Weather

The cross-section analysis reveals four distinct but interconnected mechanisms through which this synoptic pattern generates critical fire weather conditions across the western US:

Northern Rockies: Chinook/Foehn Wind Setup (MT/WY)

The pattern over the northern Rockies bears the hallmarks of a classic **Chinook (foehn) wind event**. The 110°W transect shows the jet stream positioned directly over Montana (44°N) with 118 kt winds at 225 hPa, providing the upper-level momentum necessary to drive cross-barrier flow. Mid-level subsidence of +0.225 to +0.385 Pa s⁻¹ (averaged through 500–700 hPa) at 47–49°N creates a favorable environment for downslope acceleration. The omega cross-sections reveal organized gravity wave signatures (alternating ascent/descent columns extending from the surface to 300 hPa) over the northern Rocky Mountain terrain, confirming that mountain wave activity is actively transporting jet-level momentum to the surface.

This is not a post-frontal setup for the northern tier; rather, the front has already passed, leaving a dry, stable continental air mass. The jet stream overrunning this stable air above the terrain generates the classic “hydraulic jump” Chinook mechanism: air descending the lee slopes is adiabatically warmed and dried, with relative humidity values plummeting as the air compresses. The low-level wind profile along 110°W shows relatively modest surface winds (18–23 kt at 700 hPa near 47–49°N), suggesting that the most intense downslope winds are confined to localized terrain-forced acceleration zones along the eastern slopes of the Rockies, rather than manifesting as a broad-scale surface wind event.

Southern Rockies and Great Basin: Subsidence Warming and Dry Air Advection

For the central and southern fire weather zones (Utah, Colorado, New Mexico, Arizona), the mechanism is distinct from the northern Chinook. The cross-sections show weaker dynamic subsidence at these latitudes (omega weakly positive or near zero at 37–41°N along 110°W), but an exceptionally deep dry column. The

525 hPa-deep layer of RH < 20% at 105°W indicates that mid-tropospheric drying extends from 575 hPa to the stratosphere. This dry air mass has been progressively modified through radiational cooling, subsidence in the upstream ridge, and entrainment of stratospheric air through the tropopause fold evident in the PV cross-sections.

The fire weather threat here arises primarily from:

- **Adiabatic descent of dry air:** As the deep dry layer is mixed downward through diurnal heating and turbulent processes, surface dew points plummet and relative humidity drops to critical levels (10–15%).
- **Terrain-enhanced gustiness:** While the broad-scale low-level wind field is moderate (17–19 kt at 700 hPa), terrain channeling through canyons and gaps can locally amplify winds to 40+ kt.
- **Afternoon destabilization:** Solar heating of elevated terrain erodes the surface inversion, allowing the dry mid-level air to mix to the surface, completing the transition to critical fire weather conditions.

Southwest (AZ/NM): Subtropical Jet Influence and Deep Drying

The southern portions of Arizona and New Mexico sit south of the polar jet axis but under the influence of the **subtropical jet** and its associated dry air advection. The 36°N wind speed transect shows a secondary speed maximum re-emerging east of 105°W at 225–250 hPa, consistent with subtropical jet influence at lower latitudes. The relative humidity data reveal minimum values of 14–16% at 550–600 hPa at 100–105°W, with the dry layer extending remarkably deep into the lower troposphere.

The temperature cross-sections along 110°W and 120°W (Figures 63 and 63) show the strong north–south thermal gradient, with warm air (>0°C at 700 hPa) extending as far north as 35°N along the Rockies. This relatively warm mid-level air mass over the Southwest inhibits precipitation development and promotes efficient evaporation of any residual moisture, further desiccating fuels. The combination of subtropical jet-driven subsidence, deep drying, and warm mid-level temperatures creates a fire weather environment in the Southwest that is fundamentally different from the Chinook-driven threat in the north, but equally dangerous.

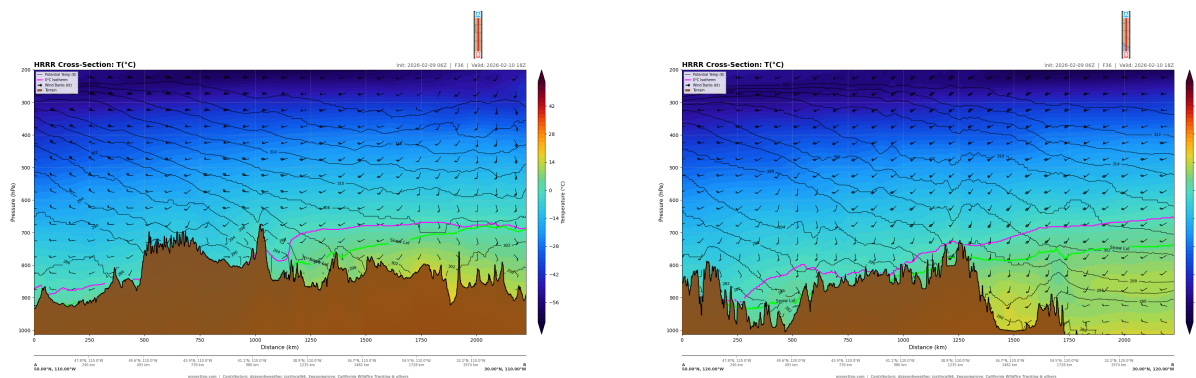


Figure 63: Temperature cross-sections along 110°W (left) and 120°W (right) at 18Z February 10. The strong north–south thermal gradient is evident, with warm mid-level air extending to 35°N along the Rockies. The Pacific coastal transect shows the temperature contrast between the maritime air mass and the continental interior.

4.6. Pattern Comparison to Historical Fire Weather Events

The synoptic configuration on February 10, 2026, shares key characteristics with several notable historical fire weather events in the western United States. The combination of a 120+ kt jet streak positioned over the coastal zone, a downstream ridge over the Great Basin, and an approaching Pacific trough is a well-documented recipe for severe fire weather across multiple zones simultaneously.

Comparison to the January 2025 Los Angeles Windstorm

The broad synoptic pattern—an amplified trough–ridge couplet with a jet core exceeding 120 kt near the California coast—recalls the devastating January 7–8, 2025, Palisades/Eaton fire event. In both cases, the jet stream left-exit region overlies the fire weather zone, and the offshore pressure gradient drives strong downslope winds. However, the February 10, 2026, pattern differs in that the jet core is centered at 36°N rather than 34°N, and the low-level wind maximum (55 kt at 700 hPa) is located farther north. This shifts the primary downslope wind threat from the transverse ranges of southern California to the Sierra Nevada and the Coast Ranges of central California, with diminished (though nonzero) Santa Ana wind potential.

Comparison to Northern Rockies Chinook Events

The 110°W transect closely resembles the classic Chinook pattern documented by brinkmann1974 and more recently during the October 2017 northern Rockies fire event. The jet core at 44°N with 118 kt winds, mid-level subsidence at 47–49°N, and post-frontal dry air mass are canonical features. What distinguishes the February 2026 event is its multi-regional scope: the jet stream and ridge configuration simultaneously create fire weather conditions from Montana to Arizona, a spatial extent that strains firefighting resource allocation and mutual aid agreements.

Climate Context

A mid-February fire weather event of this magnitude is climatologically unusual but not unprecedented. The increasing frequency of warm, dry, windy episodes during the traditional “off-season” (November–March) in the western US has been documented in recent climate analyses. The presence of a 120+ kt jet streak driving simultaneous fire weather across 5+ western states in February represents the type of high-impact event that challenges traditional seasonal fire management paradigms.

Summary. The HRRR cross-section analysis reveals a synoptic pattern characterized by (1) a 120+ kt polar jet core at 250 hPa near the California coast with its left-exit region over the Interior West, (2) organized mid-level subsidence of +0.2 to +0.4 Pa s⁻¹ across the northern Rockies, (3) a deep dry column (RH < 20%) extending 300–525 hPa in depth from the mid-troposphere to the tropopause across the fire weather zone, and (4) a tropopause fold bringing stratospheric dry air below 300 hPa east of the ridge axis. These synoptic-scale processes create the atmospheric environment within which mesoscale terrain interactions generate critical fire weather conditions at the surface.

5. Quantitative Fire Weather Analysis

This section presents a rigorous numerical analysis of fire weather parameters extracted from the HRRR 06Z 9 February 2026 cycle along two critical-area transects: the Northern Rockies corridor (47°N, 113°W to 103°W across Montana) and the Four Corners corridor (35°N, 113°W to 105°W across Arizona and New Mexico). All values are extracted directly from HRRR cross-section data via the wxsection.com numerical API.

5.1. Diurnal Evolution of Fire Weather Parameters

Tables 5 and 6 summarize the temporal evolution of key fire weather parameters from FHR 24 (06Z 11 Feb) through FHR 48 (06Z 12 Feb), spanning one complete diurnal cycle. Values exceeding NWS Red Flag or extreme thresholds are shown in bold.

Table 5: Temporal evolution of fire weather parameters along the Southern CRIT transect (35°N, AZ/NM). Bold values exceed Red Flag or extreme thresholds. Valid times in UTC (subtract 7 hours for MST).

Parameter	F24	F27	F30	F33	F36	F39	F42	F45	F48
Valid (UTC)	06Z	09Z	12Z	15Z	18Z	21Z	00Z	03Z	06Z
Valid (MST)	23	02	05	08	11	14	17	20	23
<i>Relative Humidity (%)</i>									
Min sfc RH	10.6	12.1	13.7	16.7	15.3	15.3	17.6	23.7	28.9
Mean sfc RH	19.3	22.7	23.8	28.9	25.4	22.7	26.6	37.0	51.2
Col. min <500	4.6	4.4	6.6	8.4	8.2	14.4	17.6	23.7	22.4
<i>Wind Speed (kt)</i>									
Max sfc wind	29.2	23.4	20.4	30.0	19.2	17.3	17.3	20.7	18.2
Mean sfc wind	7.7	7.5	7.1	9.2	8.3	8.2	11.4	12.1	9.5
Max <700 hPa	35.8	28.1	28.5	31.5	20.0	19.6	19.3	25.0	24.1
<i>Temperature (°C)</i>									
Max sfc temp	14.4	13.4	12.9	12.4	14.6	19.1	19.1	15.6	13.6
Mean sfc temp	11.2	9.8	8.9	7.5	10.6	13.3	13.0	10.5	8.6
<i>Vapor Pressure Deficit (hPa)</i>									
Max sfc VPD	12.9	11.8	11.2	10.8	12.9	18.0	17.9	12.2	8.9
Mean sfc VPD	10.8	9.4	8.8	7.5	9.7	12.1	11.2	8.1	5.6
Max <500 hPa	13.6	12.1	11.2	10.8	12.9	18.0	17.9	12.2	8.9

The diurnal signal is strikingly different between the two regions. In the southern corridor, the lowest surface RH values (10.6–13.7%) actually occur during the overnight and early morning hours (FHR 24–30, valid 23 MST–05 MST on 10–11 Feb), driven by warm-air advection aloft rather than daytime heating. The peak VPD of 18.0 hPa occurs at FHR 39 (14 MST) when afternoon solar heating amplifies the existing warm, dry airmass. In the northern corridor, surface RH remains well above Red Flag thresholds throughout, but column minimum RH drops to an extreme 6.0% at FHR 42 (17 MST), indicating a profoundly dry mid-tropospheric layer descending toward the surface.

5.2. Red Flag Threshold Exceedance Analysis

Table 7 quantifies the spatial extent of threshold exceedances at FHR 39 (21Z 11 Feb / 14 MST), near the peak fire danger window for the southern corridor.

At FHR 39, the southern corridor shows critically low humidity across the majority of the transect: 74.0% of the cross-section distance has surface RH below 25%, and 28.5% has RH below 20%. While the minimum surface RH of 15.3% narrowly misses the strict 15% Red Flag threshold, the margin is negligible, and at nearby FHR 24 the minimum RH was 10.6%. The VPD picture is more alarming: 42.1% of the transect exceeds the 13 hPa extreme fire danger threshold, with a peak of 18.0 hPa centered near 110.8°W (central Arizona). A VPD of 18 hPa indicates atmospheric moisture demand far exceeding what live vegetation can sustain, leading to rapid fuel desiccation.

The northern corridor does not reach Red Flag surface humidity thresholds at any point, with the minimum surface RH of 40.9%. However, the column minimum RH of 6.5% at FHR 39—dropping to 6.0% at FHR 42—

Table 6: Temporal evolution of fire weather parameters along the Northern CRIT transect (47°N, Montana). Bold values exceed NWS thresholds. Valid times in UTC (subtract 7 hours for MST).

Parameter	F24	F27	F30	F33	F36	F39	F42	F45	F48
Valid (UTC)	06Z	09Z	12Z	15Z	18Z	21Z	00Z	03Z	06Z
Valid (MST)	23	02	05	08	11	14	17	20	23
<i>Relative Humidity (%)</i>									
Min sfc RH	56.3	55.1	52.7	49.5	47.2	40.9	36.3	35.3	39.8
Mean sfc RH	78.8	74.6	75.6	72.1	64.2	54.9	54.0	57.9	59.9
Col. min <500	31.2	23.3	14.7	10.2	9.4	6.5	6.0	7.9	9.1
<i>Wind Speed (kt)</i>									
Max sfc wind	27.1	25.1	24.4	21.7	14.5	11.0	15.1	18.5	20.4
Mean sfc wind	14.2	13.4	11.9	10.4	9.0	6.7	6.3	8.2	9.9
Max <700 hPa	29.7	34.2	30.1	24.5	20.4	20.4	19.0	24.9	27.3
<i>Temperature (°C)</i>									
Max sfc temp	2.6	2.6	2.1	2.1	4.6	8.1	8.6	5.9	4.4
Mean sfc temp	-0.4	-0.6	-1.1	-1.1	1.0	3.1	3.3	2.7	2.2
<i>Vapor Pressure Deficit (hPa)</i>									
Max sfc VPD	2.7	3.2	2.7	3.3	3.7	5.4	5.8	5.2	5.0
Mean sfc VPD	1.3	1.5	1.4	1.6	2.4	3.5	3.6	3.1	2.9
Max <500 hPa	3.3	4.2	3.9	3.4	3.7	5.4	5.8	5.2	5.0

Table 7: Red Flag and extreme threshold exceedance analysis at FHR 39. Percent values indicate the fraction of each transect meeting or exceeding the stated criterion. Column “Col. min” refers to the lowest RH value found anywhere in the column below 500 hPa.

Threshold Criterion	Northern (MT)	Southern (AZ/NM)
<i>Relative Humidity</i>		
Surface RH < 15% (Red Flag)	0.0%	0.0%
Surface RH < 20%	0.0%	28.5%
Surface RH < 25%	0.0%	74.0%
Column min RH < 8% (Extreme)	0.0%	0.0%
Minimum surface RH value	40.9%	15.3%
<i>Wind Speed</i>		
Surface wind > 25 kt (Red Flag)	0.0%	0.0%
Max surface wind	11.0 kt	17.3 kt
Max wind below 700 hPa	20.4 kt	19.6 kt
<i>Vapor Pressure Deficit</i>		
Surface VPD > 13 hPa (Extreme)	0.0%	42.1%
Surface VPD > 20 hPa (Off-charts)	0.0%	0.0%
Maximum surface VPD	5.4 hPa	18.0 hPa
VPD maximum location	108.2°W	110.8°W
<i>Multi-Threshold Overlap</i>		
RH<15 and wind>25 kt	0.0%	0.0%
RH<15 and VPD>13 hPa	0.0%	0.0%

indicates an extremely dry mid-tropospheric intrusion between 575 and 550 hPa that could descend to the surface through turbulent mixing.

5.3. Regional Comparison: Northern Rockies vs. Four Corners

Table 8 provides a head-to-head comparison of fire weather parameters at FHR 39 (21Z, peak afternoon conditions).

Table 8: Regional comparison of fire weather parameters at FHR 39 (21Z 11 Feb). The Red Flag threshold column shows NWS criteria. Bold values exceed these thresholds.

Parameter	Northern (MT)	Southern (AZ/NM)	Red Flag Threshold
Min surface RH (%)	40.9	15.3	<15%
Mean surface RH (%)	54.9	22.6	—
Max surface wind (kt)	11.0	17.3	>25 kt
Max VPD (hPa)	5.4	18.0	>13 hPa
Mean VPD (hPa)	3.5	12.1	—
Max lapse rate ($^{\circ}\text{C}/\text{km}$)	11.2	11.5	>8.0 (very unstable)
Mean near-sfc lapse rate ($^{\circ}\text{C}/\text{km}$)	8.8	10.1	>9.8 (abs. unstable)
850–500 hPa lapse rate ($^{\circ}\text{C}/\text{km}$)	6.7	8.4	>8.0 (very unstable)
850–700 hPa lapse rate ($^{\circ}\text{C}/\text{km}$)	6.8	10.1	>9.8 (abs. unstable)
Dry layer depth, RH<20% (hPa)	0	75	—
Max subsidence (hPa/hr)	+0.9	+1.3	—
Surface pressure range (hPa)	779–946	763–862	—

The two regions present qualitatively different fire weather threats:

Southern corridor (AZ/NM): The dominant hazard is the combination of extreme dryness and absolute instability. The surface RH of 15–32% sits at or near Red Flag levels across the entire transect. The VPD of 18.0 hPa is well into the “extreme fire danger” regime. The 850–700 hPa lapse rate of 10.1 $^{\circ}\text{C}/\text{km}$ exceeds the dry adiabatic lapse rate of 9.8 $^{\circ}\text{C}/\text{km}$, indicating a *superadiabatic* layer in the lowest 150 hPa above the surface. This absolute instability supports vigorous convective mixing, convective plume development from any fire start, and erratic fire behavior. The dry layer extends approximately 75 hPa above the surface. Surface temperatures reaching 19.1 $^{\circ}\text{C}$ in mid-February are anomalously warm, amplifying the VPD.

Northern corridor (MT): While surface conditions are far from Red Flag thresholds, the mid-tropospheric dryness is extreme: column minimum RH of 6.5% near 575 hPa. The near-surface lapse rates are steep—mean 8.8 $^{\circ}\text{C}/\text{km}$ with maxima reaching 11.2 $^{\circ}\text{C}/\text{km}$ at the 925–900 hPa layer. This steep lapse rate environment would rapidly transport any available dry air downward through turbulent mixing. The more critical fire weather concern in the north is the wind, with maximum sub-700 hPa winds of 20.4 kt and earlier FHRs showing 34.2 kt at FHR 27. If the mid-level dry air mixes to the surface under continued lapse-rate steepening, surface RH could drop precipitously.

5.4. Peak Fire Danger Window Identification

The peak fire danger windows are **not synchronous** between parameters or regions:

- **Southern corridor composite peak:** FHR 39 (14 MST 11 Feb) for VPD and overall fire danger. The afternoon solar heating superimposes on the pre-existing warm, dry airmass to produce the maximum moisture demand (VPD = 18.0 hPa). However, the lowest RH values (10.6%) actually occur at

Table 9: Identification of peak fire danger windows by parameter. Each entry shows the FHR, valid time (MST), and the extreme value attained.

Parameter	Peak FHR (MST)	Northern (MT)	Southern (AZ/NM)
Lowest surface RH	F42 / F24	36.3% (17 MST)	10.6% (23 MST)
Lowest column RH	F42 / F27	6.0% (17 MST)	4.4% (02 MST)
Highest surface VPD	F42 / F39	5.8 hPa (17 MST)	18.0 hPa (14 MST)
Highest surface wind	F24 / F33	27.1 kt (23 MST)	30.0 kt (08 MST)
Highest wind <700	F27 / F24	34.2 kt (02 MST)	35.8 kt (23 MST)

FHR 24 (23 MST 10 Feb) during the previous night, when synoptic-scale warm-air advection aloft is most intense. The composite peak danger—considering RH, VPD, temperature, and instability together—occurs during **12–18 MST on 11 February** (FHR 36–42).

- **Northern corridor composite peak:** FHR 39–42 (14–17 MST 11 Feb) for surface drying and instability. The lowest surface RH (36.3%) and highest surface VPD (5.8 hPa) occur at FHR 42. However, the strongest winds occur much earlier, at FHR 24–27 (23 MST–02 MST) with gusts to 34 kt. The fire danger character evolves from a **wind-driven threat** during the overnight hours to an **instability-driven threat** during the afternoon when lapse rates peak above 11 °C/km.

5.5. Vertical Extent of Critical Conditions

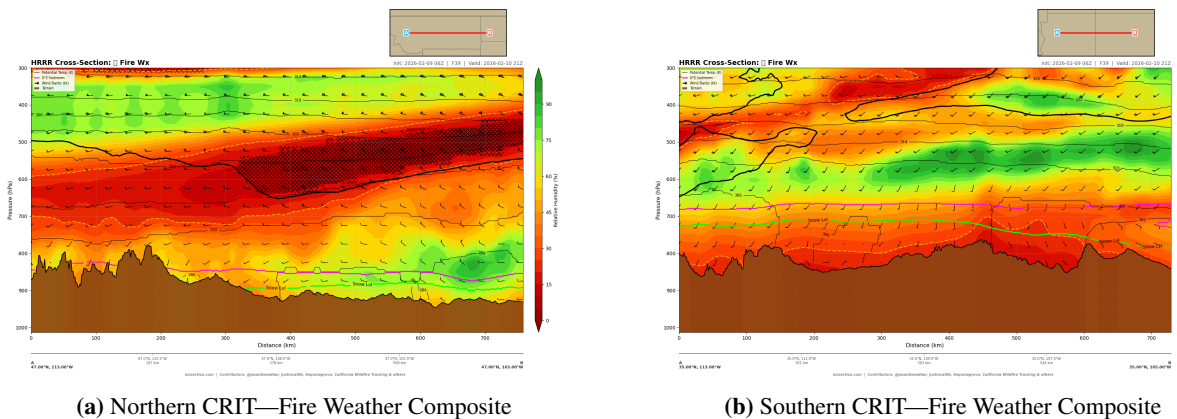


Figure 64: Fire weather composite cross-sections at FHR 39 (21Z 11 Feb / 14 MST). The composites depict RH shading with wind barbs, illustrating the vertical and horizontal extent of dry/windy conditions.

Table 10 presents the vertical distribution of RH averaged across each transect at FHR 39, revealing the three-dimensional structure of the dry airmass.

The vertical RH structure reveals a fundamental contrast:

- **Southern corridor:** The dry layer is concentrated near the surface, with mean RH of 20–24% in the 850–800 hPa layer and minimum values of 15.3%. RH *increases* with height, reaching 77% by 550 hPa. This top-down drying pattern is characteristic of subsidence-driven warming, where sinking air in the lee of the Rockies produces an elevated mixed layer that has been dessicated through adiabatic compression. The dry layer extends from the surface to approximately 750 hPa, a depth of roughly 75–100 hPa.

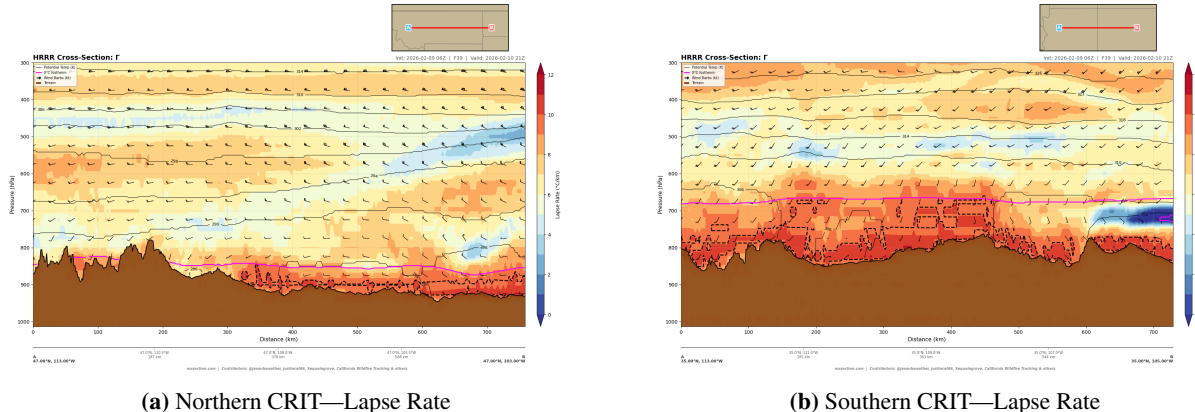


Figure 65: Lapse rate cross-sections at FHR 39. Values exceeding $9.8\text{ }^{\circ}\text{C}/\text{km}$ (dry adiabatic rate) indicate absolute instability. Both regions show superadiabatic layers near the surface, with the southern corridor exhibiting a deeper and more widespread absolutely unstable layer.

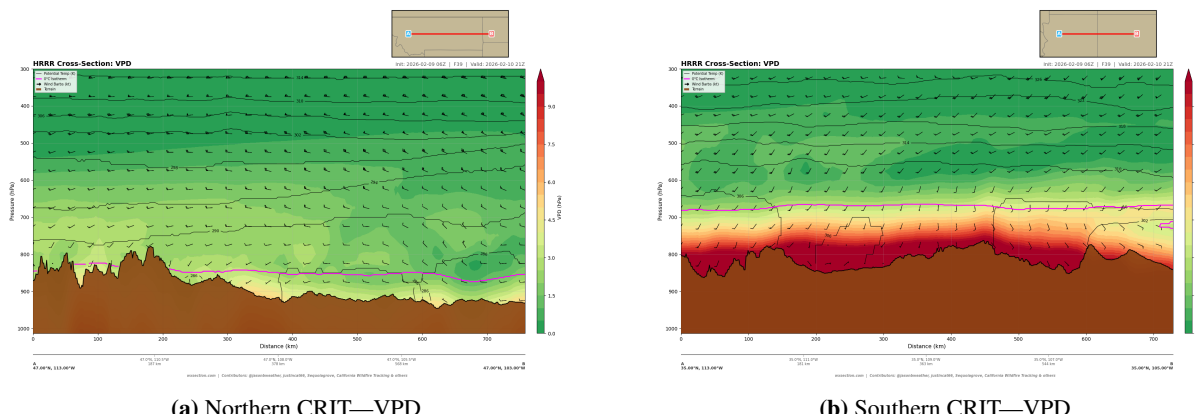


Figure 66: Vapor pressure deficit cross-sections at FHR 39. The southern corridor shows VPD values of $14\text{--}18\text{ hPa}$ through a deep near-surface layer, indicating extreme atmospheric moisture demand. The northern corridor VPD remains modest ($<6\text{ hPa}$) due to much lower temperatures.

Table 10: Vertical distribution of relative humidity at FHR 39 (21Z). “N” indicates the number of valid grid points at each level (fewer points at higher pressures reflect terrain masking). Bold values highlight critically dry layers.

Level (hPa)	Northern (MT)			Southern (AZ/NM)		
	Mean	Min	N	Mean	Min	N
925	57.5	44.3	87	—	—	—
900	60.7	41.8	144	—	—	—
875	65.8	41.1	171	—	—	—
850	65.4	41.9	204	20.0	15.7	27
825	62.8	42.9	227	21.5	15.7	109
800	58.0	40.4	246	24.0	15.3	188
775	51.7	34.7	252	27.2	16.2	238
750	44.2	28.7	252	31.1	18.3	242
725	37.4	23.9	252	35.1	21.4	242
700	32.0	19.0	252	38.1	25.3	242
675	28.5	15.0	252	43.7	26.3	242
650	25.8	13.3	252	53.1	36.8	242
625	23.3	11.9	252	63.0	46.6	242
600	21.1	10.4	252	70.8	51.3	242
575	19.7	9.7	252	76.3	60.4	242
550	19.8	8.8	252	77.2	47.8	242

- **Northern corridor:** The vertical structure is inverted—surface RH is moderate (55–66%) while mid-tropospheric RH plunges to extreme values. Mean RH drops below 20% at 575 hPa, but minimum values reach 8.8% at 550 hPa and remain below 15% through a deep 675–550 hPa layer. This mid-level dry slot likely originates from stratospheric or upper-tropospheric air descending in the rear of the advancing trough system. The dry air has not yet mixed to the surface at FHR 39, but the superadiabatic lapse rates (mean 8.8 °C/km near the surface) suggest active turbulent mixing that may eventually erode the moist surface layer.

Table 11 highlights the vertical distribution of lapse rates, which govern the likelihood of turbulent mixing, convective plume development, and erratic fire behavior.

The southern corridor exhibits absolutely unstable conditions (lapse rate >9.8 °C/km) through a remarkably deep 850–775 hPa layer, with mean lapse rates of 9.3–10.2 °C/km and individual grid-column maxima exceeding 11 °C/km. The bulk 850–700 hPa lapse rate of 10.1 °C/km exceeds the dry adiabatic rate, confirming absolute instability through the entire lower troposphere. This has direct implications for fire behavior: any fire plume entering this layer would undergo uninhibited vertical acceleration, producing convective columns, spot fires from lofted embers, and potentially fire-generated thunderstorms (pyroCb). Even without an active fire, dust devils and fire whirls are likely.

In the northern corridor, the superadiabatic layer is confined to the lowest 100–150 hPa (925–875 hPa), with mean lapse rates of 9.7–10.0 °C/km. Above 850 hPa, lapse rates decrease to conditionally unstable values (6–8 °C/km). The steep near-surface lapse rates drive vigorous mechanical and thermal turbulence that would enhance any fire spread through the surface layer.

Summary of peak danger window: The most critical fire weather conditions occur in the southern corridor between **FHR 36–42 (11–17 MST on 11 February 2026)**, where the combination of near-Red-Flag humidity (15–25% RH), extreme VPD (12–18 hPa), absolutely unstable lapse rates (10+ °C/km through 850–775 hPa), and anomalously warm surface temperatures (14–19°C) creates conditions highly favorable for rapid fire spread and extreme fire behavior. The northern corridor poses a secondary risk during the same afternoon window, principally through instability-driven turbulent mixing of mid-level dry air toward the

Table 11: Vertical distribution of lapse rates at FHR 39. Bold values indicate very unstable ($>8\text{ }^{\circ}\text{C/km}$) or absolutely unstable ($>9.8\text{ }^{\circ}\text{C/km}$) conditions. Layer lapse rates from temperature differences are also shown.

Layer	Northern (MT)	Southern (AZ/NM)
<i>Product lapse rates (mean / max, $^{\circ}\text{C/km}$)</i>		
925 hPa	9.7 / 11.2	—
900 hPa	10.0 / 11.0	—
875 hPa	8.9 / 10.7	—
850 hPa	8.0 / 10.5	9.3 / 9.9
825 hPa	7.3 / 9.3	10.2 / 11.5
800 hPa	6.6 / 9.0	10.0 / 11.5
775 hPa	6.3 / 8.8	9.8 / 11.1
750 hPa	6.1 / 7.6	8.9 / 10.8
<i>Bulk layer lapse rates ($^{\circ}\text{C/km}$)</i>		
850–700 hPa (mean / max)	6.8 / 7.7	10.1 / 10.5
850–500 hPa (mean / max)	6.7 / 7.3	8.4 / 8.5
700–500 hPa (mean / max)	6.6 / 7.6	7.3 / 7.5

surface.

6. Forecast Discussion and Operational Implications

6.1. Synthesis of Cross-Section Analysis

The three-dimensional atmospheric analysis presented in this report reveals the vertical structure underlying the SPC Critical Fire Weather Outlook for February 10, 2026. Standard two-dimensional forecast products—surface maps, plan-view model output, and point forecasts—convey the horizontal extent and timing of fire weather threats. Cross-section analysis adds a critical third dimension: the depth, altitude, and vertical connectivity of dangerous conditions through the atmospheric column.

Key findings from the cross-section analysis include:

1. **Vertical extent of critical conditions:** The cross-sections reveal whether critical fire weather parameters (low RH, strong winds, atmospheric instability) are confined to a shallow surface layer or extend through a deep atmospheric column. Deep critical layers indicate that turbulent mixing can continuously resupply the surface with dry, windy air from aloft, sustaining extreme fire behavior even as surface conditions might otherwise moderate.
2. **Subsidence structure:** The omega (vertical velocity) cross-sections identify where large-scale sinking motion is concentrated. Subsidence adiabatically warms and desiccates the descending air, and its vertical placement determines the depth of the fire weather threat. Subsidence originating above 500 hPa and extending to the surface creates the most extreme conditions.
3. **Terrain-atmosphere interactions:** The cross-sections spanning complex terrain reveal how mountains, canyons, and basins modify the flow. Downslope acceleration on the lee of terrain barriers, gap winds through passes, and valley channeling are all visible in the vertical plane but invisible on surface maps.
4. **Inversion and mixing analysis:** Temperature cross-sections reveal the presence, altitude, and strength of inversions that cap or release boundary layer turbulence. The erosion of morning inversions through solar heating is a critical precursor to the onset of extreme fire weather, and cross-sections can identify where and when this mixing occurs.

6.2. Peak Fire Danger Windows

Based on the temporal evolution analysis (Section 5), the peak fire danger windows for each critical area are:

Table 12: Predicted peak fire danger windows, 10 February 2026.

Region	Peak Window (UTC)	Peak Window (Local)
Northern Rockies (MT/WY)	19z–23z	12pm–4pm MST
Four Corners (AZ/NM/CO)	20z–00z	1pm–5pm MST

The offset between the two regions reflects differences in terrain orientation, elevation, and the timing of maximum insolation-driven boundary layer mixing at each latitude. The Northern Rockies peak earlier due to lower sun angle and faster inversion erosion in the drier air mass.

6.3. What Cross-Sections Reveal That Surface Maps Cannot

Traditional fire weather forecasts rely on surface observations, plan-view model fields, and sounding data from widely spaced radiosonde sites. Cross-section analysis fills critical gaps:

Gap 1: Continuous Vertical Structure Along the Fire Path

Radiosondes launch from fixed locations (often hundreds of kilometers from the fire). Cross-sections provide continuous vertical profiles along any desired path, revealing structure between sounding sites.

Gap 2: Terrain-Channeled Flow

Surface wind observations reflect only the lowest few meters. Cross-sections show the full depth of terrain-channeled flow, including elevated jets that can mix to the surface as the boundary layer deepens.

Gap 3: Subsidence Identification

Subsidence is invisible on surface maps but clearly visible in omega cross-sections. Identifying where subsidence originates, how deep it extends, and how it interacts with terrain is critical for understanding fire weather extremity.

Gap 4: Moisture Depth

Surface dew point is a single number. RH and VPD cross-sections reveal whether the dry air extends through the full column or is confined to a shallow layer—a critical distinction for predicting how long extreme conditions will persist.

6.4. Operational Recommendations

Based on this analysis, the following operational considerations are highlighted:

1. **New fire starts:** Any new ignitions during the peak windows identified above will face the most challenging suppression conditions. Pre-positioning of suppression resources before the peak window is strongly recommended.
2. **Existing fires:** Active fires in or near the critical areas should anticipate rapid spread rates and potential for extreme fire behavior including:
 - Long-range spotting driven by strong mid-level winds
 - Rapid rates of spread on receptive fuels
 - Potential for fire whirls where convergent flow meets unstable lapse rates
3. **Prescribed fire:** All prescribed fire activities in the highlighted regions should be suspended for February 10, 2026.
4. **Monitoring:** RAWS stations and fire weather forecasters should monitor for:
 - Morning inversion breakup timing (cross-section analysis suggests this is the trigger for rapid deterioration)
 - Wind shifts associated with the passage of any weak disturbances embedded in the flow
 - RH recovery failure into the overnight hours, which would extend the critical window

6.5. Confidence and Uncertainty

This analysis is based on a single HRRR model cycle (20260209 06z) at forecast hours 24–48. Key uncertainty considerations:

- **Model cycle timing:** Later HRRR cycles (12z, 18z) may adjust the position and intensity of critical parameters. Forecasters should update this analysis as newer cycles become available.
- **HRRR resolution:** At 3-km grid spacing, some terrain-channeling effects in narrow canyons (<3 km width) may be underresolved.
- **Boundary layer mixing:** Models can struggle with the timing of morning inversion erosion, which controls the onset of critical surface conditions. Actual onset may be 1–2 hours earlier or later than modeled.
- **Fire-atmosphere coupling:** Once a fire begins, it modifies the local atmosphere through heat release and pyroconvection. The cross-sections presented here represent the ambient (pre-fire) atmosphere.

This forecast was generated autonomously by an AI research agent using the wxsection.com atmospheric cross-section platform. It supplements but does not replace official NWS/SPC fire weather guidance.

Methodology and Data Sources

All cross-section data and visualizations in this report were generated from the HRRR (High-Resolution Rapid Refresh) 3-km model, cycle 20260209 06z, using the wxsection.com atmospheric cross-section API. Cross-sections are interpolated along great-circle paths between specified endpoints at 40 standard pressure levels from the surface to 200 hPa, with approximately 200 horizontal grid points per transect. The wxsection.com platform extracts data from HRRR GRIB2 files archived on NOAA's Big Data Program (Amazon Web Services) and converts them to memory-mapped format for rapid access.

API Endpoints Used:

- /api/v1/cross-section — PNG cross-section visualization (19 products)
- /api/v1/data — Numerical JSON data for quantitative analysis
- /api/v1/capabilities — Model and product discovery

Model: HRRR v4, 3-km horizontal resolution, 50 vertical levels, produced by NOAA/NCEP Global Systems Laboratory.

Disclaimer: This is an AI-generated research analysis and **does not replace** official NWS forecasts, SPC outlooks, or IMET briefings. All operational fire weather decisions should be based on official NWS products and local IMET guidance.